NTIS # PB2015-

SSC-471

STRUCTURAL LOAD PREDICTION FOR HIGH SPEED PLANING CRAFT

SHIP STRUCTURE COMMITTEE

2015

Ship Structure Committee

RDML Paul F. Thomas
U. S. Coast Guard Assistant Commandant,
for Prevention Policy
Co-Chair, Ship Structure Committee

RDML Bryant Fuller
Chief Engineer and Deputy Commander
For Naval Systems Engineering (SEA05)
Co-Chair, Ship Structure Committee

Mr. H. Paul Cojeen
Society of Naval Architects and Marine Engineers

Mr. Howard Fireman
Senior Vice President
American Bureau of Shipping

Mr. Kevin Kohlmann
Director, Office of Ship Construction
Maritime Administration

Ms. Julie Gascon
Executive Director, Domestic Vessel Regulatory Oversight
and Boating Safety, Transport Canada

Mr. Kevin Baetsen
Director of Engineering
Military Sealift Command

Dr. Neil Pegg
Group Leader - Structural Mechanics
Defence Research & Development Canada - Atlantic

Mr. Jeffrey Lantz,
Director, Commercial Regulations and Standards
U.S. Coast Guard

Mr. Matthew Garner
Director, Structural Integrity and Performance Division
Naval Sea Systems Command

Mr. Albert Curry
Deputy Assistant Commandant for Engineering and
Logistics – U.S. Coast Guard

Dr. Paul Hess
Director, Ship Systems and Engineering Research
Division
Office of Naval Research

SHIP STRUCTURE SUB-COMMITTEE

AMERICAN BUREAU OF SHIPPING (ABS)

Mr. Craig Bone
Mr. Daniel LaMere
Mr. Richard Delpizzo

DEFENCE RESEARCH & DEVELOPMENT CANADA ATLANTIC (DRDC)
Mr. Malcolm Smith
Mr. Cameron Munro
Dr. Layton Gilroy

MARITIME ADMINISTRATION (MARAD)
Mr. Chao Lin
Mr. Richard Sonnenschein
Mr. Todd Ripley
Mr. Todd Hiller

MILITARY SEALIFT COMMAND (MSC)

NAVSEA/ NSWCCD
Mr. David Qualley
Mr. Gerard Mercier
Mr. Dean Schleicher

TRANSPORT CANADA
Mr. Bashir Ahmed Golam

UNITED STATES COAST GUARD (CVE)

CAPT Ben Hawkins
Mr. Jaideep Sirkar
Mr. Charles Rawson

SOCIETY OF NAVAL ARCHITECTS AND MARINE ENGINEERS (SNAME)
Mr. Rick Ashcroft
Dr. Roger Basu
Dr. Robert Sielski
Mr. Paul H. Miller

UNITED STATES COAST GUARD (ELC)

OFFICE OF NAVAL RESEARCH (ONR)

Member Agencies:

American Bureau of Shipping
Defence Research and Development Canada
Maritime Administration
Military Sealift Command
Naval Sea Systems Command
Office of Naval Research
Society of Naval Architects & Marine Engineers
Transport Canada
United States Coast Guard

Ship
Structure
Committee

Address Correspondence to:

COMMANDANT (CG-ENG-2/SSC)
ATTN (EXECUTIVE DIRECTOR/SHIP
STRUCTURE COMMITTEE)
US COAST GUARD
2703 MARTIN LUTHER KING JR. AVE SE
WASHINGTON DC 20593-7509
Website: http://www.shipstructure.org

SSC – 471
SR – 1470

September 21, 2015

STRUCTURAL LOAD PREDICTION FOR HIGH SPEED PLANING CRAFT

There is on-going interest in high-speed planing boats, especially for government patrol boats, but also increasingly in the civilian sector for competitive ferry and freight services.

The objective of this project was to develop and verify a practical method to use time-domain stimulation to drive structural design of high speed planing craft. Computer simulators were utilized, enhanced, and modified so as to calculate panel pressures, vessel kinematics, and loads for use in Finite Element Method (FEM) programs for structural analysis. Specifically, low aspect ratio strip theory was employed via the computer program POWERSEA to predict transient slamming loads created when a high-speed craft travels through irregular seas.

Simulation affords the designer the opportunity to study the impact of a broad range of loading and operating conditions, and further consider the consequences of hull geometry on structural loads. Time-Domain simulation is shown to be able to predict the capability of the vessel hull to withstand a variety of sea states without damage. By means of resulting pressures, force distribution, stresses, and strains the designer can better optimize the material use in their hull structure to create a more resilient, yet still lighter vessel.

We thank the authors and Project Technical Committee for their dedication and research toward completing the objectives and tasks detailed throughout this paper and continuing the Ship Structure Committee's mission to enhance the safety of life at sea.

PAUL F. THOMAS
Rear Admiral, U.S. Coast Guard
Co-Chairman, Ship Structure Committee

L. BRYANT FULLER
Rear Admiral, U.S. Navy
Co-Chairman, Ship Structure Committee

1. Report No. SSC - 471	2. Government Accession No.	3. Recipient's Catalog No.
4. Title and Subtitle STRUCTURAL LOAD PREDICTION FOR HIGH-SPEED PLANING CRAFT		5. Report Date 09/21/2015 6. Performing Organization Code
7. Author(s) Akers, Richard H.		8. Performing Organization Report No. SR-1470
9. Performing Organization Name and Address Maine Marine Composites LLC 2 Portland Fish Pier, Suite 211 Portland, ME 04101-4699		10. Work Unit No. (TRAIS) 11. Contract or Grant No.
12. Sponsoring Agency Name and Address Ship Structure Committee U.S. Coast Guard (CG-ENG-2/SSC) 2703 Martin Luther King Jr. Ave. SE Washington, DC 20593-7509		13. Type of Report and Period Covered Final Report **11/2011-09/2015** 14. Sponsoring Agency Code **CG-5P**
15. Supplementary Notes Sponsored by the Ship Structure Committee. Jointly funded by its member agencies		

16. Abstract

The lack of information about hydrodynamic loads is an obstacle in the structural design of high-speed planing boats. The goal of this project is to develop and verify a practical method to use time domain simulation to drive structural design of high speed planing craft. The simulator predicts planing boat motion by calculating 2D forces and integrating the results to solve the equations of motion. Sectional pressures are expanded into transverse pressure distributions using models from Smiley (1951), which are converted to Finite Element Method (FEA) load maps for structural analysis. Results are compared with measured data from a fiberglass ski boat and with data from Jones and Allen (1972).

17. Key Words	18. Distribution Statement Distribution is available to the public through: National Technical Information Service U.S. Department of Commerce Springfield, VA 22151 Ph. (703) 487-4650		
Finite Element Analysis, High Speed Planing, Strip Theory, Seastate, Vessel Accelerations, Hydrodynamic, Ship Structure, Slamming			
19. Security Classif. (of this report) Unclassified	20. Security Classif. (of this page) Unclassified	21. No. of Pages	22. Price

CONVERSION FACTORS
(Approximate conversions to metric measures)

To convert from	to	Function	Value
LENGTH			
inches	meters	divide	39.3701
inches	millimeters	multiply by	25.4000
feet	meters	divide by	3.2808
VOLUME			
cubic feet	cubic meters	divide by	35.3149
cubic inches	cubic meters	divide by	61,024
SECTION MODULUS			
$inches^2$ feet	$centimeters^2$ meters	multiply by	1.9665
$inches^2$ feet	$centimeters^3$	multiply by	196.6448
$inches^3$	$centimeters^3$	multiply by	16.3871
MOMENT OF INERTIA			
$inches^2$ $feet^2$	$centimeters^2$ $meters^2$	divide by	1.6684
$inches^2$ $feet^2$	$centimeters^4$	multiply by	5993.73
$inches^4$	$centimeters^4$	multiply by	41.623
FORCE OR MASS			
long tons	tonne	multiply by	1.0160
long tons	kilograms	multiply by	1016.047
pounds	tonnes	divide by	2204.62
pounds	kilograms	divide by	2.2046
pounds	Newtons	multiply by	4.4482
PRESSURE OR STRESS			
$pounds/inch^2$	$Newtons/meter^2$ (Pascals)	multiply by	6894.757
kilo $pounds/inch^2$	mega $Newtons/meter^2$ (mega Pascals)	multiply by	6.8947
BENDING OR TORQUE			
foot tons	meter tons	divide by	3.2291
foot pounds	kilogram meters	divide by	7.23285
foot pounds	Newton meters	multiply by	1.35582
ENERGY			
foot pounds	Joules	multiply by	1.355826
STRESS INTENSITY			
kilo $pound/inch^2$ $inch^{½}$ ($ksi\sqrt{in}$)	mega Newton $MNm^{3/2}$	multiply by	1.0998
J-INTEGRAL			
kilo pound/inch	$Joules/mm^2$	multiply by	0.1753
kilo pound/inch	kilo $Joules/m^2$	multiply by	175.3

TABLE OF CONTENTS

LIST OF ILLUSTRATIONS

LIST OF TABLES

1 INTRODUCTION

The objective of this project is to develop and verify a practical method to use time domain simulation to drive structural design of high speed planing craft. Existing and developmental time-domain simulators will be enhanced and modified so as to calculate panel pressures, vessel kinematics, and loads for use in Finite Element Method (FEA) programs for structural analysis. Specifically, low aspect ratio strip theory will be extended to predict transient slamming loads created when a high-speed craft travels through irregular seas. The new analysis method must meet the following requirements:

- Predict transient hydrodynamic panel pressures for use in Finite Element Method programs.
- Predict velocities, rates and accelerations for use in FEA programs.
- Calculate instantaneous shear forces and longitudinal bending moments for comparison and verification of FEA results.

Maine Marine Composites (MMC) has been working continuously for almost two decades on a computer program to predict the surge, heave and pitch motion of a planing boat in regular and irregular seas. The program POWERSEA was derived starting with a computer program developed and published by Ernest Zarnick (1978) of David W. Taylor Naval Ship R & D Center. POWERSEA calculates the instantaneous motions of a planing boat by:

- Calculating the forces on each one of hundreds of hydrodynamic stations (sections) by using the following algorithms: impacting wedge, linear 2D buttock flow, viscous drag using Reynold's Number-based drag coefficients, and crossflow drag in fully-wetted regions
- Adding the sectional force components together in a weighted sum using weighting coefficients derived from more than 100 model and full-scale tests
- Calculating the added mass for each section using empirical formulas based on the sectional deadrise
- Integrating the forces and added masses for each degree of freedom
- Multiplying the inverted mass matrix times the force vector to obtain the accelerations in surge, heave and pitch; and then integrating the accelerations to find velocities and rates, and then integrating again to find positions and angles.

For SSC Project SR-1470 the POWERSEA program was modified to export forces and pressures within an operator-specified subset of the entire geometric mesh describing the hull. A load mapping algorithm was developed to export the forces in a form suitable for FEA analysis so that the strain in the structural panels of the planing boat can be predicted. This strain can be used to test the capability of the boat hull to withstand a particular sea state without damage.

The specific goal of this SSC project is to show that POWERSEA's sectional pressures can be converted to panel pressures which can be used in a Finite Analysis Method (FEA) program to predict stress and strain in the hull structure.

1.1 Background

There is on-going interest in high-speed planing boats, especially for government patrol boats. The USCG is in the middle of a long-term acquisition program for the RB-S and RB-M patrol craft. USSOCOM has issued a contract for the CCM Mark I, a replacement craft for the workhorse 11m RIB. In the civilian sector, high-speed craft are important for new, competitive ferry services and possibly for high-speed freight services, both regulated by US Coast Guard.

Structural assessment of these craft has an important impact on their operational safety. A major problem in the design of high-speed planing boats such as fast ferries and patrol craft is predicting the panel loads

for structural analysis. It is very difficult to predict the loads for quasi-static operation of planing boats, and even more difficult to predict the instantaneous loads in irregular sea states. Often algorithms such as CFD are used to predict hydrodynamic loads, but these methods are computationally intensive and cannot be used in long time-domain simulations of planing craft.

To illustrate the difficulty of designing high-speed planing craft, the Mark V is an 82-foot aluminum boat built to carry Special Operations Forces (SOF), primarily SEAL combat swimmers. The vessel has an estimated top speed of 47-50+ knots in SS2, and can cruise at 25-35 knots in SS3. This vessel was designed taking into account ABS rules, but the vessel's severe missions have resulted in structural failures and injuries to crew and passengers (Ensign, 2000). A better method of predicting structural loads is necessary for the design of future high-speed patrol boats and high-speed ferries.

Empirical algorithms have a limited range of applicability and are not well suited to time domain simulation. Spencer (1975) proposed a methodology for structural design of aluminum crewboats, using Savitsky's method (1964) to predict the trim angle of the vessel, data from Fridsma (1971) to predict peak accelerations, and a technique from Heller and Jasper (1960) to predict hull pressure distributions. Given a pressure distribution, engineers can calculate maximum frame spacings and minimum panel thicknesses. This method is an historical basis for the dynamic pressure used in the USCG's NVIC 11-80 (1980). Unfortunately the method makes assumptions about sea states, missions, and hull geometry. Any significant deviations from these assumptions introduce uncertainty into the design process.

The Ship Structure Committee funded a project to study and compare "…the application, requirements and methods for the structural design of high speed craft..." used by various classification societies. Results of the comparison appear in Report SSC-439 (Stone, 2005). Classification society rules use empirical formulas to predict vertical accelerations, which are used in structural design calculations. A more direct method would be to use time-domain simulation to predict panel pressures for structural design.

Planing hull simulation programs based on low aspect ratio strip theory have been in existence for several decades (Zarnick, 2978). These programs can predict the vertical accelerations of a planing monohull operating in a seaway with good engineering accuracy (Akers, 1999a, b). Maine Marine Composites, LLC recently was awarded a contract to extend low aspect strip theory to support a wide range of hull forms and to predict transverse forces (Office of Naval Research contract N00014-10-C-0196). The result of this effort is a computer program called POWERSEA.

1.2 Justification for Project

The American Bureau of Shipping (ABS, 2003) recognizes that time domain simulation is an effective way of predicting hull pressures for structural analysis of high speed craft:

> "Slamming loads cause whipping response of the entire hull particularly for high-speed craft operating in severe seas. The resulting dynamic stresses in the hull girder can be of the same order of magnitude as those induced by quasi-static wave bending moments. But their frequencies are much higher than those generated by wave and motion-induced loads, closer to the lowest natural frequency of the hull girder. Therefore, slam-induced whipping response of the hull could also have significant influence on the strength requirements…
>
> "For detailed analysis, direct time-domain simulation involving short-term predictions are recommended as a minimum requirement for strength assessment for monohulls. In most cases involving high speeds, the absolute motions or relative motions will be of such large amplitude that nonlinear calculations will need to be employed..."

2 PROCEDURE

The goal of this project is to advance the ability of the engineer to predict instantaneous structural loads on planing boats. This is accomplished by:

- Calculating the instantaneous sectional forces on a planing boat as it passes through irregular seas,
- Integrating the sectional forces to find the rigid body surge and heave forces and the pitching moment on the boat, and
- Solving the equations of motion to find the instantaneous attitude of the boat.

If the simulator accurately predicts the surge, heave and pitch motions, then it is likely that the sectional forces are at least qualitatively close to the actual forces. Once the sectional forces are known, they can be converted to transverse force distributions according to the theories of Zhao (1993, 1996), Faltinsen (2007), Smiley (1951), and others.

A low aspect ratio, time-domain simulator for planing hulls operating in the vertical plane was modified for this project. The program is a "2 ½ D" simulator that calculates two-dimensional section forces and integrates them over the longitudinal coordinates by replacing the longitudinal coordinate with a function of time.

2.1 Time-Domain Planing Boat Simulator

2.1.1 Capabilities of Planing Simulator

The Planing Simulator can synthesize irregular seas according to Pierson-Moskowitz, JONSWAP, ITTC and Ochi 6-Parameter spectra.

The Planing Simulator can run the following constrained simulations:

- Constant or ramped surge velocity
- Constant or ramped effective thrust or power (free in surge velocity)
- Constant or ramped shaft RPM driving waterjets or propellers (free in surge velocity)

In addition, the user can instruct the Planing Simulator to constrain the heave and pitch degrees of freedom:

- Free to move
- Fixed or ramped in position or angle
- Driven sinusoidally in position or angle to simulate a planar motion mechanism in a towing tank

The Planing Simulator can plot or list time-histories of accelerations, velocities and positions (collectively called "motions"), and can post-process simulation results to calculate:

- Fourier transforms and spectral density functions of motions
- Statistical summaries of motions
- Motion-sickness dosage values and Shock dosage values
- Static Effective Dosage (SED) per ISO 2651

2.1.2 Geometry Models in the Planing Simulator

The geometry kernel in the Planing Simulator is based on the IGES 5.3 specification (IGES, 1997). Most of the geometric entities in the specification are supported in the Planing Simulator kernel including points, curves and surfaces. The CAD human interface supports a subset of these entities. It can display almost all of the geometric entities properly, but only includes provisions for creating and editing:

- Points
- Straight Lines
- Parametric Curves
- BSpline Curves
- Composite Curves
- Ruled Surfaces
- Group Associativity Entities (e.g. groups of surfaces in a hull, groups of buttock curves)

The user may define boat hulls using BSpline surfaces, NURBS surfaces, surfaces of rotation, and other IGES entities, but they must create and edit their designs outside of the Planing Simulator environment, convert them into IGES or DXF files (Autodesk, 2013), and then import them into the Planing Simulator. In the Planing Simulator kernel each geometric entity is converted to vertices and straight line segments. The user can control the fineness of the geometry mesh by specifying the number of divisions and subdivisions that should be used for each entity.

The Planing Simulator geometry mesh is derived from its internal representation of entities that define the hull. A mesh is a list of hydrodynamic sections and hydrodynamic buttock lines. These lines are created by:

1. Finding the intersection points of a plane (e.g. a constant X-plane for a station and a constant Y-plane for a waterline) with all of the Planing Simulator hull entities,
2. Sorting the points in an order perpendicular to the intersection plane, removing duplicates, and
3. If necessary adjust points so that the order of points is monotonic and so that deadrise is held between 0 and 90 degrees.

The resulting sorted point set becomes the vertices for piecewise-linear stations and buttock lines. If the user specifies reasonable resolution values (e.g. 8 divisions, 4 subdivisions) then the accuracy of the results rivals the accuracy of direct calculations of each vertex.

2.1.2.1 Calculating Forces and Moments; Simulating Motion

At each time step, the Planing Simulator:

1. Calculates the force vector and moment vector contributed by each station (refer to Appendix 1).
2. Calculates the added mass contributed by each station
3. Integrates the station force and moment vectors over the entire hull to find the total force vector and moment vector
4. Integrates the added mass over the entire hull to find the total added mass and added pitch inertia
5. Solves the equations of motion to find instantaneous angular and radial accelerations

$$|\mathbf{A}| = (|\mathbf{M}| + |\mathbf{Added\ M}|)^{-1} * |\mathbf{Total\ Force/Moment}|$$

6. Integrates the accelerations to find velocities and the velocities/angular rates to find positions/angles

The sectional force and moment vectors calculated in Step 1 are the basis for calculating the vector forces exported to FEA.

2.2 Calculating Pressures for Structural Analysis

2.2.1 Transverse Pressure Distribution

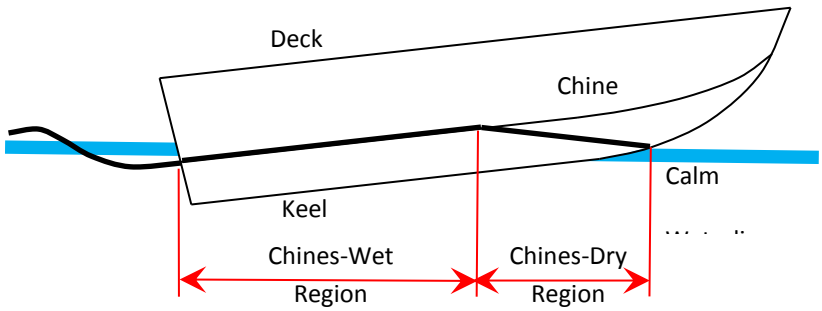

Figure 1 Planing Regions

The transverse pressure distributions can be categorized by their region of operation (refer to Figure 1). Starting at the bow of the planing boat, the most forward wetted point on the keel occurs at the calm waterline. Moving aft, the water rises above the calm waterline because the water displaced by the boat piles up to port/starboard, resulting in an increase of the sectional draft. Eventually the piled-up water reaches the chine. The "chines-dry region" is the range between the most forward wetted point and the station for which the pile-up water reaches the chine. The transverse flow separates off of the chine, so the piled-up water stops at the chine. The distance abaft the end of the "chines-dry region" is, of course, called "chines-wet."

From many model tests (e.g. Kapryan, 1955; Broglia, et. al. 2010) it is apparent that the transverse pressure distribution follows a curve that resembles the curves in Figure 2. The similarity between the pressure distributions at different longitudinal locations is apparent in this figure. The distributions with a peak occur in the "chines-dry" region, while the ones without a peak occur in the "chines-wet" region.

As seen in Figure 2 the transverse pressure distribution in the chines-dry region is dramatically different than that in the chines-wet region. In the chines-dry region the pressure reaches a peak value along a stagnation line and drops off quickly toward the keel. After the stagnation line reaches the chine in the chines-wet region, the pressure distribution becomes much more constant, tapering off as it nears the chine.

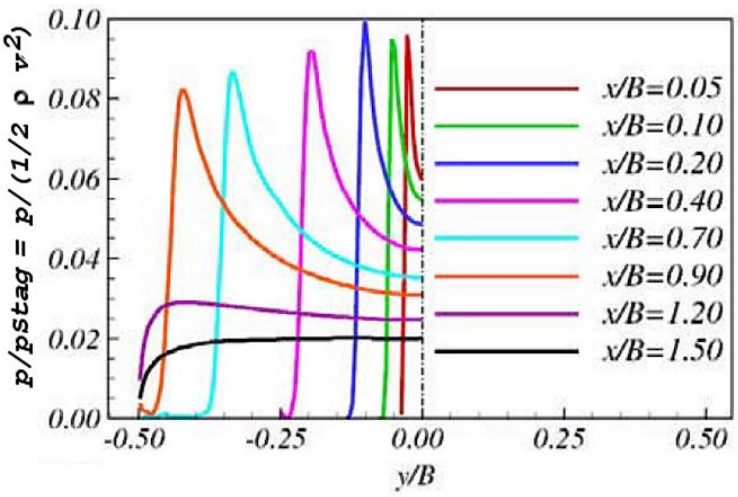

Figure 2 Transverse pressure distribution measured on boat with 0-heel angle. "y/B=0.05" is bow and "y/B=1.50" is stern (Broglia, et. al., 2010, Figure 7). Curves with peaks are in chines-dry region, curves at x/B=1.2 and 1.5 are in chines-wet region.

In both the chines-dry and chines-wet regions, much of the curvature in the pressure distribution occurs near the outer edge of the wetted surface. To make sure that the pressure points exported by the simulator have sufficient density to model the rapid pressure changes, the simulator models each section with up to 50 pressure panels. To avoid creating extremely small panels, the minimum panel size is limited to the maximum wetted beam divided by 250.The vertices of the panels are calculated by stepping the y coordinate (transverse) from 0 to 1, where the step size is inversely proportional to the cube of the fraction of the transverse wetted beam left to be covered by panels.

The procedure for calculating pressure loads at any point on the hull is to calculate the total sectional half pressure (force/unit length for the port or starboard side of the hull) and use the models summarized in Smiley (1951) to scale a transverse pressure distribution from the sectional forces. Smiley suggests two different methods of modeling the pressure distribution, one for the forward chines-dry region and one for the aft chines-wet region of the boat.

2.2.1.1 Modeling the Transverse Pressure Distribution: Chines-Dry Region

The transverse pressure distribution in the chines-dry region is modeled using Equations 1, 2 and 3. The variable K is the water-rise ratio.

$$K \approx \frac{\pi}{2}\left(1 - \frac{3\tan^2\beta\cos\beta}{1.7\,\pi^2} - \frac{\tan\beta\sin^2\beta}{3.3\,\pi}\right) \quad (1)$$

The deadrise β is assumed to be constant for each station, defined as the angle between the keel point and the chine point. For computational efficiency a spline curve is precalculated to compute K from β (refer to Figure 4).

Pierson (1948) and Pierson and Leshnover (1950) suggest Equation 2 to calculate a modified deadrise θ taking into account the running trim of the boat. The value K was precalculated using the spline curve described above.

$$\tan(\theta) = \frac{\pi}{2}\sqrt{\frac{\sin^2\beta + K^2\tan^2\tau}{K^2 - 2K\sin^2\beta - K^2\sin^2\beta\,\tan^2\tau}} \quad (2)$$

Smiley's transverse pressure distribution uses this in the form of cot(θ) = 1/tan(θ). The transverse pressure distribution is modeled by Equation 3 with an appropriate scale factor.

$$\frac{p\left(\frac{\hat{\eta}}{c}\right)}{p_{SECTION}} \propto \left[\frac{\pi \cot(\theta)}{\sqrt{1-\left(\frac{\hat{\eta}}{c}\right)^2}} - \frac{1}{\left(\frac{c}{\hat{\eta}}\right)^2 - 1}\right] \tag{3}$$

Equation 3 includes a variable η which is related to the transverse distance from the keel toward the chine. The term (η/c) represents the normalized wetted half beam ranging from 0 to 1. The equation goes to -∞ when η=c, corresponding to the pressure at the outer edge of the wetted surface c. The pressure curve passes through 0 close to that point, and the zero crossing is the effective outer edge of the wetted beam model. In other words the model is not accurate over the entire range of normalized half beam, but has to be scaled slightly. A value $\hat{\eta}$ is defined that maps η from the keel to the zero crossing.

At each time-step, the trim angle τ is known, so a second constant c1 is calculated.

$$c1 = 2\sqrt{\frac{K\,(K\,(1-sin^2\beta\,tan^2\tau) - 2\,sin^2\beta)}{sin^2\beta + K^2 tan^2\tau}} \tag{4}$$

Instead of ranging from 0 to 1, the value of $\hat{\eta}$ ranges from 0 to $\hat{\eta}_{MAX}$ as calculated as in Equation 5.

$$\hat{\eta}_{MAX} = \frac{1}{2}\sqrt{2\,c1\,\sqrt{c1^2+4} - 2\,c1^2} \tag{5}$$

A factor of proportionality is chosen so that the integral of Equation 3 from $\hat{\eta} = 0$ to $\hat{\eta}_{MAX}$ is equal to 1. The direct integral of this formula can be shown to be Equation 6. The total transverse half pressure calculated by this formula over the entire wetted beam is proportional to the sectional half pressure.

$$\hat{p}_{TOTAL} = c1\,\text{asin}(\hat{\eta}_{MAX}) + \hat{\eta}_{MAX} + \frac{1}{2}\ln\left(\frac{1-\hat{\eta}_{MAX}}{1+\hat{\eta}_{MAX}}\right) \tag{6}$$

The scale factor $\hat{p}_{TOTAL}$ can be used to make Equation 3 an equality. Figure 3 is a chart of the transverse pressure for three different values of deadrise β, all shown for a constant trim τ = 4 degrees.

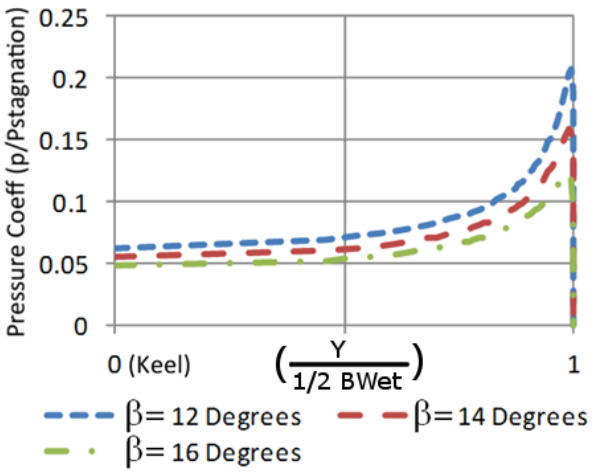

Figure 3 Sample chines-dry transverse pressure distributions for three different deadrise angles. All three distributions were calculated at a running trim of 4 degrees.

Note that Equation 3 defines a hull pressure in terms of the stagnation pressure ½ ρ v^2. Instead of pressures, the following procedure calculates forces by scaling the panel pressure by the panel girth.

Steps in scaling the sectional half forces in the Chines Dry region are:

1. Calculate all of the sectional half forces using the conventional low aspect ratio planing algorithm. These are the sum of the hydrostatic and the hydrodynamic forces as applied to one side of each section of the hull.

   (Continue for each section in the Chines-Dry region…)

2. Using the keel-to-chine deadrise, calculate K using Equation 1. Using the instantaneous trim angle calculate an effective deadrise value θ. Only tan(θ) is required so Equation 2 is used.
3. Find the transverse coordinate scale factor by using Equation 4 and Equation 5 to calculate the value $\hat{\eta}_{MAX}$ corresponding to the point where Equation 3 is undefined. Since this corresponds to the wetted beam c(t), the transverse coordinate scale factor is KYscale = $\hat{\eta}_{MAX}/_{c(t)}$
4. Find the area under the $p\left(\frac{\hat{\eta}}{c}\right)$ curve by using Equation 6. Find the force scale factor by assuming that the stagnation pressure is 1.0 and calculating: $= F_{HalfSection}/p\left(\frac{\hat{\eta}}{c(t)}\right)$.
5. For each panel in the section, map the transverse coordinate of its midpoint ymid to the η̂ domain by multiplying ymid by KYscale. Use Equation 3 and KPScale to calculate a pressure, $\hat{p}$. Assuming that the stagnation pressure is 1.0, this is actually a force, $\hat{f}$.
6. Convert $\hat{f}$ to f_{PANEL} by scaling it by the inverse of the transverse scale factor and the section spacing $1/(\text{KYScale} * \Delta X)$.

The results of this algorithm will be a set of forces applied at the transverse midpoint of an array of sectional panels. The total force contribution from each section is twice the sum of these forces because these forces only cover one half of each hull section.

2.2.1.2 Modeling the Transverse Pressure Distribution: Chines-Wet Region

The transverse pressure distribution in the Chines-Wet Region does not have the bump at the stagnation line that the Chines-Dry distribution has. Instead it starts with a flat region near the keel and rolls off as it approaches the chine (refer to Figure 2, curve "y/B=1.5"). Smiley (1951) uses the results of a derivation from Korvin-Kroukovsky and Chabrow (1948) to model the pressure distribution in the chines-wet region. Variables in the following equations are:

b	Half beam of boat	h	(Constant)
β	Deadrise, radians	k	(Constant)
ϵ	Auxiliary variable, radians	η	Transverse distance from keel, positive toward chine

Equation 7 and Equation 8 map the deadrise β to a constant value k. For efficiency an array of pairs of (β, k) are precalculated and mapped with a spline function so that k can be calculated quickly for any value of β (refer to Figure 4).

$$h = \frac{\pi - 2\beta}{\pi} \tag{7}$$

$$\frac{1}{k} = 4\,cos\beta \int_0^{2\pi} (1 + \sin(\epsilon))^h (\cos(\epsilon)^{1-h} \sin(\epsilon))\, d\epsilon \tag{8}$$

Equation 9 maps the transverse location η to a non-dimensional value ϵ and Equation 10 maps ϵ to non-dimensionalized pressure:

$$\frac{\eta}{Beam_{SECTION}} = 2k\ cos\beta\ \int_{\varepsilon}^{2\pi}(1+\sin(\epsilon))^{h}(\cos(\epsilon)^{1-h}\sin(\epsilon))\,d\epsilon \quad (9)$$

$$\frac{p(\eta)}{P_{Section}} \propto 1-\left(\frac{\cos(\epsilon)}{1+\sin(\epsilon)}\right)^{2h} \quad (10)$$

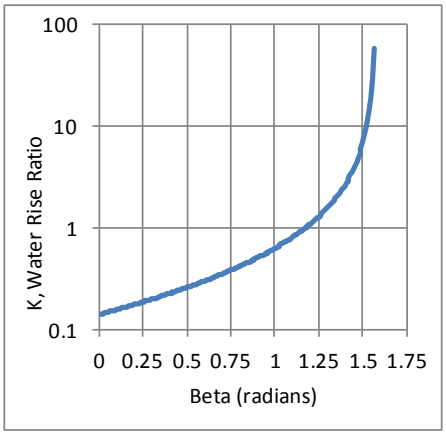

Figure 4 Constant used in chines-wet transverse pressure calculations, plotted versus deadrise β, corresponding to Equation 7 and Equation 8.

Steps in scaling the sectional half forces in the Chines Wet region are:

1. Precalculate a spline to map deadrise β to ε using Equation 7 and Equation 8.
7. Calculate all of the sectional half forces using the conventional low aspect ratio planing algorithm. These are the sum of the hydrostatic and the hydrodynamic forces as applied to one side of each section of the hull.

   (Continue for each section in the Chines-Wet region…)

2. Using the sectional deadrise and the spline from step 1, calculate k.
3. Evaluate Equation 9 using ε values ranging from 0 to π/2. The result will be an array of mapping between (η, ε) values. Evaluate Equation 10 for each ε value in the mapping array. The results will be an array of η, ε, and p(η) values. Fit an interpolation spline to the η, p(η) values.
4. Find the total area under the η, p(η) curve by using quadrature integration of Equation 10 from η=0 to $\eta=\eta_{MAX}$. Calculate a pressure-to-force scale factor KPScale by assuming that the stagnation pressure is 1.0 and calculating $KPScale = F_{HalfSection}/(N_{Panels} * \int p(\eta))$.
5. For each panel in the section, calculate the normalized pressure value for ymid using the spline from Step 4. Multiply this by the sectional half force (which can be a 3-dimensional value), by the panel spacing ΔY, and by KPScale to calculate f_{PANEL}. f_{PANEL} will also be a 3-dimensional value.

As in the previous section, the results of this algorithm will be a set of forces applied at the transverse midpoints of each panel in an array of sectional panels. The total force contribution from each section is twice the sum of these forces because these forces only cover one half of each hull section.

2.2.1.3 Combining Force Vectors to Predict Structural Panel Pressures

The previous sections describe a method to convert a 3-component longitudinal force vector contributed by each station to individual panel forces. These force vectors are applied at a point on the hull and resemble the point pressures measured with small pressure sensors. As discussed by Allen, et al. (1978)

predicting the structural force on a panel requires the designer to consider multiple pressure values over the panel area, averaging them to calculate an effective panel pressure. To calculate instantaneous effective panel pressures the following steps were implemented in the Planing Simulator:

1. Preprocessing steps:
    a. The hull surface is tessellated into small triangles that approximate the curvature of the hull. This hull mesh does not necessarily line up with the hydrodynamic sections. Its role is to represent the fine shape and curvature of the hull.
    b. A set of four hull vertices were specified. Each vertex includes an x (longitudinal) and y (transverse) coordinate. As the hull cannot have negative deadrise, there only can be one z (vertical) offset corresponding to an (x, y) pair.
    c. The centroid of each tessellation panel is tested to see if it is in the hull area enclosed by the four vertices. If so it is added to a list for efficient processing during simulation.
2. At each time step:
    a. Sectional panel forces are calculated as in previous sections. These are converted to panel pressures by dividing each panel force by its area (panel girth times station spacing).
    b. The pressure at each enclosed tessellation triangle is calculated by interpolating pressures between sectional panel pressures. The force on each tessellation triangle is calculated by multiplying the pressure times the triangle area.
    c. The forces on the enclosed tessellation triangles are summed and divided by the total area of the enclosed tessellation triangles.

The interpolation algorithm takes advantage of the regular section spacing in the time-domain simulator model. Sections (stations) are defined as having constant X coordinates, so the first step in the interpolations is to identify the pair of stations that bound the target vertex. Once the stations have been identified, the Y-coordinate of the vertex is used to find the pair of offset locations in each station that bound the vertex. Finally linear interpolation between the four offset locations (two on each section) is used to calculate the pressure that corresponds to the vertex. If a higher order interpolation algorithm such as quadratic interpolation was used, the time-domain simulator could export fewer pressure points, and the pressure mesh might be slightly more accurate.

2.2.2 Communication between Simulator and FEA

The simulation mesh and the FEA simulation will not be identical and a load mapping step is required. It is likely that some of the individual FEA panels will map to multiple simulation pressure panels and vice versa. To avoid many of these problems, a fine mesh is created and a large number of pressure panels are exported for each section of the simulation model. As a result, any error due to the mismatch between simulation panels and FEA panels will be small.

2.2.2.1 Geometry Algorithms to Export Pressures to FEA

To export a pressure map for use in FEA:

- The FEA system creates a mesh.
- The simulator creates a cloud of sectional panel forces.
- An interpolation tool reads the FEA mesh, reads the simulation scalar data, and interpolates to find the force at the center of each FEA face. Refer to Section 2.2.1.3 for details of the interpolation.
- The interpolation tool exports a pressure file formatted to be read by the finite element analyzer.

Special attention must be paid to the case in which there is a large FEA face covering many of simulator vertices, some with high pressure (e.g., the stagnation line in the chines-dry region) and most with low pressure or zero pressure (e.g. above the wetted surface). Interpolation is challenging because the average of all of these pressures is not necessarily the best value to use, and a polynomial interpolation may fail due to oscillations in the polynomial. In this project these problems have been addressed by using a fine mesh in both the time-domain simulator and the FEA models.

3 Calculating Reference and Design Pressures

Heller and Jasper (1960) proposed a method for predicting bottom pressures by comparing the natural frequency of the boat to the rise time of the wave encounters and modeling the resulting pressures by a Dynamic Load Factor. Further Heller and Jasper recognized that the longitudinal and transverse pressure distributions can be captured by using impact load factors.

Spencer (1975) extended the method by using the method of Savitsky (1964) to determine running trim angles, the method of Fridsma (1971) to predict vertical accelerations, and the work of Heller and Jasper to calculate hull pressures.

Allen and Jones (1978) extended this work by relating actual spatial pressure distributions to equivalent static design pressures. The hull bottom is represented by a reference area AR and the peak pressures are calculated or measured for this area. A smaller design area AD representing the hull area near a structural feature is defined. The pressure is estimated for this area based on the ratio of AR/AD and on the longitudinal location of the design area.

This method has been extended and revised by Koelbel (1995) and others, and is the basis for the ABS *Rules for Building and Classing High Speed Craft* (ABS HSC, 2015). Section 3.2.2 of ABS HSC describes a method for estimating hull reference pressures and design detail pressures for structural analysis of planing boats.

The first steps in this procedure are to select load conditions, sea states, and operating speeds. Table 1 in ABS HSC, 3.2.2 specifies that the appropriate sea state for an ocean-going planing boat is Hsig=13 feet. Assuming that the sea is fully developed, a single parameter Pierson-Moskowitz spectrum can be used for this analysis. The ABS HSC describes three load conditions, 10% of the maximum operating deadweight, 50%, and full load, and it recommends that the craft run at full speed for the 10% case.

Vertical Accelerations: For a fixed mass the force applied to the mass will be proportional to the acceleration of the mass. Accordingly, there should be a correlation between the peak accelerations at a particular panel on the hull it and the pressure applied to that point. The ABS HSC Rules specify that the acceleration history at the center of gravity of a boat can be used as the basis for the accelerations anywhere on the hull. The Rules provide a formula to estimate the average of the $1/100^{th}$ highest accelerations at the center of gravity, and then provides charts to extrapolate the effects of this acceleration longitudinally along the hull by using a vertical correction factor F_V.

Reference Area: Once the conditions are established, the ABS HSC Rules specify that a maximum hull pressure should be calculated for the entire hull reference area A_R. The Rules specify a formula for the reference area, based on the displacement and the stationary draft at the midpoint of the design waterline. The Rules do not take the deadrise into account, presumably because they are targeted at boats with similar deadrise distributions.

Design Area: The area A_D is calculated for a structural feature such as a panel spanning transverse longitudinal and transverse stiffeners. Structural features range from simple panels to entire hull sections defined by bulkheads or major frames. Accordingly their longitudinal coordinates and their design areas can vary widely. The ABS HSC Rules define a dynamic correction factor F_D that depends on the ratio of each design area A_D and the reference area A_R. The correction factor ranges from a high value of 1.0 to a minimum value of 0.2.

Dynamic Panel Pressure: The dynamic panel pressure PBXX is calculated by a formula that takes into account the vessel displacement, the length and beam, the average of the $1/100^{th}$ vertical accelerations at the center of gravity, and the correction factors F_V and F_D.

This report describes an alternative method of calculating panel pressures based on time-domain simulation.

3.1 Numerical Example

A notional design was created, based loosely on the Mk V Special Operations Craft (SOC). Principal characteristics for this vessel were derived from the MS Thesis of Todd Whalen (2002) and are listed in Table 1.

Table 1 Principal Characteristics, High Speed Patrol Boat

Parameter	Value	Units	Parameter	Value	Units
LOA	82	feet	Z-Chine (Min)	4.75	feet
Bmax	17.5	feet	Beta Fore	35	degrees
Half Beam	8.75	feet	Beta Mid	29	degrees
Depth (keel to Shear)	7.75	feet	Beta Min	28.5	degrees
LCG (fwd of Transom)	52	feet	Pitch Rad. Of Gyr. (RG)	20	feet
VCG (ABL)	2.5	feet	Displacement	119,000	Lb
Propulsion	2x Waterjets				

This boat has a high deadrise value and a very moderate longitudinal deadrise distribution and was chosen because of its simplicity. A CAD model was created for this boat using MultiSurf (AeroHydro, 2013). Lines drawings for this model are shown in Figure 5 and Figure 6.

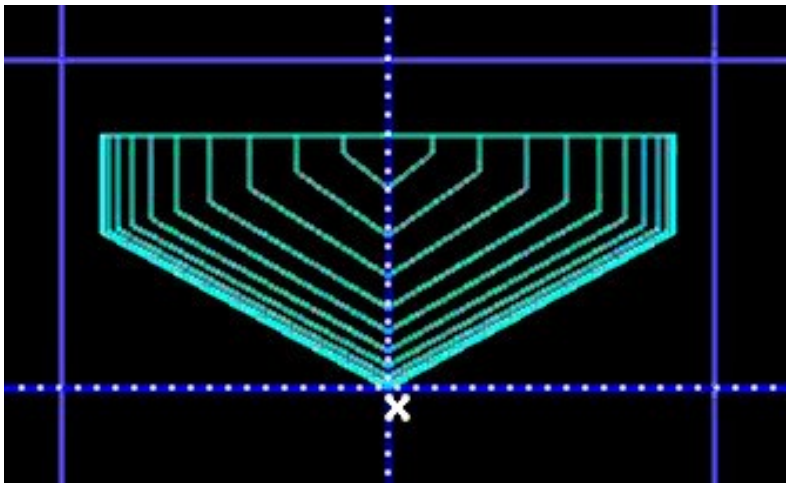

Figure 5 Body Plan, Patrol Boat

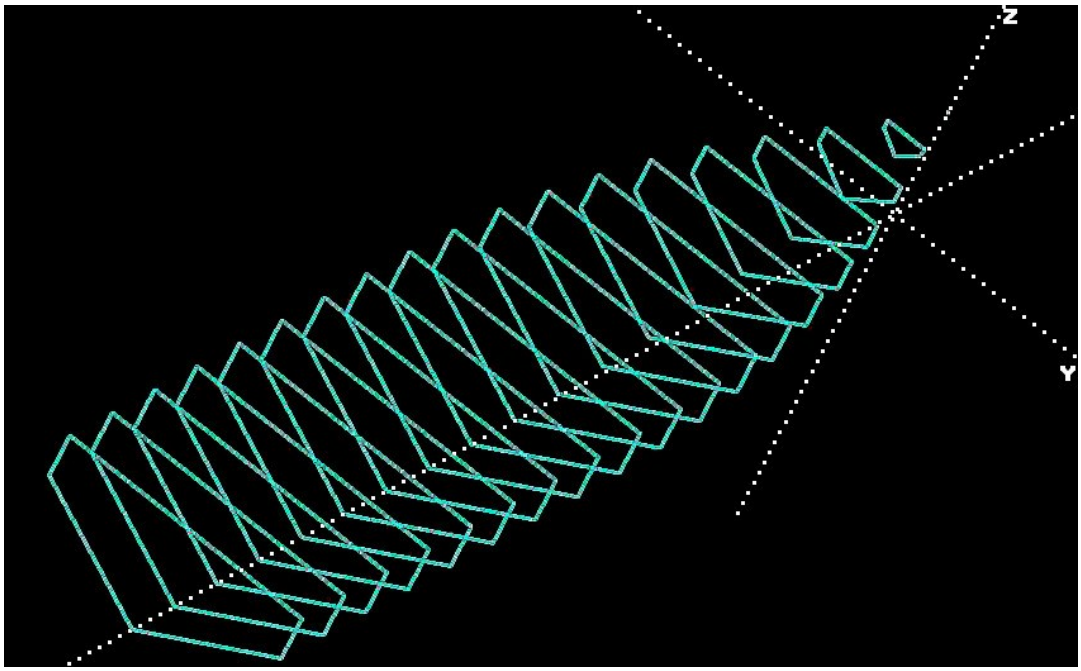

Figure 6 Offset Lines, Patrol Boat, perspective view

A hydrostatic analysis was performed on this hull as designed and the results are shown in Table 1.

Table 2 Hydrostatics and Principal Characteristics of Patrol Boat model

Position			**Center of Buoyancy**		
Sink	4.883	ft	X	52.034	ft
Trim	-0.659	deg	Y	0	ft
Heel	0	deg	Z	2.951	ft
Center of Gravity			**Center of Flotation**		
`X	52	ft	X	50.238	ft
Y	0	ft	Y	0	ft
Z	0	ft	Z	4.304	ft
Specific Weight			**Waterplane**		
	64	lb/ft^3	W.P. Area	952.96	ft^2
			LCF (%WL)	56.62%	
Coefficients					
Waterplane	0.818		**Dimensions**		
Prismatic	0.739		WL Length	73.222	ft
Block	0.369		WL Fwd X	8.778	ft
Midsection	0.5		WL Aft X	82	ft
Disp/L	135.32		WL Beam	15.915	ft
			Draft	4.32	ft
			Displacement	119000	lb

Initial Stability	Transverse		Longitudinal		
Moment of Inertia	16699	ft^4	328844.6	ft^4	
Metacentric Height	11.932	ft	179.809	ft	
R.M. per degree	24782	ft-lb	373451.7	ft-lb	
Volume	1859.4	ft^3			
LCB (%WL)	59.08%		**Center of W.S. Area**		
			X	50.208	ft
Wetted Surface			Y	0	ft
W.S. Area	1087	ft^2	Z	2.356	ft

Figure 7 is a CAD rendering of the model. Patches representing structural design areas are shown in this figure. Large and small forward and aft patches (A and B, C and D) were defined, centered at common longitudinal location (Table 3). These will be used to illustrate the inverse relation between panel size and design pressures.

Table 3 Sample Design Areas

	Fore Panel		Aft Panel	
	Large (A)	Small (B)	Large (c)	Small (D)
Area	35.9	8.99	36.3	9.07
Distance abaft Bow	36.4	36.4	63.8	63.8

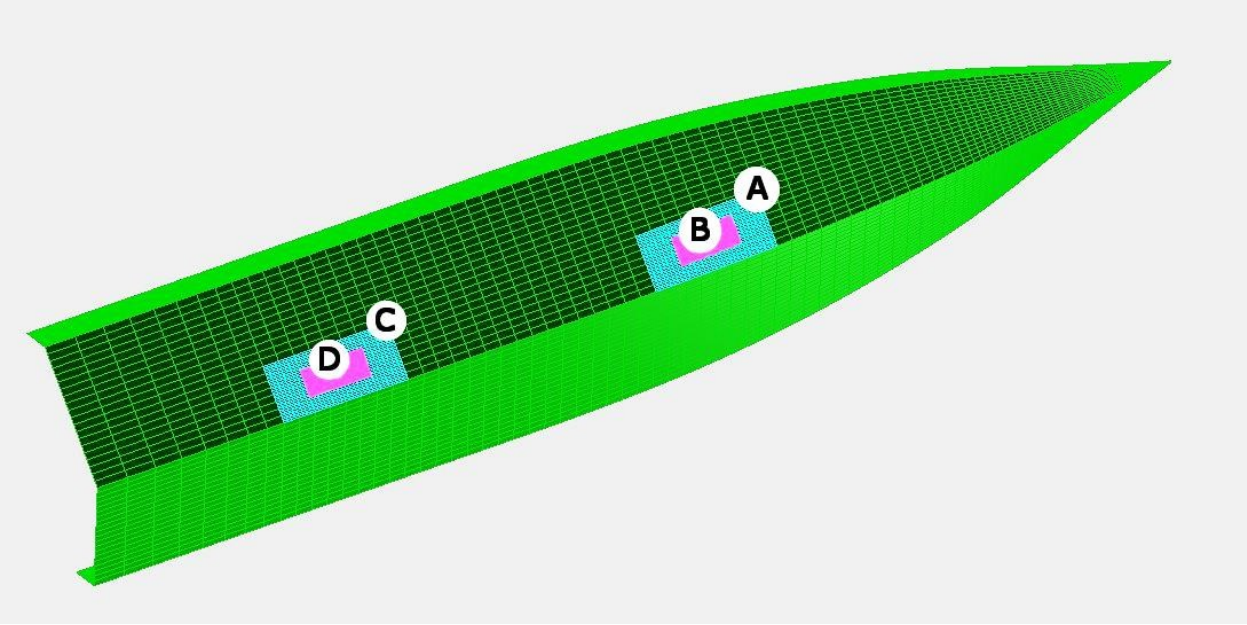

Figure 7 Perspective view of Patrol Boat as seen from below. Small patches (magenta) are centered in larger patches (cyan).

A simulation was performed on this boat operating for 500 seconds at 35 knots in a head sea described by a pseudo-random Pierson-Moskowitz spectrum with Hsig=13 feet. Statistical results from this simulation

are listed in Table 4. As illustrated in Figure 8, the boat experienced vertical accelerations up to about 16 g's at the center of gravity.

Table 4 Simulation Results for Patrol Craft at 35 knots, Hsig=13 feet (P-M spectrum)

	Heave Loc	Pitch	Wave Ht, X=FP	Surge Vel	Heave Vel	Pitch Vel	Eff Thrust	Eff Power	Surge Accel	Heave Accel	Pitch Accel
	feet	degr	feet	ft/sec	ft/sec	RPM	lbf	HP (British)	G's	G's	Degr /sec**2
Min	-8.56	-9.56	-10.59	56.36	-33.97	-3.92	-100	-11.206	-0.209	-1.705	-376.35
Mean	0.01	1.49	0.03	59.09	-0.16	0.05	8887.1	951.4	0.000	-0.005	19.53
Max	15.70	12.59	14.13	61.63	16.89	8.00	30000	3335.7	0.721	8.020	2012.40
Std Dev	3.34	3.09	3.23	0.59	6.39	1.47	7573.3	810.3	0.047	0.580	200.84
MAX VALUE BETWEEN MEAN CROSSINGS (REL TO MEAN):											
Abs Min	0.56	0.32	0.36	0.06	0.67	0.15	859.9	81.27	0.005	0.060	22.79
Ave	4.31	3.47	4.13	0.67	6.96	1.91	11565	1226.6	0.085	1.098	163.83
Abs Max	15.70	11.10	14.10	2.54	17.05	7.95	21112	2384.3	0.720	8.025	1992.80
Ave(1/3)	7.58	5.55	6.84	1.39	10.80	3.26	19446	2080.9	0.194	2.150	352.25
Ave(1/10)	10.55	7.41	8.65	2.05	13.32	4.62	21112	2301	0.358	3.513	633.90
MIN VALUE BETWEEN MEAN CROSSINGS (REL TO MEAN):											
Abs Min	-8.57	-11.05	-10.62	-2.73	-33.81	-3.97	-8987.	-962.6	-0.209	-1.700	-395.88
Ave	-4.11	-4.71	-4.16	-0.68	-10.11	-1.94	-7181.	-765.5	-0.053	-0.633	-63.98
Abs Max	-0.46	-0.32	-0.43	-0.06	-0.67	-0.18	-826.3	-93.18	-0.005	-0.059	-20.22
Ave(1/3)	-6.03	-7.33	-6.58	-1.35	-17.24	-2.86	-8987.	-962.4	-0.106	-1.004	-100.60
Ave(1/10)	-7.04	-9.13	-8.07	-2.09	-22.69	-3.33	-8987.	-962.5	-0.151	-1.119	-186.81
ALL MAXIMA:											
Abs Min	-1.40	-0.33	-2.27	58.83	-2.56	-0.33	5878.3	627.4	-0.180	-0.930	-21.49
Ave	4.03	4.76	3.75	59.78	6.49	1.87	19536	2130.6	0.062	0.946	204.72
Abs Max	15.70	12.59	14.13	61.63	16.89	8.00	30000	3335.7	0.647	8.020	1770.50
Ave(1/3)	7.37	6.92	6.54	60.52	10.49	3.22	27077	2972.6	0.152	1.885	375.70
Ave(1/10)	10.39	8.82	8.41	61.16	13.06	4.52	30000	3244.3	0.283	3.009	581.50
ALL MINIMA:											
Abs Min	-8.56	-9.56	-10.59	56.36	-33.97	-3.92	-100	-11.206	-0.209	-1.705	-376.35
Ave	-3.93	-3.05	-3.54	58.37	-10.02	-1.76	1984.4	218.83	-0.039	-0.276	-48.68
Abs Max	0.73	2.37	2.98	59.03	3.33	0.47	11458	1227.7	0.146	2.342	520.50
Ave(1/3)	-5.92	-5.70	-6.28	57.70	-17.07	-2.77	-100	-10.978	-0.094	-0.867	-96.58
Ave(1/10)	-6.98	-7.59	-7.88	56.97	-22.64	-3.25	-100	-11.098	-0.138	-1.072	-193.07
ALL MAXIMA ABOVE MEAN:											
Abs Min	0.12	1.59	0.09	59.13	-0.04	0.08	9028.5	968.4	0.000	0.000	55.62
Ave	4.06	4.73	3.80	58.34	6.54	1.88	19253	2105.4	0.066	0.959	204.84
Abs Max	15.70	12.59	14.13	61.63	16.89	8.00	30000	3335.7	0.647	8.020	1770.50
Ave(1/3)	7.16	6.81	6.35	60.48	10.29	3.19	26644	2933.2	0.125	1.827	375.70
Ave(1/10)	9.55	8.26	7.84	61.07	12.40	4.40	30000	3237.5	0.176	2.740	572.00

ALL MINIMA BELOW MEAN:											
Abs Min	-8.56	-9.56	-10.59	56.36	-33.97	-3.92	-100	-11.206	-0.209	-1.705	-376.35
Ave	-3.94	-3.09	-3.62	58.37	-10.04	-1.77	1674.2	181.59	-0.043	-0.380	-51.55
Abs Max	-0.09	1.38	-0.17	59.03	-0.17	0.03	8793.3	939.3	0.000	-0.010	0.04
Ave(1/3)	-5.89	-5.61	-5.95	57.70	-16.91	-2.74	-99.99	-10.964	-0.085	-0.642	-95.62
Ave(1/10)	-6.89	-7.37	-7.12	56.97	-22.26	-3.13	-100	-11.076	-0.113	-0.764	-188.40

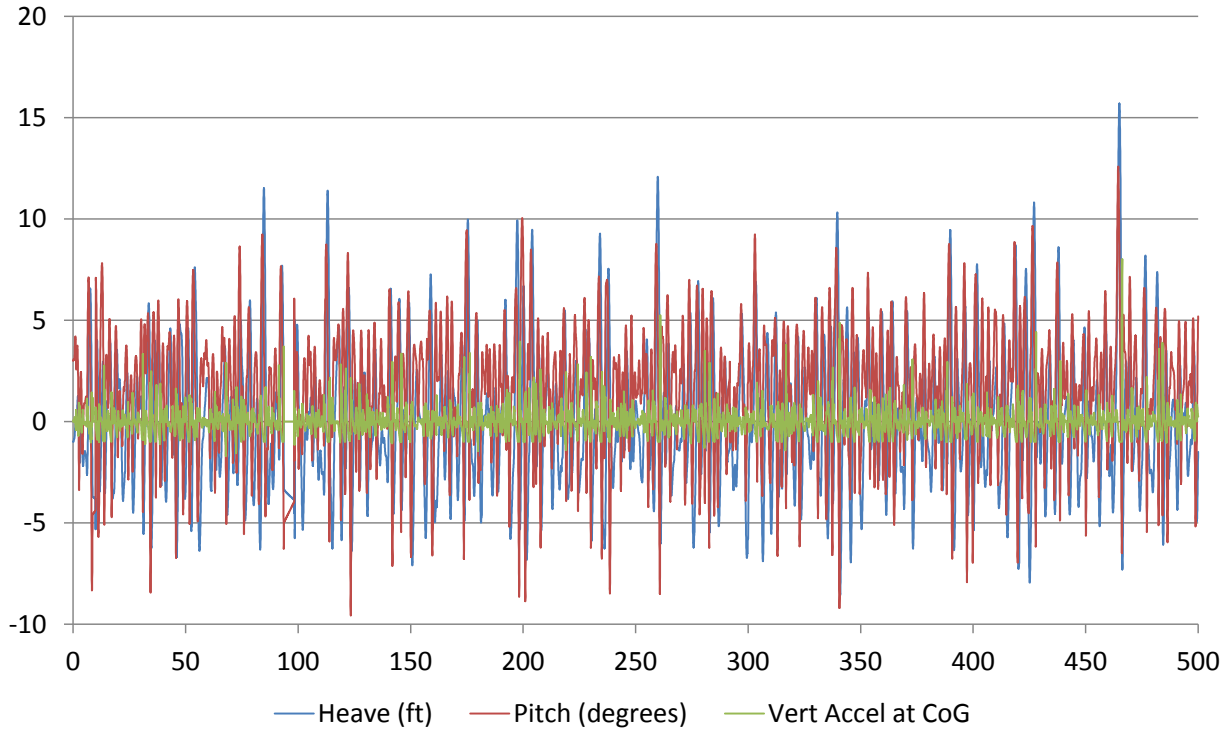

Figure 8 Time-domain simulation results for Patrol Boat, Vk=35 knots, Hsig=13 feet

The motion of the patrol boat is extreme, including an instance in which the boat stuffs into a wave completely submerging the keel and chine (simulation time = 97 seconds, Figure 9 and Figure 10). Further, there is at least one instance in which the boat is completely out of the water (simulation time=113 seconds, Figure 9 and Figure 10). In real life the coxswain would slow down well before these points, but they are included as extreme examples of the maximum loads that could cause structural failures.

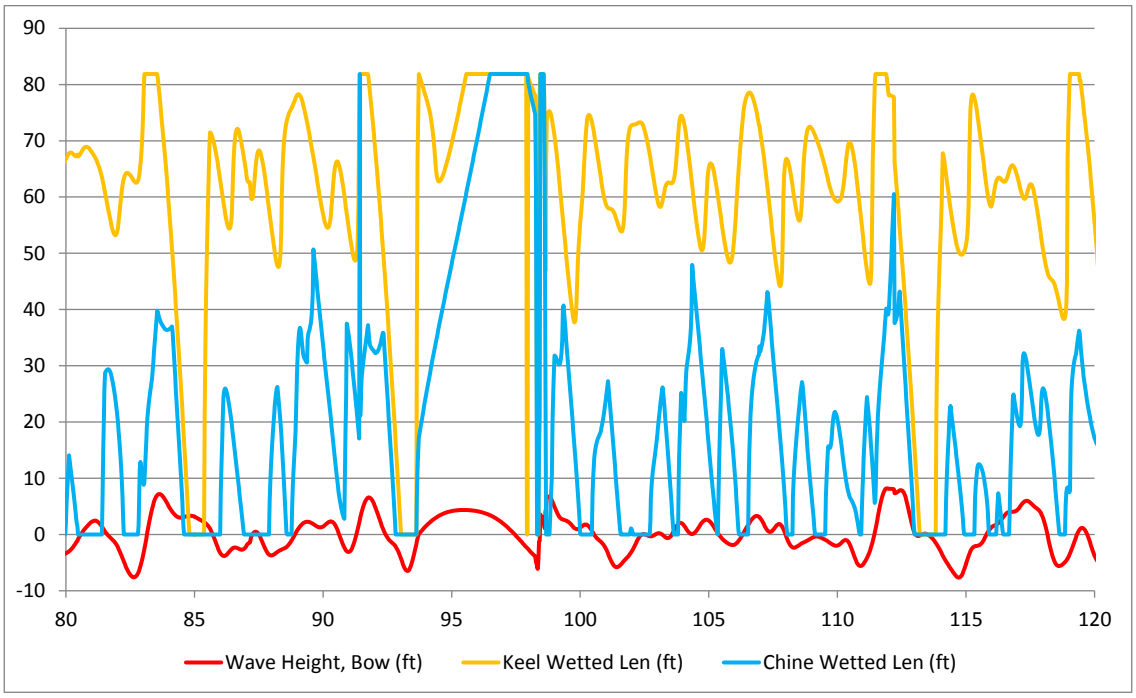

Figure 9 Chine and keel wetted lengths for Patrol Boat (Vk=13 knots, Hsig=13 feet)

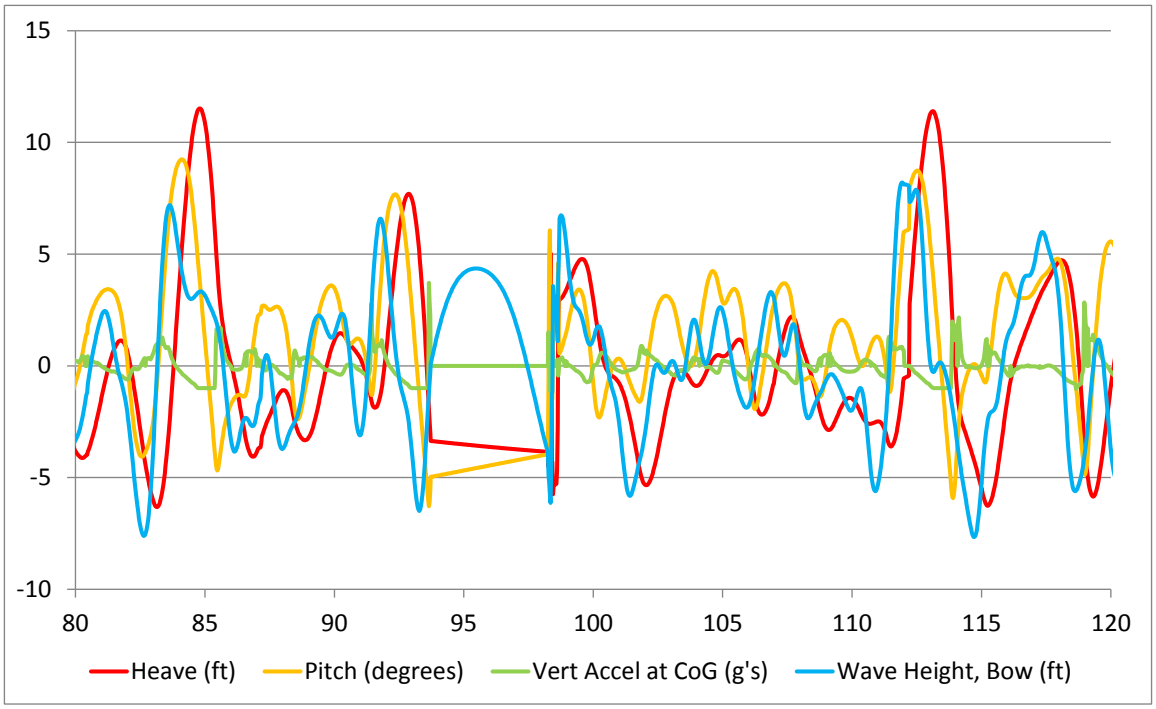

Figure 10 Heave, pitch and vertical acceleration motions for Patrol Boat (Vk=35 knots, Hsig=13 feet)

The instantaneous magnitudes and phase relationship between vertical accelerations at the center of gravity and the pitch acceleration determine the magnitude of the vertical accelerations at any point on the boat. Table 5 lists the accelerations observed during this simulation and Figure 11 shows the relationship

between longitudinal coordinates and observed accelerations. This figure can be compared with Figure 6 in Heller and Jasper (1960). It is important to balance the high accelerations expected in far forward and aft sections with the relatively lower bending moments created in the fore and aft regions as a result of these accelerations. The ABS HSC Rules address this with the vertical acceleration factor K_V.

Table 5 Maximum acceleration values at a range of longitudinal coordinates. All values at z=2.5 feet ABL.

Dist Abaft Bow (ft)	0	8.2	16.4	24.6	32.8	41	49.2	57.4	65.6	73.8	82
Min (g's)	-10.55	-8.88	-7.22	-5.56	-3.89	-2.23	-1.71	-5.88	-14.82	-23.75	-32.69
Ave (g's)	0.55	0.46	0.38	0.29	0.20	0.11	0.02	-0.06	-0.15	-0.24	-0.33
Max (g's)	56.66	47.72	38.79	29.85	20.92	11.99	7.45	9.12	10.80	12.47	14.14
St Dev (g's)	5.65	4.78	3.91	3.04	2.19	1.36	0.67	0.78	1.52	2.36	3.22

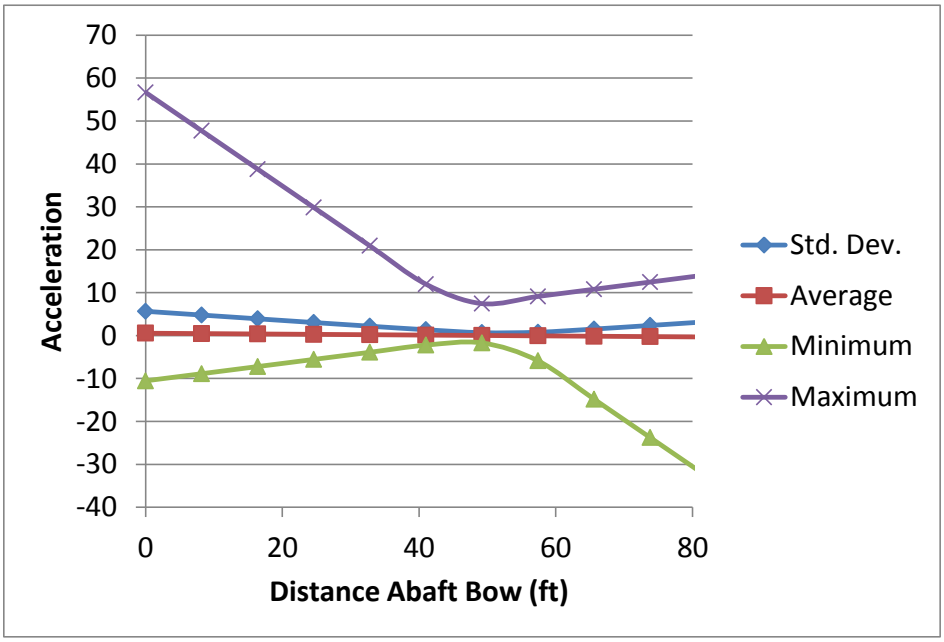

Figure 11 Vertical acceleration values predicted by simulation. Minimum accelerations are predicted at X=50 feet abaft the bow, near the longitudinal center of gravity.

Figure 12 and Figure 13 are a histogram and cumulative histogram respectively of the peak values of the sum of all of the sectional panel forces over the reference area A_R. The vertical line in Figure 12 represents the static weight of the patrol boat, 119,000 lbf.

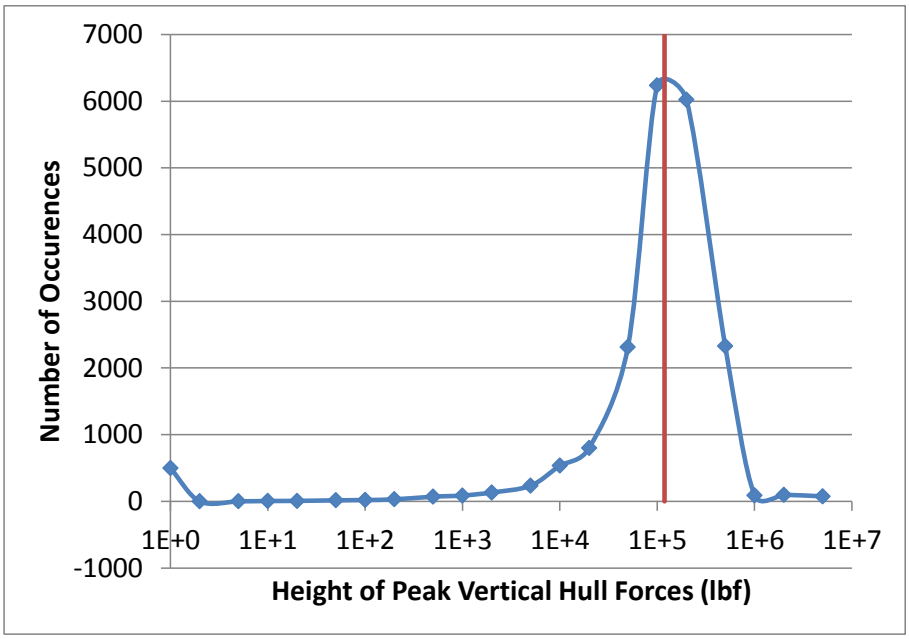

Figure 12 Peak values of effective hull pressure during 500 second simulation. Vertical line represents static weight of boat and cargo.

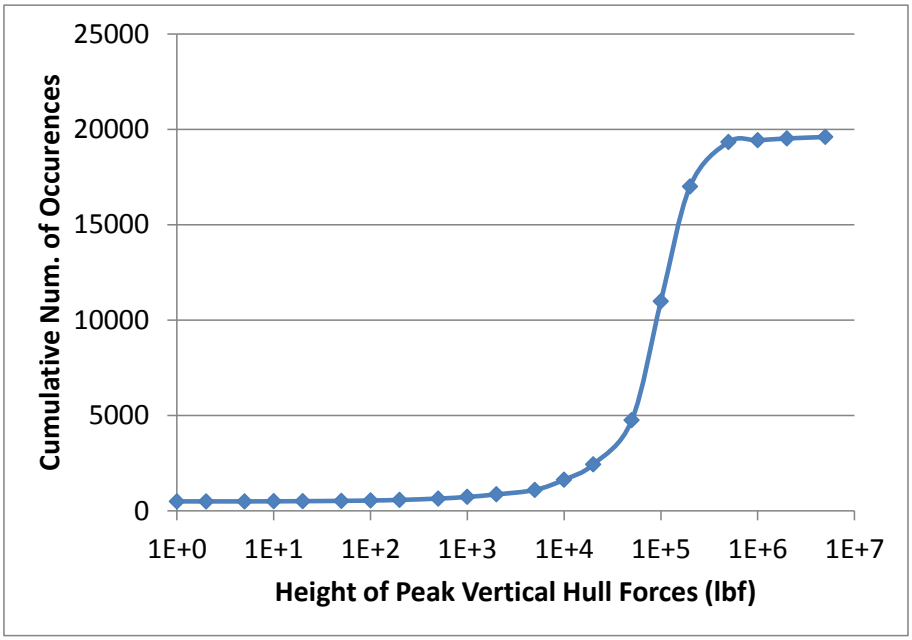

Figure 13 Cumulative values of peak "total vertical hull force" predicted by 500 second simulation.

3.1.1 Standard G

The high-speed boat community have developed and used many different definitions for acceleration amplitudes. To eliminate acceleration predictions based on numerical jitter rather than on physics, early versions of the Planing Simulator would calculate the standard deviation of a signal as the basis for a hysteresis filter. If the signal motion of a signal (e.g. vertical acceleration, pitch angle, etc.) exceeded the

hysteresis threshold the peak or trough was included in the output; otherwise it was discarded. While this was useful in eliminating numerical noise, it did not address the problems of tailoring the filter to match the application (structural versus human factors), of comparing data from one lab to another (choosing a filter type), and of documenting the steps in post-processed data.

As discussed in Riley (2010), and expanded in Zseleczky (2012), Riley (2012), and McCue (2012), a standardized method for time and amplitude filtering and threshold selection is required. The results of work by these authors is a procedure called "Standard G". This procedure filters the data with standardized analog filters, time filters it with a window based on the type of analysis, and threshold filters it with a value based on the standard deviation of the signal in question.

As pressure data has a strong relation to acceleration data, the same arguments apply to post-processing pressure data as to post processing acceleration data. Pressure data used in the remainder of this example was processed with the Standard G algorithm. The data was prefiltered with a 3-pole Butterworth filter with a cutoff frequency of 10 hz. The data was time-windowed with a span of 0.5 seconds, chosen based on intuition regarding the width of pulses that could damage structure. The data was threshold-filtered with the built-in standard deviation-based filter. A summary of the results is listed in Table 6

Table 6 Pressures predicted by Planing Simulator for Patrol Boat (Vk=35 knots, Hsig=13 ft, P-M Spectrum)

	Fore Panel		**Aft Panel**		**Entire Hull**	
	Large	**Small**	**Large**	**Small**		
Panel	**A**	**B**	**C**	**D**		
Area	35.9	8.99	36.3	9.07	1328	in^2
Num. Peaks	281	283	76	70	136	
Press. 1/100	2586.7	2241.6	N/A	N/A	3099.2	psi
Press. 1/10	949.8	816.1	2412.6	2204.7	763.5	psi
Press. 1/3	697.1	587.9	1267.6	1193.2	489.7	psi
Press Average	468.4	399.2	753.6	715.0	342.6	psi
Press, Max	3515.2	3039.7	7684.0	7323.7	3099.2	psi

3.1.2 Comparing Simulation to ABS High Speed Craft Rules

The ABS High Speed Craft Rules define the reference area A_R as:

A_R = reference area, cm2 (in2), 6.95Δ/d cm2 (1.61Δ/d in2)

Where Δ is the displacement of the boat in kg or lbf, and d is the stationary draft of the boat at X=1/2 of wetted keel length. From the AeroHydro (MultiSurf) hydrostatics analysis the draft d is 4.32 feet. Accordingly the reference area A_R is 3695.8 in^2 or 25.67 ft^2. Multiple definitions for AR can be defined from simulation as summarized in Table 7. There is a great discrepancy in planing hull area definitions. This work will use two values 308.0 ft^2 for ABS HSC Rule calculations and 807.7 ft^2 for Planing Simulator calculations.

Table 7 Reference area (hull area), calculated by ABS HSC rules and by simulation.

ABS Reference Area (3.2.2-1.1.3), A_R	44349.5	in^2
	308.0	ft^2
Planing Area bounded by chine/Transom (CAD)	1328.0	ft^2
Waterplane Area (CAD)	953.0	ft^2
Static Wetted Surface (CAD)	1087.0	ft^2
Planing Simulator Wetted Surface , Average	807.7	ft^2
Maximum	1321.9	ft^2

The design pressures for Panel A and Panel B (refer to Table 3) will be calculated using the ABS HSC rules and using the Planing Simulator panel pressure method. The results of these calculations are included here as Table 8 and Table 9.

Table 8 General design pressure calculations in ABS HSC Rules

Description	Symbol	Value	Units
Reference Area	AR	308	ft^2
Length Over All	L	82	ft
ABS HSC Constants	N1	0.069	
	N2	0.0016	
	N3	0.44	
Displacement	Δ	119000	lbf
Length on Waterline	Lw	60.3	ft
Beam on Waterline	Bw	17.5	ft
Static drat	d	4.32	ft
Significant Wave Height	H1/3	13	ft
Running Trim	τ	4	degrees
Deadrise at Center of Gravity	BetaCG	29	degrees
Boat Speed	V	35	knots
Wave Parameter	H	13.39	ft
Calc. Vert. Accel. At CoG	EtaCG	4.20	g's
Hydrostatic Design Pressure	Pd	5.67	psi

Table 9 Design pressure calculations for structural panels.

Panel Pressures from ABS HSC Rules						
	Panel	A	B	C	D	
		Fore Big	Fore Little	Aft Big	Aft Little	
X coord of center of panel, abaft bow	X Loc	36.4	36.4	63.8	63.8	
Design Area of Panel	AD	35.9	8.99	36.3	9.07	ft^2
Area Ratio	AD/AR	0.117	0.029	0.118	0.029	
Design Area Factor	FD	0.36	0.57	0.36	0.57	
Relative Long. Coordinate of Panel	% of LW	0.244	0.245	0.698	0.698	
Vertical Accel. Factor	FV	1	1	0.66	0.66	
Hydrodynamic Design Load	Pbxx	14.57	23.07	9.62	15.22	psi

Panel Pressures from Planing Simulator						
	Ave. of 1/100	15.57	17.96	N/A	N/A	
	Ave. of 1/10	5.67	6.60	15.31	16.75	psi
	Ave. 1/3	4.08	4.84	8.29	8.80	psi
	Average	2.77	3.25	4.97	5.23	psi
	Maximum	21.11	24.41	50.86	53.36	psi
	2*Pr_1/3	8.16	9.68	16.57	17.61	psi

Figure 14 is a comparison of the results of the two methods. A number of values can be chosen from the simulator results for comparison with the ABS HSC Rule results. For the aft panels a reasonably good match is found by comparing twice the significant panel pressures (2 times average of 1/3 highest pressures) with the results from the Rule.

There is a significant discrepancy between predicted structural pressures for the forward panels and pressures predicted by the ABS HSC Rules. This occurs because the quasistatic trim and heave of the boat is such that much of the time the panel is partially or completely out of the water (refer to Figure 15). This skews the effective pressures predicted by the Planing Simulator. On the other hand the ABS HSC Rule does not take this into account as it assumes small variations from the quasistatic trim and draft.

More research is required to determine which method is better and to determine whether the individual methods can be extended to recognize the non-linear transient behavior of the wetted surface of a high speed planing hull.

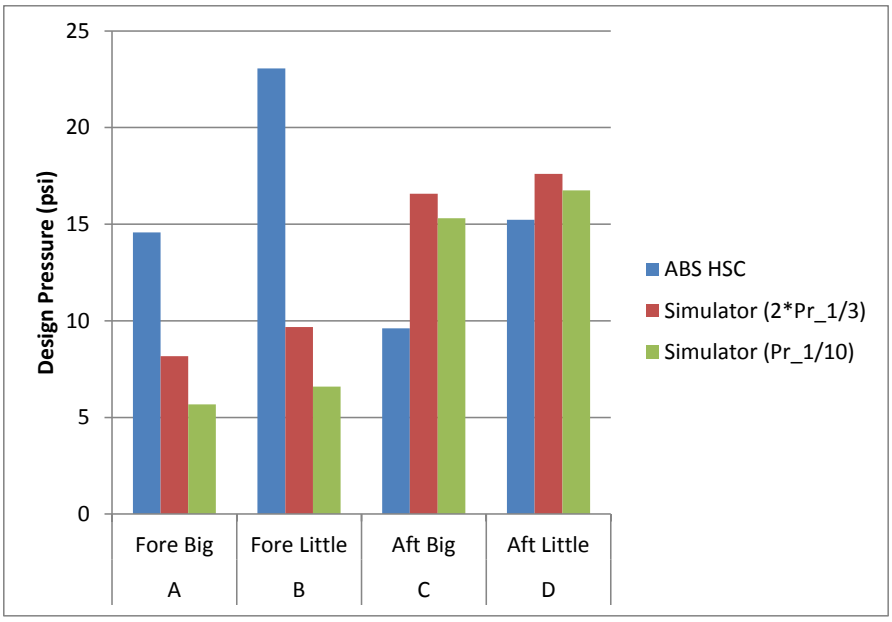

Figure 14 Structural panel pressures predicted by ABS HSC Rules and by Planing Simulator

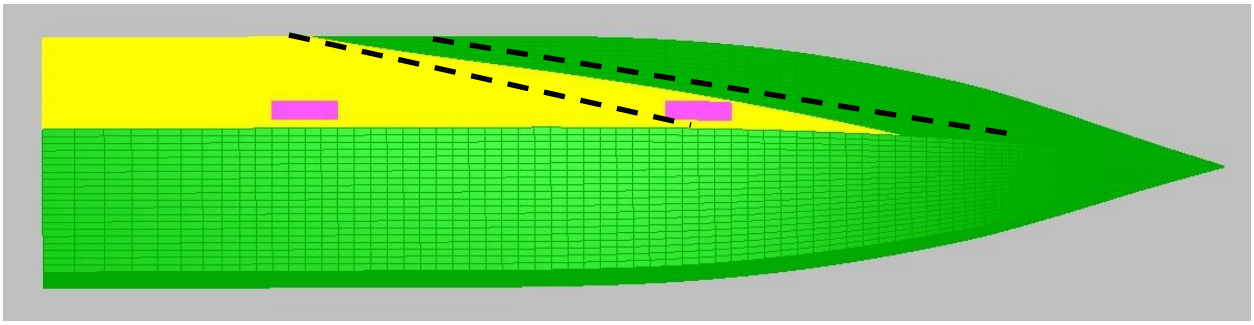

Figure 15 Wetted surface on Patrol Boat. Large yellow wedge (top, aft) represents starboard quasistatic wetted surface. Dashed lines show instantaneous variations in wetted surface.

4 VALIDATION

4.1 Test Case: Recreational Planing Boat

To test the ability of the modified version of the simulator to export accurate pressures, simulated results were compared with pressure measurements taken on a ski boat built by Hydrodyne Boat Company, in Fort Wayne, Indiana. The following description of the boat is quoted from Royce (2001).

> "[Hydrodyne Boat Company of Fort Wayne, IN] agreed to build a modified 21 ft. long competition ski boat solely for the purpose of gathering experimental data. The hull was made using a production mold and the modifications were limited to changes in the laminate schedule and outfitting of the boat.
>
> "Hydrodyne's standard construction consisted of a cored laminate schedule in which E-glass roving and cloth was used in conjunction with a balsa core. The balsa core was largely omitted in favor of a ¼ inch thick layer of chopped strand laminate, while the internal structure (longitudinal frames) remained unchanged. Additionally, no pigment was used in the protective gel coat layer which resulted in a translucent hull that aided in the visual identification of the wetted foot print from within the boat.
>
> "The hull was outfitted with 200 through-hull manometer taps in the port side bottom. During fitting out, the arrangements and floor-boards for the port half of the hull were excluded, allowing direct access to the manometer taps and an un-obscured view for the visual identification of the spray root location... The body plan view shows that the deadrise varies from 47 degrees at the bow to 10 degrees at the transom and a lifting strake at the chine runs the entire length of the planing surface."

The principle characteristics of the test boat are listed in Table 10. Photos of the boat and locations of the manometer pressure sensors are included as Figure 16 and Figure 17.

Table 10 Principal characteristics of Ski Boat.

LOA	20.5 ft.	Displacement	2780 lbs.
LWL	18.0 ft.	Chine Beam	5.7 ft.
LCG	6.5 ft.	Shaft Angle	15.8 degrees
VCG	1.4 ft.	Shaft Depth	1.0 ft.

Figure 16 Recreational Ski Boat. Translucent hull makes location of manometer taps visible in this view. Figure reproduced from Royce (2001).

Figure 17 Row of manometer taps in hull of Ski Boat. Figure reproduced from Royce (2001).

4.1.1 Geometric Model

The lines of the Ski Boat are shown in Figure 18 and Figure 19. These drawings were plotted from the offsets using Microsoft Excel. The bulges in the lines at the chine are artifacts of the plotting process, not the hull form itself. Figure 20 through Figure 22 show a 3D CAD model created in MultiSurf. In these figures the keel flat can be seen in the green hull bottom. The red surface is the chine flat. The MultiSurf CAD model was modified to meet the needs of the simulator, and then was exported as an IGES graphics file.

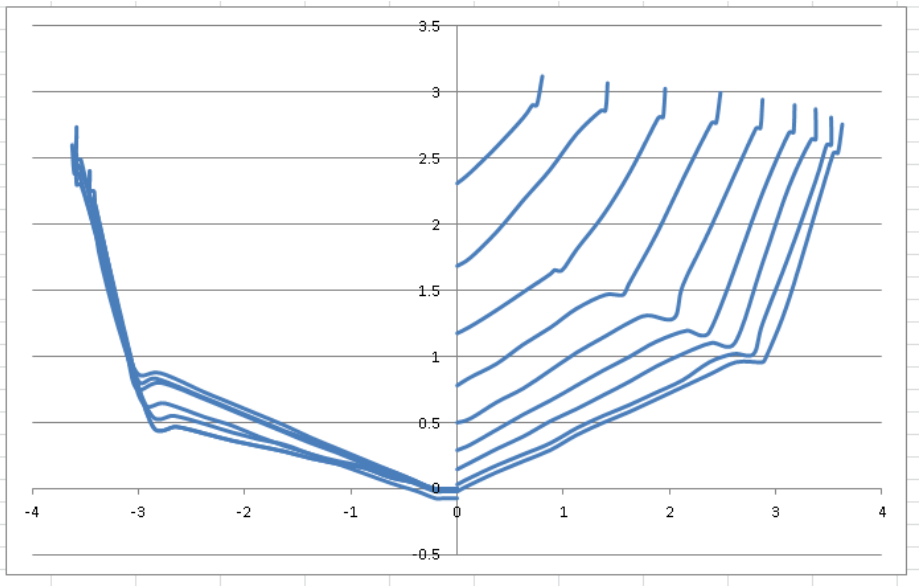

Figure 18 Body Plan lines for "Ski Boat"

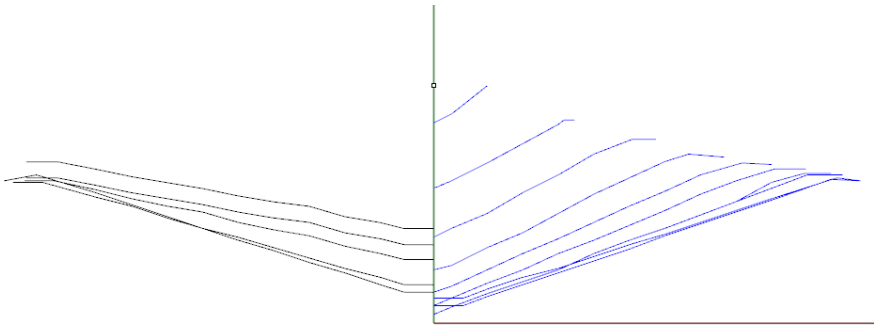

Figure 19 Submerged planing surfaces of Ski Boat

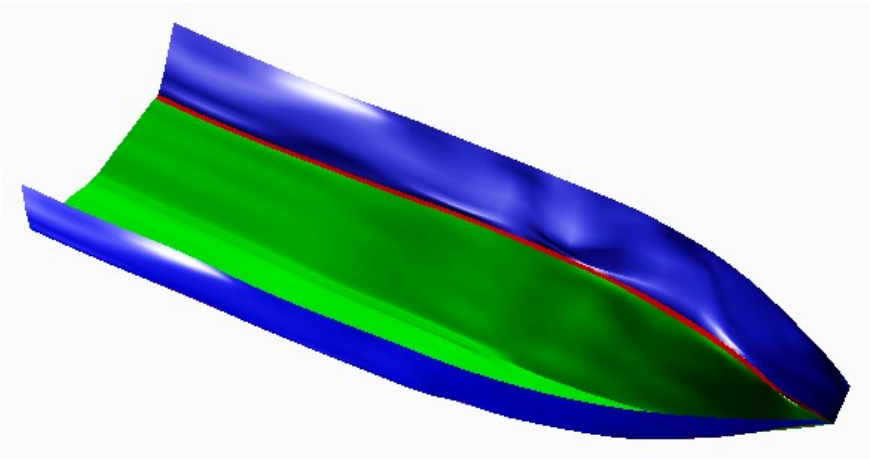

Figure 20 MultiSurf rendering of Ski Boat

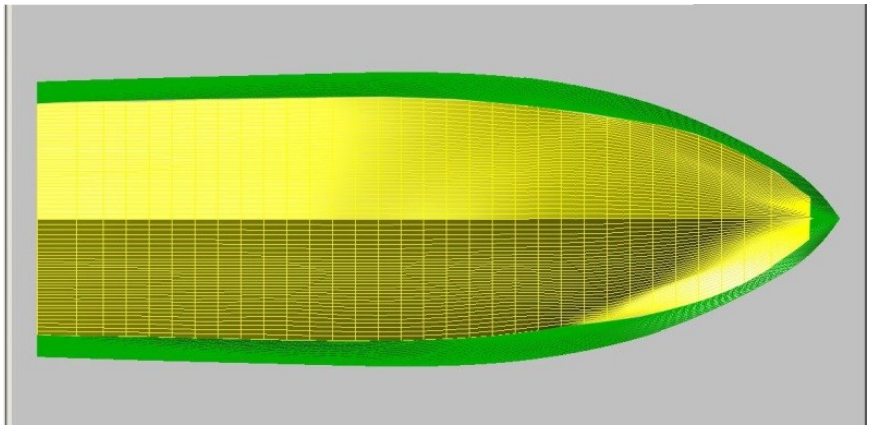

Figure 21 Rendering in plan view of model of Ski Boat. Outer, darker section represents the actual hull. Inner, lighter section is the subset of the hull modeled in the simulator.

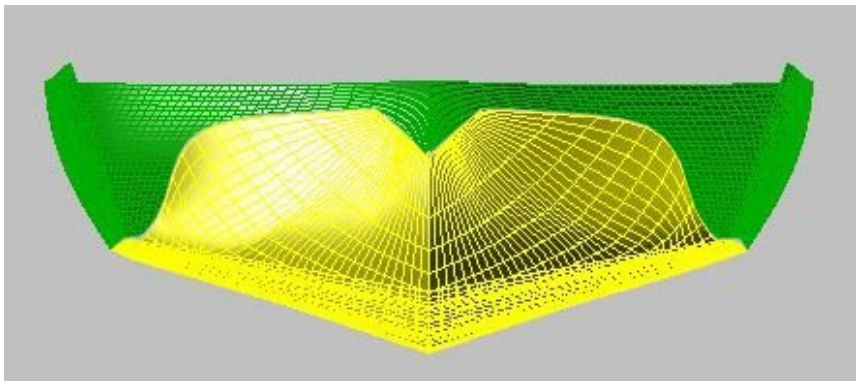

Figure 22 Rendering in bodyplan view of model of Ski Boat. The inner, lighter section is the simulator model showing the section of bow flare included in the model.

4.1.2 Test Program, Quasi-Static Results

To compare the results of the simulator-based pressure calculation with measured data, the Ski Boat model was simulated at a constant speed of 20 mph in fresh water with a fixed trim angle of 3.07 degrees. The model was loaded to a weight of 2,780 lbs. to match the Royce measurements. The model was allowed to be free in heave. The simulator predicted a slightly smaller draft than was reported by Royce, but this comparison is difficult because it was unclear exactly how the draft was measured on the real boat.

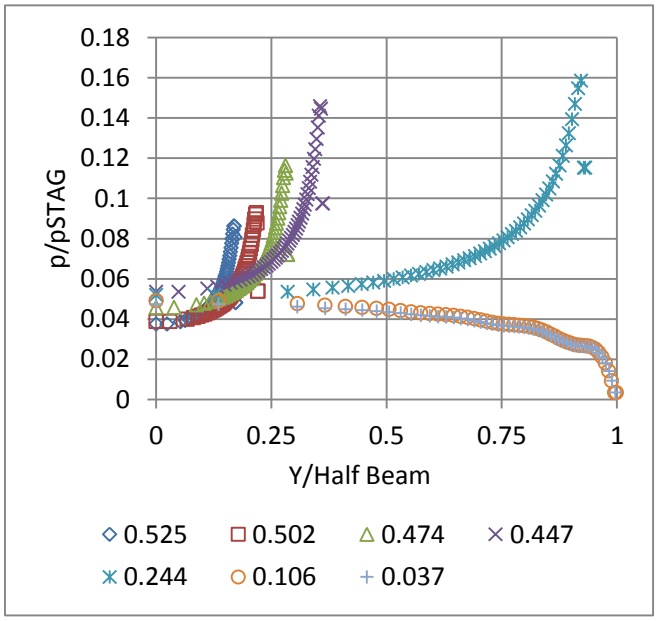

Figure 23 Transverse pressure distributions from simulation, scaled by wetted half beams and by the stagnation pressure. X coordinates of each distribution are scaled by LOA.

In Figure 23 through Figure 27 transverse coordinates Y are scaled by the individual sectional wetted beam, and pressure values are normalized by the stagnation pressure $\frac{1}{2}\rho V^2$. Since results from the simulator and the actual boat varied, individual scale factors varied slightly as well. The results indicate rather good correlation between predicted and measured pressures. Figure 23 illustrates some transverse

pressure distributions from the simulator analysis. Notice the pressure peaks towards the outer edge of the distributions in the chines-dry region and the tapering of distributions in the chines-wet region.

Figure 24 through Figure 27 compare the pressure distributions predicted by the time-domain simulator and measurements taken by Royce using the manometer bank in the Ski Boat. In each case the longitudinal coordinate of the pressure distributions is labeled as X' = X / LOA of the boat. Because the simulator predicted a slightly different draft than was measured, slightly different calculated and measured X' locations are used in these charts.

There is tremendous variation in the measured data, but some observations can be made from these figures.

- Overall, the shape of the calculated and measured pressure distributions is similar.
- Measured data indicates more of a longitudinal drop in the chines-wet region than is predicted by the simulator.
- Due to the difference in draft predictions the mean wetted length is slightly different between the simulated and measured boats.
- The chine flat and the keel flat were not modeled as severely as they are represented in the actual boat, so there may be differences in pressure distributions in the experimental data due to rapid change in transverse deadrise.

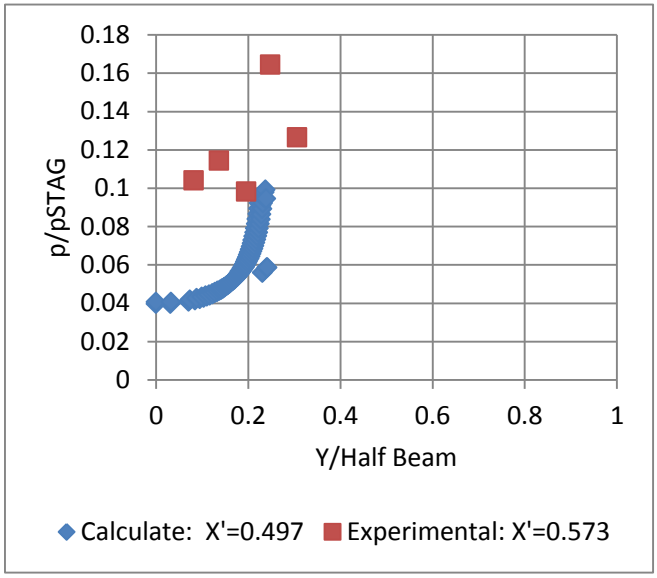

Figure 24 Measured and calculated transverse pressure distribution in forward chines-wet region. Scaled by wetted half beams and by the stagnation pressure.

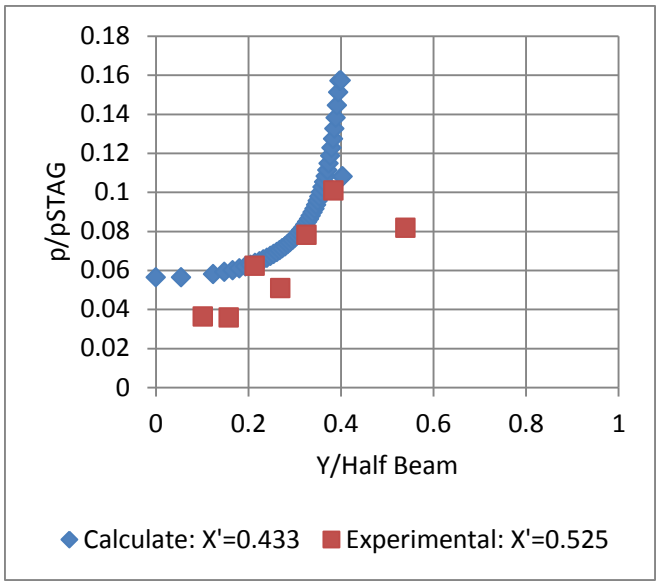

Figure 25 Measured and calculated transverse pressure distribution in chines-wet region. Scaled by wetted half beams and by the stagnation pressure.

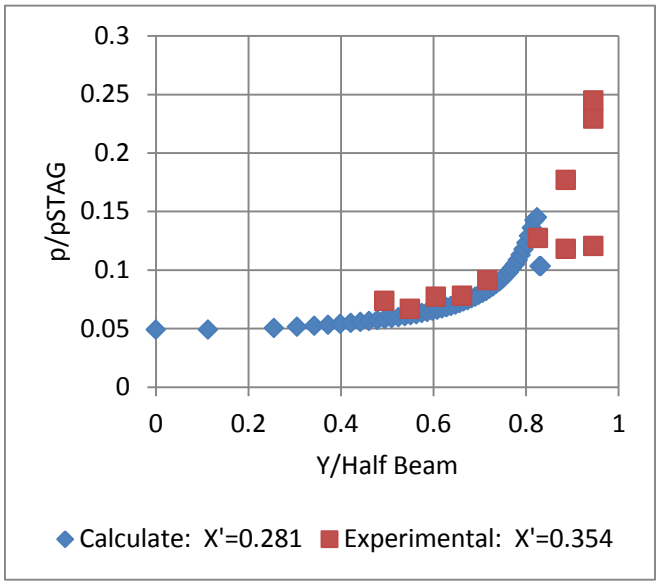

Figure 26 Measured and calculated transverse pressure distribution aftward in the chines-wet region. Scaled by wetted half beams and by the stagnation pressure.

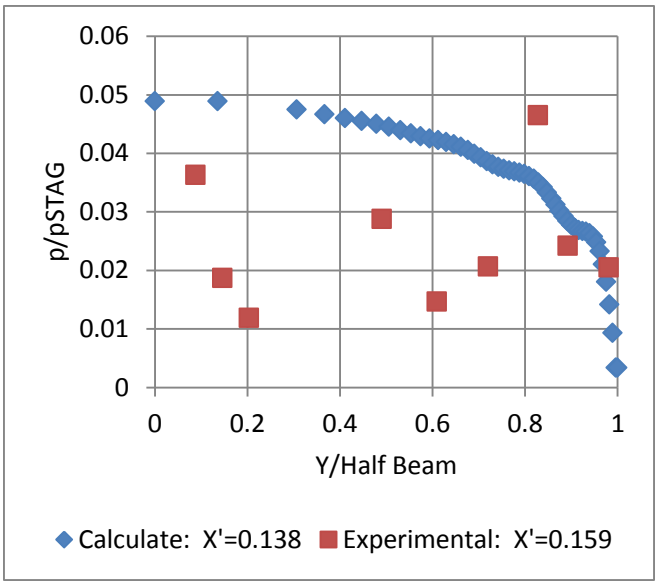

Figure 27 Measured and calculated transverse pressure distribution chines-dry region. Scaled by wetted half beams and by the stagnation pressure.

4.2 Test Case 2: Aluminum Fishing Boat

To reduce the risk in this project, while maintaining the validity of the results, MMC simplified the physical data collection phase by collecting strain gage data on an aluminum boat instead of pressure data on the same boat. This has three significant advantages over the pressure collection method.

1. Strain gage sensor technology has existed for many decades. Techniques for mounting strain gages, conditioning the data and interpreting the results are well established and well understood.
2. The original proposal did not specify the construction of the sample high-speed boat. It has been difficult to find a composite (FRP) boat suitable for this application, because the laminate schedule of the boat is critical for proper finite element analysis, but the laminate schedule is rarely available for a commercial vessel. Instead MMC has made arrangements to test an aluminum planing boat. Aluminum is isotropic and the panel thicknesses are easy to measure, so FEA results will not be encumbered by questionable assumptions about panel composition.
3. This approach was intended to test the entire design technique. Since the goal is to show that computer analysis can predict stress and strain in the hull, using strain gages to measure the hull arguably is a better validation system than using pressure sensors to measure hull pressure.

4.2.1 Case Study: Aluminum Fishing Boat

As a case study, the offsets were taken from an existing aluminum fishing boat built by Grumman (see Figure 28 and Figure 29).

Figure 28 Grumman aluminum fishing boat

The hull has formed transverse stiffeners, visible in Figure 29, that serve to limit the panel size in the hull. In addition to the transverse stiffeners, there are longitudinal strakes (not shown) in the forward sections. For purposes of this exercise, a section of panel was chosen that spans the distance uninterrupted from the keel to the formed chine.

A full 3D CAD model of the aluminum hull was created using the MultiSurf program (Figure 30). In this figure surfaces are rendered as semi-transparent so that the complete inner structure of the boat is visible. The goal of this study is to explore the stress imposed in this panel by the boat travelling over regular waves with a wavelength of about five boat lengths. From experience, that sea condition will cause the boat to exhibit large vertical motions, possibly launching and slamming depending on the size of the engine.

Figure 29 Structure of aluminum fishing boat. Transverse stiffeners are visible on the hull.

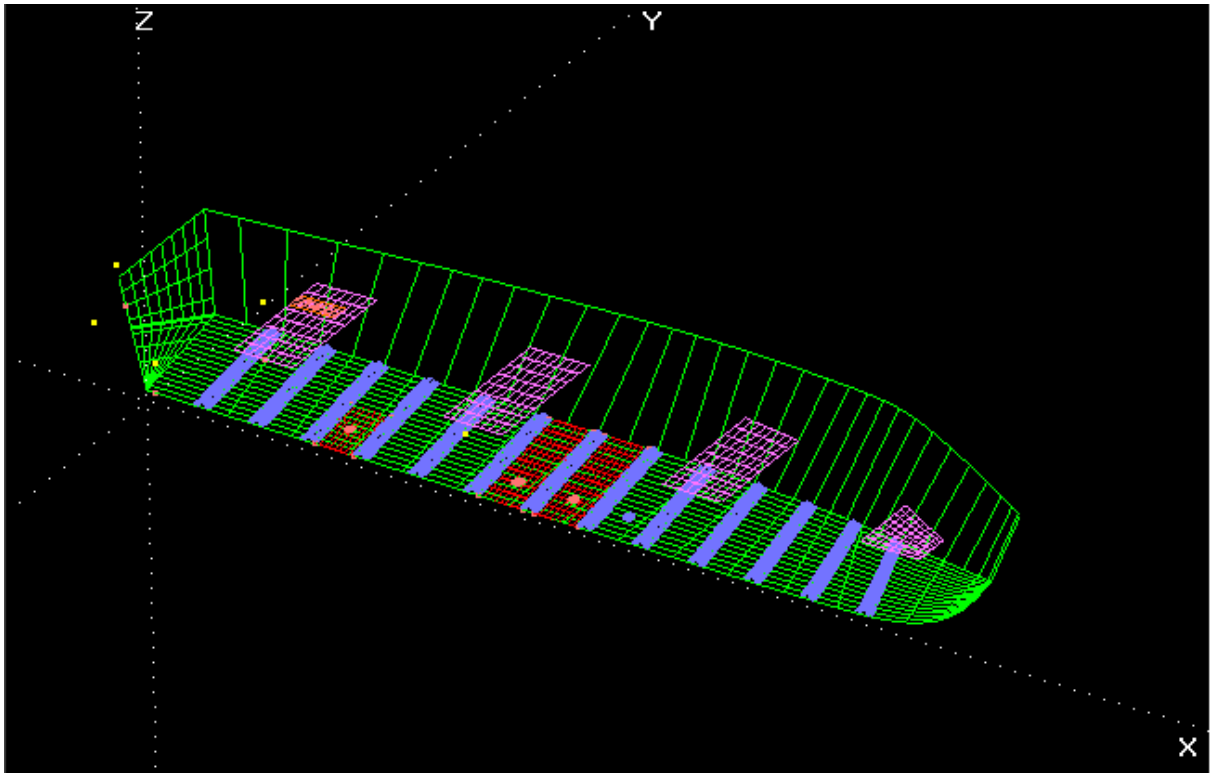

Figure 30 Wireframe model of Fishing Boat, built using offset measurements. Green surfaces are hull, side and transom. Magenta surfaces are seats. Cyan surfaces are ribs/stiffeners in hull bottom. Red surfaces in hull are panels that are structurally isolated for FEA. Bright red dots on hull show locations of strain gages.

For this case study, a single panel was selected from the hull bottom for analysis. This panel is circled in Figure 31.

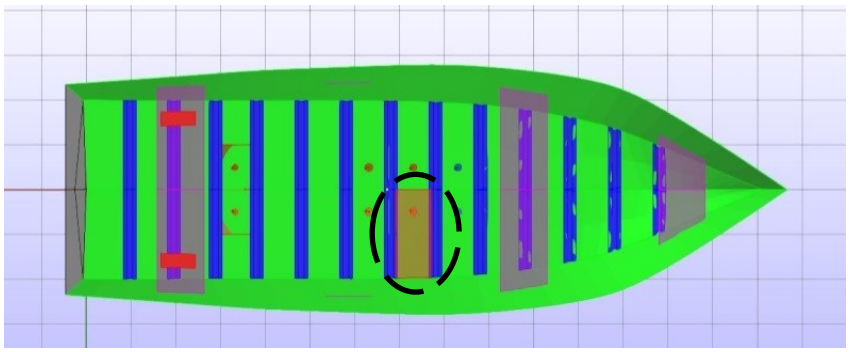

Figure 31 MultiSurf (3D CAD) model of aluminum Fishing Boat (third seat not shown). Test panel between aluminum transverse stiffeners is circled.

The exact dimensions of the test panel are given in Figure 32. As the test boat was on-loan it was not possible to cut into the hull to measure the hull plating thickness, nor was there historical documentation listing the hull plating thickness. For purposes of this analysis the plating was estimated to be 5.0 mm. The mechanical properties of the hull plating were assumed to be:

Young's Modulus	69 GPa (Aluminum)
Poisson ratio	0.333

The mesh created for that panel was created using a commercial meshing program, but is a regular matrix of 189 'S4' shell elements that could have been created by hand. The mesh is shown in Figure 47. The panel was modeled as being locked in all degrees of freedom on edge nodes, considered to be consistent with the structure in the hull.

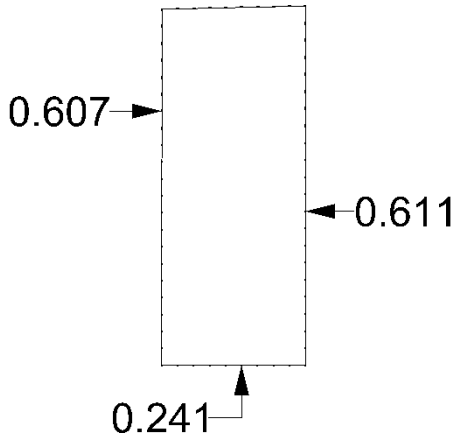

Figure 32 Test panel dimensions. The panel is not perfectly rectangular.

4.2.2 Simulation Results

The aluminum fishing boat was simulated at a constant speed of 14 knots operating in regular waves with a height (double amplitude) of 1.0 feet and a wavelength of 100 feet, about five boat lengths. The simulator predicted that the boat would perform as shown in Figure 33 and that the vertical accelerations at the center of gravity and the forward seat would be as shown in Figure 34. From the acceleration chart the boat never entirely launches out of the water because there is no protracted period with a constant -1 G acceleration. On the other hand, the boat does get subjected to some extreme loads as it pitches and heaves out of phase with the waves that it is encountering.

A set of hull pressures were calculated by the simulator at 0.1 second time steps starting at Time=7.0 seconds to Time=8.0 seconds. The hull pressures obtained from simulation using the method presented in this paper are shown Figure 35 through Figure 45.

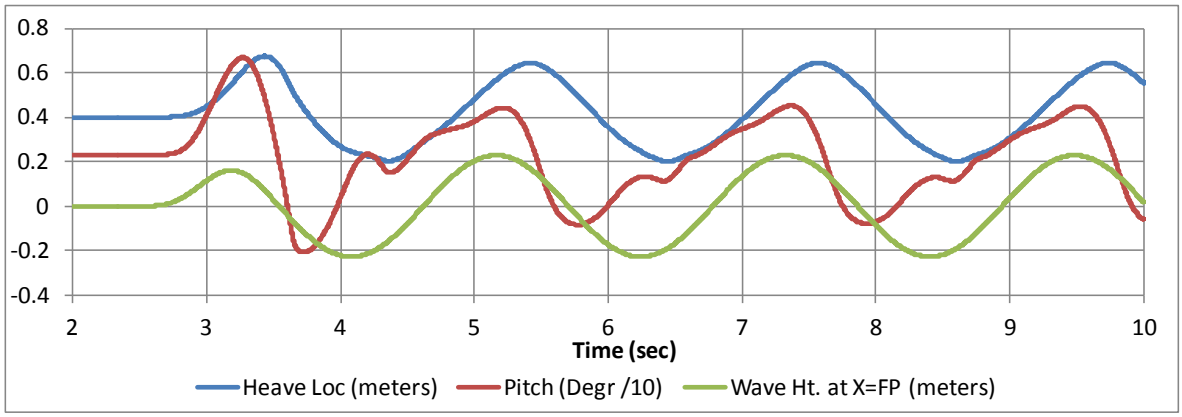

0

Figure 33 Motion of aluminum fishing boat in regular waves (height=1.0 feet, wavelength=100 feet) predicted by simulation.

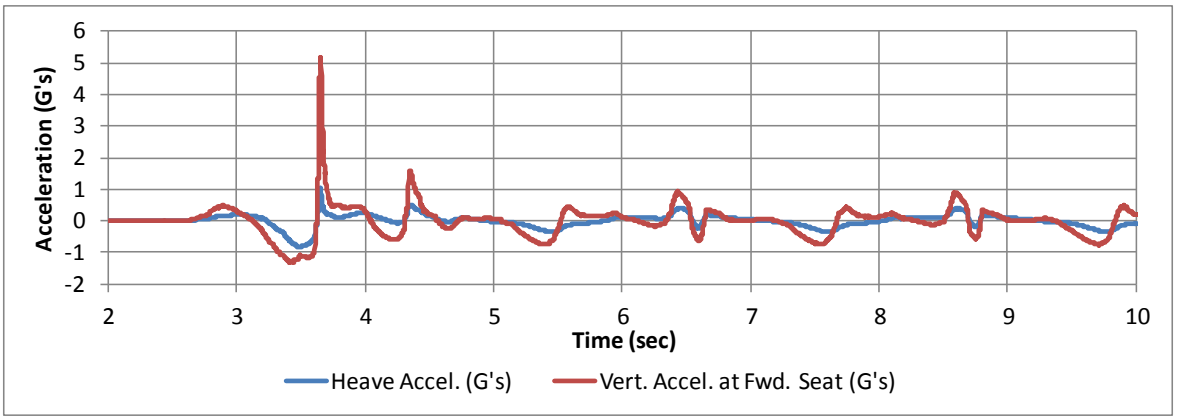

Figure 34 Accelerations on aluminum fishing boat predicted by simulation. Time series between 7 and 8 seconds were used for FEA.

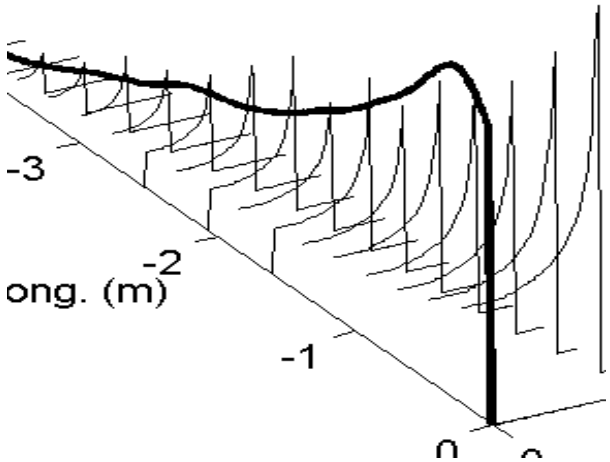

Figure 35 Trans. pressure distribution from sim., Time =7.0 sec

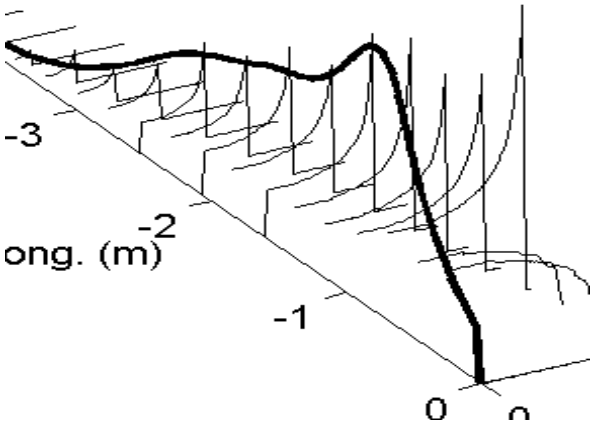

Figure 36 Trans. pressure distribution from sim., Time =7.1 sec

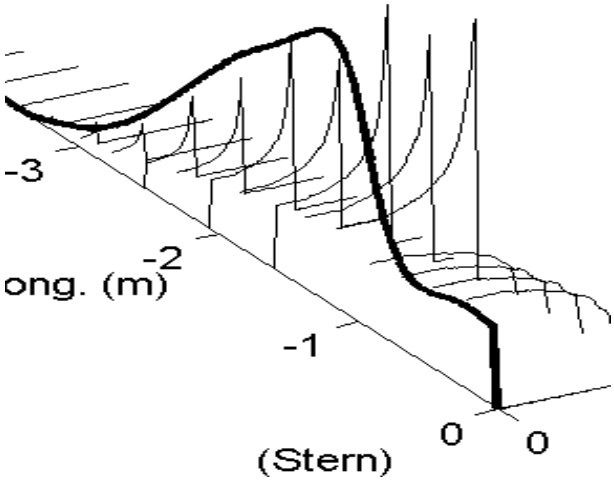

Figure 37 Trans. pressure distribution from simulation, Time =7.2 seconds

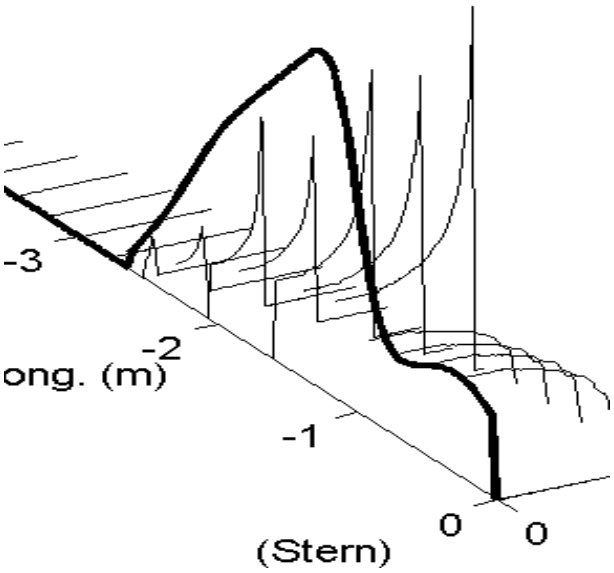

Figure 38 Trans. pressure distribution from simulation, Time =7.3 seconds

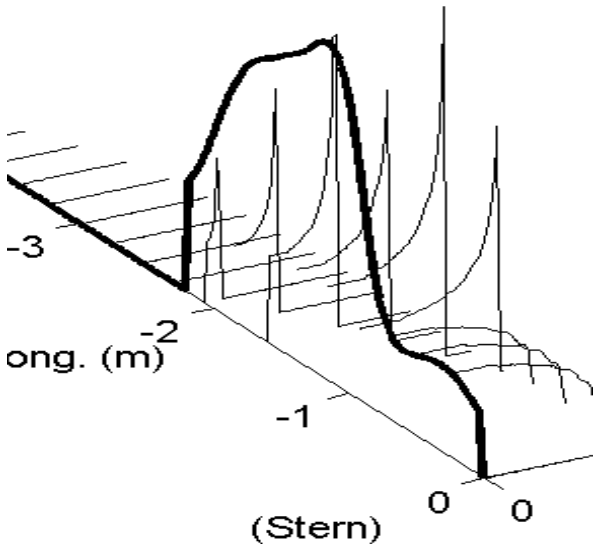

Figure 39 Trans. pressure distribution from simulation, Time =7.4 seconds

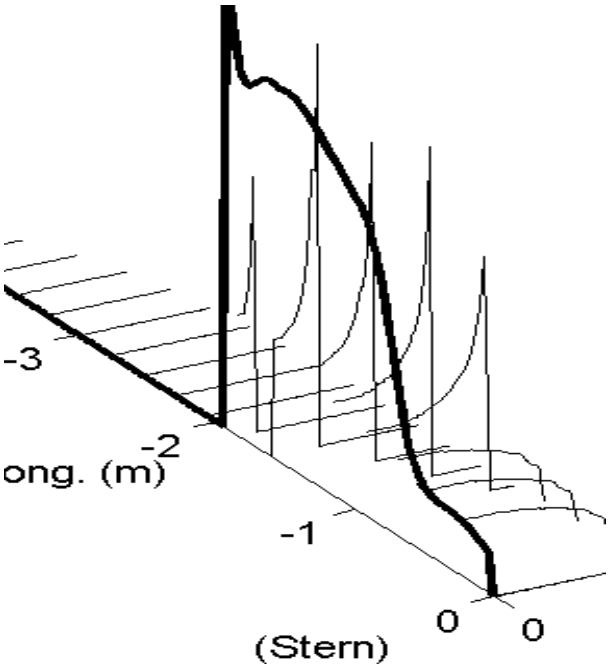

Figure 40 Trans. pressure distribution from simulation, Time =7.5 seconds

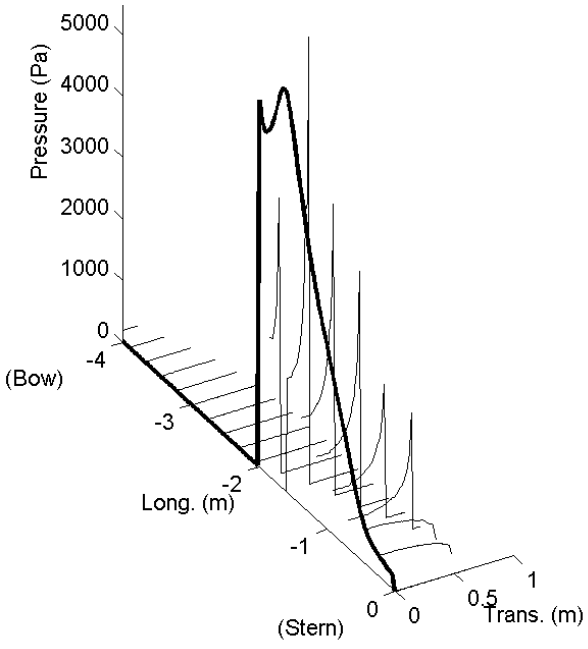

Figure 41 Trans. pressure distribution from simulation, Time =7.6 seconds

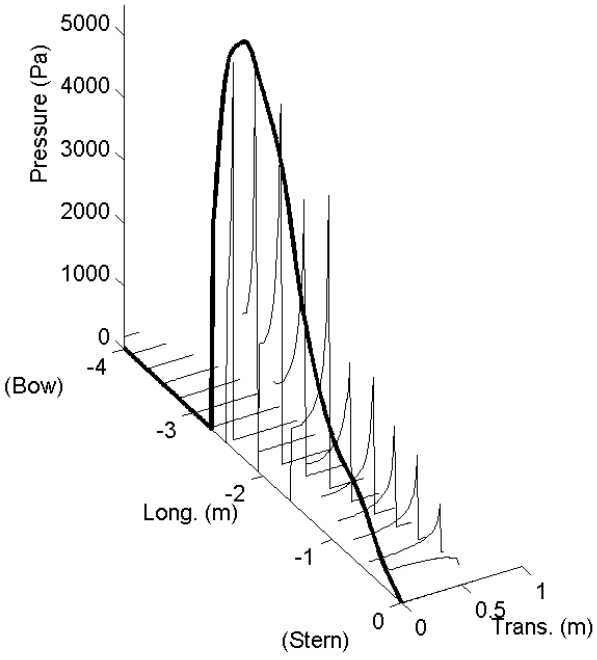

Figure 42 Trans. pressure distribution from simulation, Time =7.7 seconds

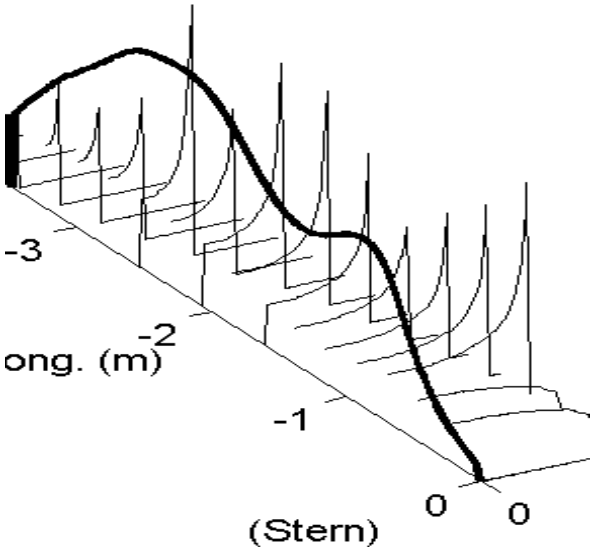

Figure 43 Trans. pressure distribution from simulation, Time =7.8 seconds

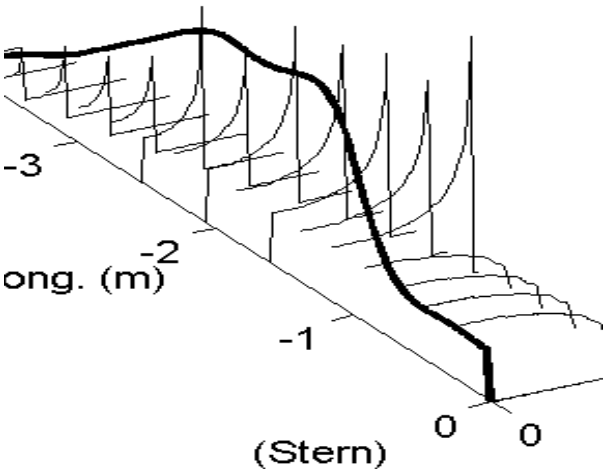

Figure 44 Trans. pressure distribution from simulation, Time =7.9 seconds

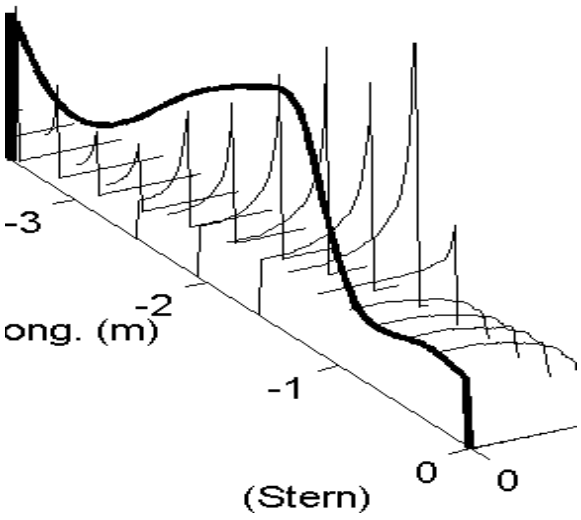

Figure 45 Trans. pressure distribution from simulation, Time =8.0 seconds

4.2.3 Finite Element Analysis

The original plan was to connect the Planing Simulator to a finite element tool using a "neutral file format" to be identified. MMC determined that there is no accepted industry-wide neutral file format. On the other hand, each vendor supports a proprietary, open text file format for input/output.

Accordingly the task of selecting a file format has changed to the task of selecting a target FEA system. The project team has demonstrated success with using a simple text format (comma-separated-variable format, "CSV") to provide supply pressure loads for use in FEA. The open source FEA program CalculiX (Wittig, 2013) was chosen for this case study. CalculiX input files are in Abacus text format, so an algorithm was developed to export panel pressures in Abacus format.

The mesh input for this program is in the same format as used by the commercial ABACUS program. Further, the open source program SALOME includes a meshing tool that can create and export an FEA mesh in ABACUS format. Figure 46 shows the progression of the hull from CAD model to SALOME/ABACUS/CalculiX mesh.

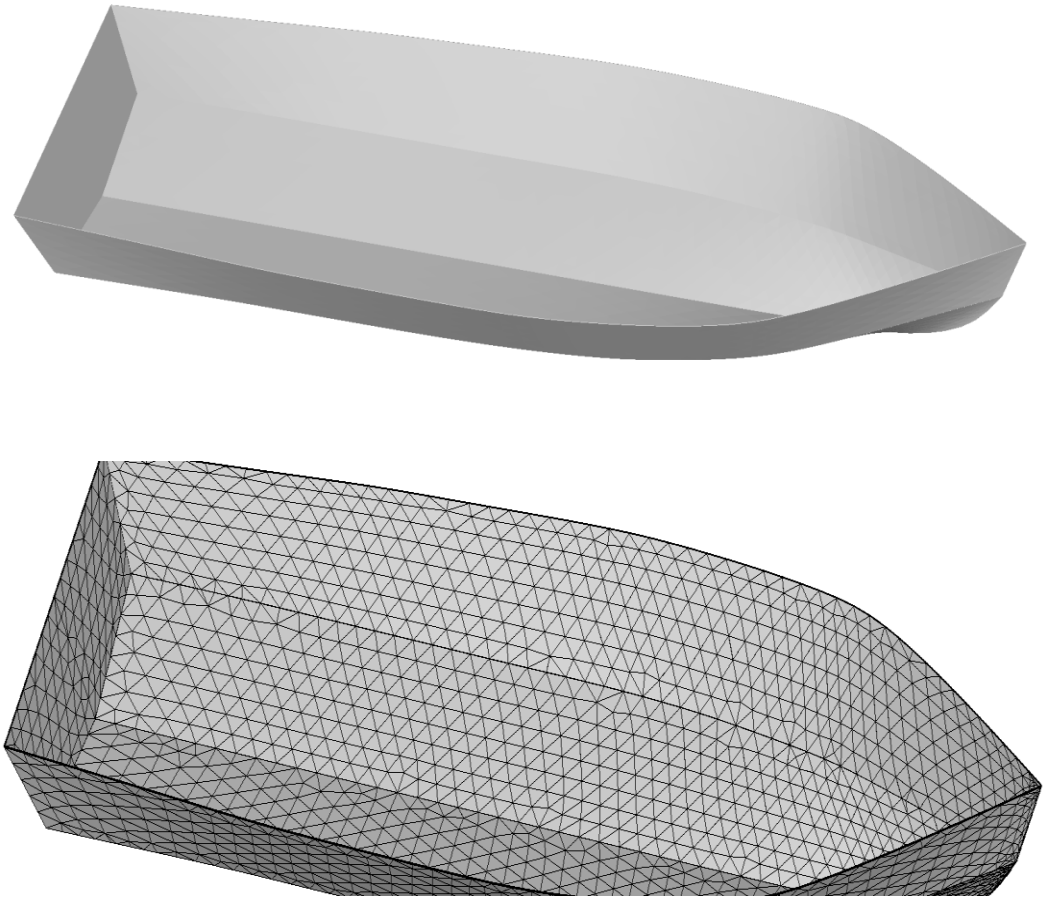

Figure 46 Outer hull of aluminum fishing boat. Meshing function in "Salome" used to crate ABAQUS shell elements (S3).

As discussed earlier, a hull panel suspended between stiffeners was chosen for finite element analysis. This panel is described by a subset of the entire CalculiX mesh (Figure 47).

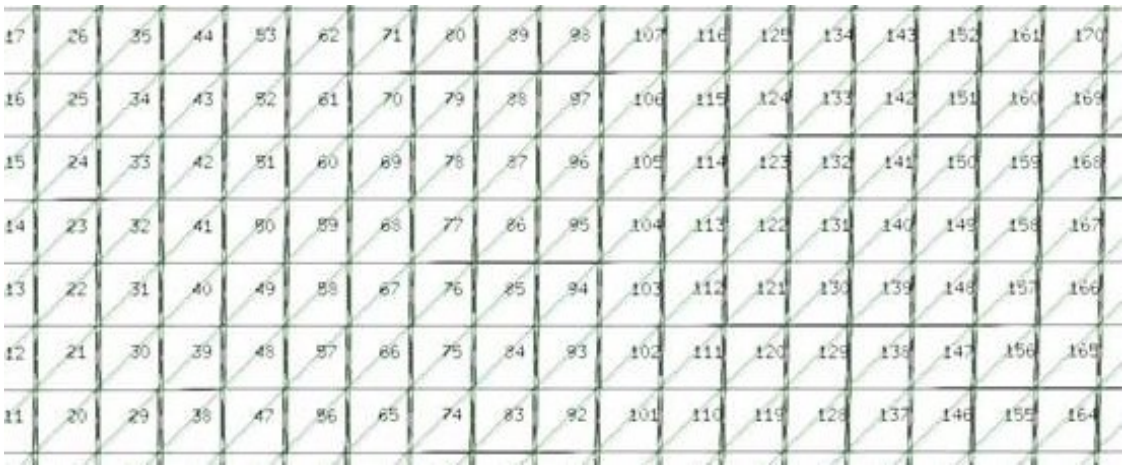

Figure 47 Mesh of fishing boat hull panel created using commercial meshing program.

Each hull pressure distribution was exported from the simulation program into a text file containing coordinate/pressure pairs. A load mapping program was used to interpolate between simulator vertices and FEA vertices. Finally the load mapping program was used to allocate pressure loads to the elements in the CalculiX model. The CalculiX FEA program was used to estimate the Von Mises stress in the aluminum hull panel. The results are included here as Figure 48 through Figure 56. In these figures the bow is on the left side of the panel and the stern on the right. At time 0.74 seconds the panel is barely wet, so the strain indicated by the FEA program is uniformly 0 except for a small point near the keel (see Figure 52). The panel is completely dry at time steps 7.5 and 7.6, so only one strain figure is included for this case (Figure 53).

The strain pattern shows relatively low, even strain when the boat is between waves. As the boat crosses a wave the wetted surface narrows and the pressure is concentrated near the keel, finally disappearing when the panel is dry. When the panel becomes wet at the next wave the high pressure from the chines-dry region of operation appears near the keel and then spreads out to cover the entire panel.

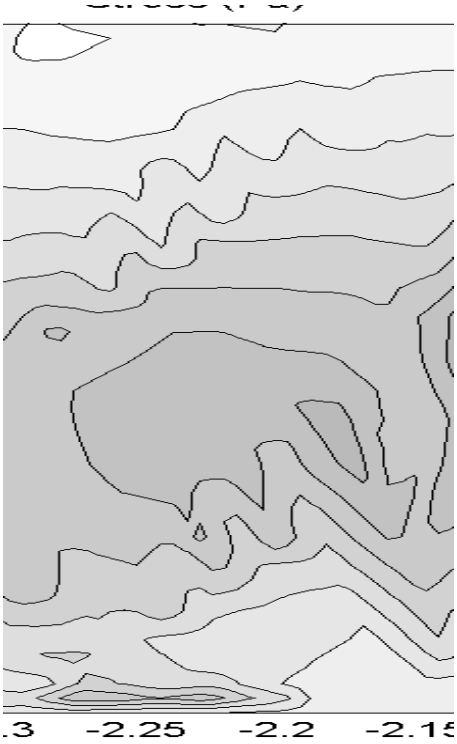

Figure 48 Stress in panel, Time=7.0

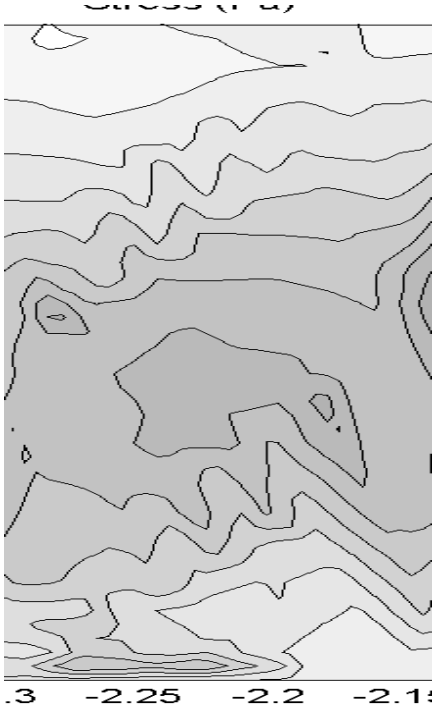

Figure 49 Stress in panel, Time=7.1

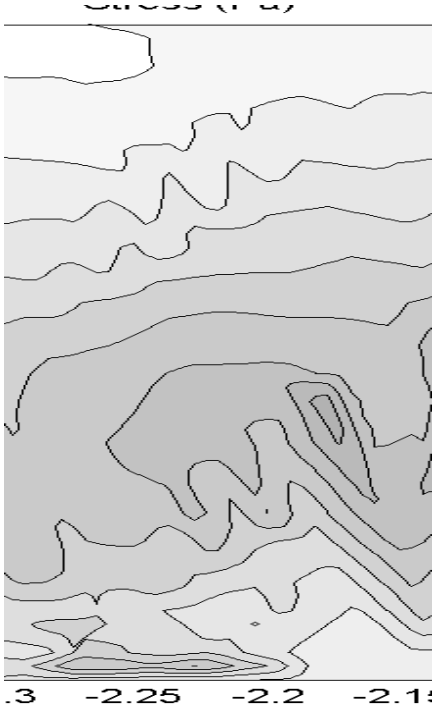

Figure 50 Stress in panel, Time=7.

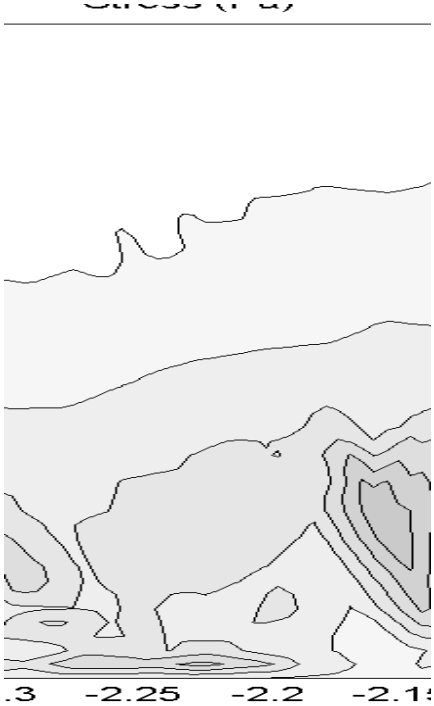

Figure 51 Stress in panel, Time=7.3

Figure 52 Stress in panel, Time=7.4-7.6

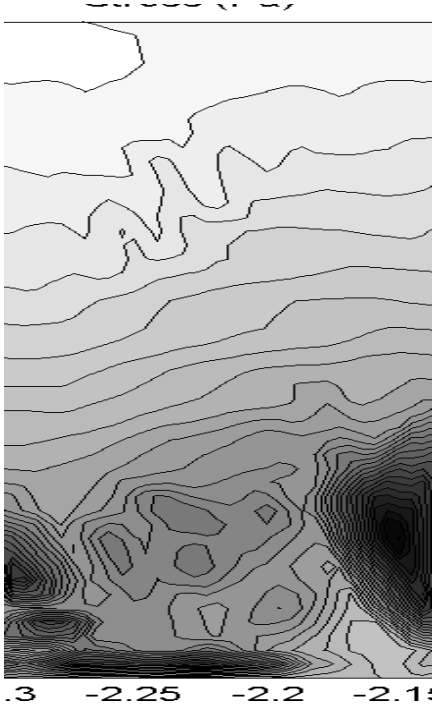

Figure 53 Stress in panel, Time=7.7

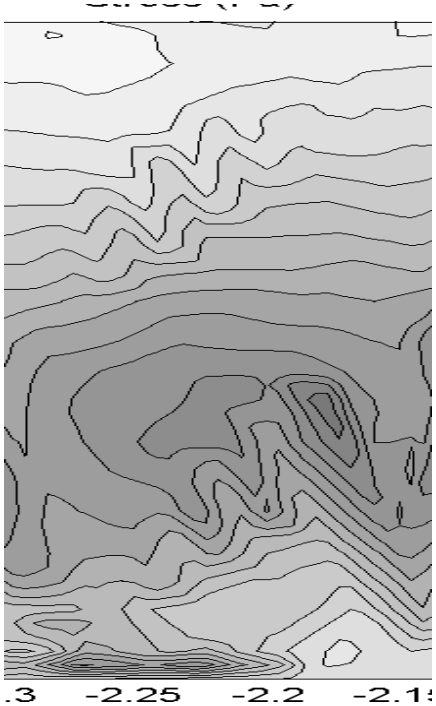

Figure 54 Stress in panel, Time=7.8

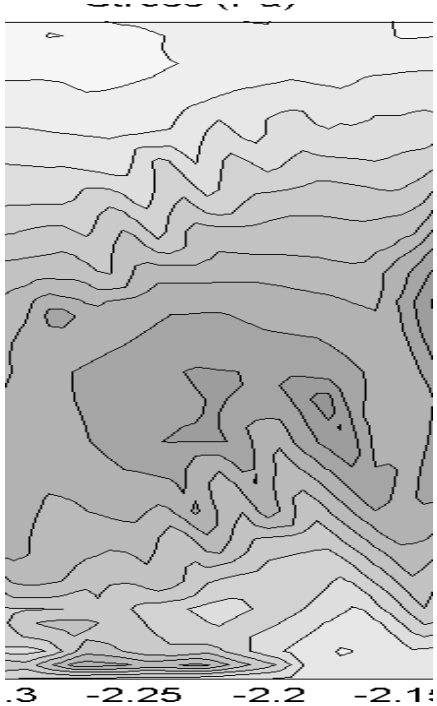

Figure 55 Stress in panel, Time=7.9

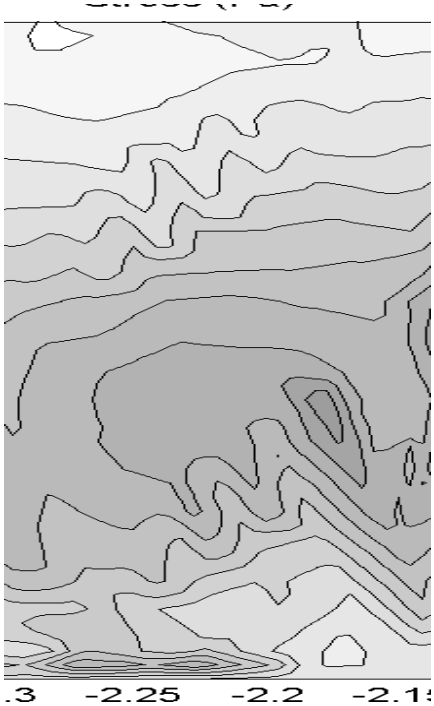

Figure 56 Stress in panel, Time=8.0

5 CONCLUSIONS

This work has shown that time-domain simulation can predict instantaneous and statistical design pressures on structural hull panels. Time-domain simulation results were validated by comparing motions and pressures measured on a Ski Boat with pressures predicted by the simulator. Structural loads were further validated, with some caveats, by comparing the design pressures predicted by the simulator with design pressures calculated using the ABS High Speed Craft rules.

Simulation affords the designer the opportunity to study the impact of a broad range of loading and operating conditions. The simulation model can be designed to reflect expected load conditions, outside the expected range of loads and centers of gravity expected by classification society rules. Further, simulation allows the designer to study the impact of extreme storm events, including wind, waves and even currents, and these conditions can be well outside the range of conditions codified in classification society rules.

Simulation allows the designer to consider the impact of hull geometry on structural loads. The simulator can account for longitudinal and transverse deadrise variations, thrust vectors from propulsors, loads from tabs and other ride control systems, and even the loads from towed bodies. Classification society rules must be somewhat broad to cover an entire class of boat, so they cannot account for the infinite range of possible designs.

Predicting structural panel pressures on planing hulls using time-domain simulation gives the designer a new way to optimize the material use and structure of their hull designs. By determining localized loads it is possible to shift material or the orientation of material to better handle stress. This has the dual advantage of lightening a boat, while better addressing structural challenges facing the boat.

6 RECOMMENDATIONS

While time-domain simulation of planing hulls has been shown to make useful predictions as to the motions and loads on a particular boat, there is still much to be done in this area.

Algorithms in planing simulators that calculate forces and force distributions need to be refined, taking into account three dimensional effects and geometric discontinuities such as strakes and spray rails. Further, these algorithms need to be extended to handle multi-physics coupling between flexible metal or composite hull panels and high pressure flow against and along these panels. As a panel warps response to a hydrodynamic load, the changing shape changes they hydrodynamic load.

Additional work should be done regarding panels that are partly or completely out of the water. It is possible that the classification society rules are overly conservative for these panels. On the other hand, a procedure should be developed that takes rare impacting events into account with respect to structural design pressures.

The meshing algorithms in the Planing Simulator employed in this work need additional work. The load mesh is recreated at every time step, which means that the level of effort required to map loads from the Planing Simulator to an FEA program is quite high. Geometric methods should be developed that streamline this process, especially since it is repeated at every time step.

From the standpoint of finite element analysis, the industry needs to establish a common data transfer file format. The industry is mature and there is little reason to maintain proprietary load file formats.

In the future much of this work will be accomplished using computational fluid dynamics (CFD). The industry would do well to anticipate this trend and to make sure that design tools and analysis tools are compatible. The designer should have a choice between tools and algorithms and not be limited by file formats, conventional design methodology, and software architecture.

7 REFERENCES

ABS (American Bureau of Shipping). *RULES FOR BUILDING AND CLASSING HIGH-SPEED NAVAL CRAFT*, American Bureau of Shipping, Houston, TX, 2013 (downloaded from "http://www.eagle.org" 12-Feb-2014).

ABS, Guidance Notes on 'Dynamic Load Approach' And Direct Analysis For High Speed Craft,' American Bureau of Shipping, Houston, Texas, February 2003.

(AeroHydro), MultiSurf 8.5 User's Manual, AeroHydro, Southwest Harbor, ME, 2013.

Akers, Richard H. "Dynamic Analysis of Planing Hulls in the Vertical Plane," Presented to Society of Naval Architects and Marine Engineers, New England Section, April 29, 1999a.

Akers, Richard H., Hoeckley, Stephen A., Peterson, Ronald S., and Troesch, Armin W. "Predicted vs. MeasuredVertical-Plane Dynamics of a Planing Boat," *5th Int. Conf. on Fast Sea Transportation FAST*, 1999b.

Allen, R. G. and Jones, R. R. "A Simplified Method ofr Determining Structural Design-Limit Pressures on High Performance marine Vehicles," AIAA/SNAME Advanced Marine Vehicles Conf., San Diego, CA, April 1978.

Autodesk, "AutoCAD Services & Support, DXF Reference," http://usa.autodesk.com/adsk/servlet/item?linkID=10809853&id=12272454&siteID=123112, Accessed Feb. 2013.

Broglia, R., A. Iafrati, A. "Hydrodynamics of Planing Hulls in Asymmetric Conditions," *28th Symposium on Naval Hydrodynamics*, Pasadena, California, 12-17 September 2010.

Ensign, W., Hodgdon, J. A., Prusaczyk, W. K., Shapiro, D., and Lipton, M. "A Survey of Self-Reported Injuries among Special Boat Operators," Report No. 00-48, Naval Health Research Center, San Diego, CA, Nov. 2000.

Fridsma, Gerard. *A Systematic study of the Rough Water Performance of Planing Boats (Irregular Waves -- Part II)*. Report 11495, Davidson Laboratory, Stevens Institute of Technology, Hoboken, New Jersey, 1971.

Garme K. *Time-domain model for high-speed vessels in head seas [Thesis]*. KTH, Department of Vehicle Engineering; 2000.

Heller, S. R. Jr., and Jasper, N. H. "On the Structural Design of Planing Craft," *Quarterly Transactions of the Royal Institution of Naval Architects*, July, 1960.

IGES, *Initial Graphics Exchange Specification, IGES 5.3*, U.S. Product Data Association, N. Charleston, SC, 1997.

IGES/PDES Organization (September 23, 1996), Initial Graphics Exchange Specification: IGES 5.3, N. Charleston, SC: U.S. Product Data Association, "Formerly an ANSI Standard September 23, 1996 – September 2006".

Jones, R. R. and Allen R. G. *A Semiempirical Computerized Method for Predicting Three-Dimensional Hull-Water Impact Pressure Distributions and Forces on High-Performance Hulls*, Report 4005, Naval Ship Research and Development Center, Bethesda, MD, December 1972.

Kapryan, W. J., Boyd, Jr., G. M. *Hydrodynamic Pressure Distributions Obtained During a Planing Investigation of Five Related Prismatic Surfaces*, National Advisory Committee For Aeronautics, Technical Note 3477, Langley Aeronautical Laboratory, Langley Field, VA, September 1955.

Koelbel, J. G. Jr. "Comments on the Structural Design of High Speed Craft," *Marine Technology*, Vol. 32, No. 2. Soc. of Naval Architects and Marine Engineers, April 1995.

Korvin-Kroukovsky, B. V., and Chabrow, Faye R.: The Discontinuous Fluid Flow past an Immersed Wedge. Preprint No. 169, S.M.F. Fund Paper, Inst. Aero. Sci. (Rep. No. 334, Project No. NR 062-012, ONR, Exp. Towing Tank, Stevens Inst. Tech.), Oct. 1948.

Lasdon, Leon S., Richard L. Fox, and Margery W. Ratner. *Nonlinear Optimization Using the Generalized Reduced Gradient Method*. No. TM-325. Case Western Reserve University, Cleveland, OH. Dept. of Operations Research, 1973.

Martin, M., Theoretical Predictions of Motions of High-Speed Planing Boats in Waves. David W. Taylor Naval Ship Research and Development Center, DTNSRDC#76/0069, 1976.

McCue, L., Jacobson, D., Weil, C., Zeleczky, J. "A Look at the Impact of Filter Selection on Characterization of Vertical Acceleration Peaks," Third Annual Chesapeake Power Boat Symposium, Annapolis, MD, June 2012.

Pierson, John D.: On the Pressure Distribution for a Wedge Penetrating a Fluid Surface. Preprint No. 167, S.M.F. Fund Paper, Inst. Aero. Sci. (Rep. No. 336, Project No. NR 062-012, ONR. Exp. Towing Tank, Stevens Inst. Tech.), June 1948.

Pierson, John D., and Leshnover, Samuel: A Study of the Flow, Pressures, and Loads Pertaining to Prismatic Vee-Planing Surfaces. S.M.F. Fund Paper No. FF-2, Inst. Aero. Sci. (Rep. No. 382, Project No. NR 062-012, ONR Exp. Towing Tank, Stevens Inst. Tech.), May 1950.

Riley, M. R., Haupt, K. D., Jacobson, D. R., "A Generalized Approach and Interim Criteria for Computing A1/n Accelerations Using Full-Scale High-Speed Craft Trials Data," Naval Surface Warfare Center Carderock Division Report NSWCCD-23-TM-2010/13, April 2010.

Riley, M. R. and Coats, T. W., "A Simplified Approach for Analyzing Accelerations Induced by Wave-Impacts in High-Speed Planing Craft, "Third Annual Chesapeake Power Boat Symposium, Annapolis, MD, June 2012.

Rosén, A. "Loads and Responses for Planing Craft in Waves", PhD Thesis, TRITA-AVE 2004:47, ISBN 91-7283-936-8, Division of Naval Systems, KTH, Stockholm, Sweden, 2004.

Royce, Richard. Thesis: "2-D Impact Theory Extended to Planing Craft with Experimental Comparisons," University of Michigan, August 2001.

Savander, B. R., Scorpio, S. M., And Taylor, R. K. "Steady Hydrodynamic Analysis of Planing Surfaces," SNAME, *Journal of Ship Research*, Vol. 46, No. 4, 2002.

Savitsky, D. "Hydrodynamic Design of Planing Hulls," *Marine Technology*, 1, 1, pp. 71-95, 1964.

Shuford, Charles L., Jr., "A Theoretical and Experimental Study of Planing Surfaces Including Effects of Cross Section and Plan Form," NACA Report-1355; 1958.

Smiley, Robert F.: A Semiempirical Procedure for Computing the Water Pressure Distribution on Flat and V-Bottom Prismatic Surfaces During Impact Or Planing. NACA TN 2583, Langley Aeronautical Laboratory, Washington, DC, December 1951.

Spencer, John. "Structural Design of Crewboats," *Marine Technology*, 12, 3, pp. 267-274, 1975.

Stone, Kevin F., P.E. *Comparative Structural Requirements for High Speed Craft*, Report Number SSC-439, Ship Structure Committee, Washington, DC, February 2005.

Tveitnes, T., Fairlie-Clarke, A.C. and Varyani, K. "An experimental investigation into the constant velocity water entry of wedge-shaped sections," *Ocean Engineering*, 35:14-15, 1463-1478, 2008.

USCG. Structural Plan Review Guidelines for Aluminum Small Passenger Vessel, Navigation and Vessel Inspection Circular No. 11-80. U. S. Coast Guard, Washington, D.C., 1980.

Von Karman, T., *The Impact on Seaplane Floats during Landing,"* National Advisory Committee for Aeronautics (NACA), TN-321, Washington, DC, 1929.

Vorus, William S., "A Flat Cylinder Theory for Vessel Impact and Steady Planing Resistance". *Journal of Ship Research*, Vol. 40(2), pp 89-106, 1996.

Wagner H., Uber Stoss-und Gleitvorgange an der Oberflache von Flussigkeiten. Z. angew. Math. Mech.;12(4):193–215, 1932.

Whalen, T. E., Optimal Deadrise Hull Analysis and Design Space Study of Naval Special Warfare High Speed Planing Boats, MS Thesis, Massachusetts Inst. of Tech., June 2002.

Wittig, Klaus; *CalculiX USER'S MANUAL*, Version 2.6, July 6, 2013, [downloaded from http://www.dhondt.de/cgx_2.6.1.pdf, 26-Jan-2014].

Zarnick, Ernest E. "A Nonlinear Mathematical Model of Motions of a Planing Boat in Regular Waves". David W. Taylor Naval Ship R & D Center, DTNSRDC-78/032, 1978.

Zhao, R., Faltinsen, O.M., "Water entry of two-dimensional bodies," J. Fluid Mech., Vol. 246, pp. 593–612, 1993.

Zhao, R., Faltinsen, O.M., Aarsnes, J.V. "Water entry of arbitrary two-dimensional sections with and without flow separation," 21st Symposium on Naval Hydrodynamics, 1996.

John Zseleczky, "Behind the Scenes of Peak Acceleration Measurements," Third Annual Chesapeake Power Boat Symposium, Annapolis, MD, June 2012.

Appendix A. Theory of the Planing Simulator Program

A1.1. History of POWERSEA

In March, 1978, E. E. Zarnick of the David W. Taylor Naval Ship Research and Development Center published a paper entitled "A Nonlinear Mathematical Model of Motions of a Planing Boat in Regular Waves". This paper (number DTNSRDC-78/032) describes a low-aspect ratio strip theory that can be used to predict the vertical-plane motions of planing craft. The theory described in this paper is the basis for the POWERSEA program, and Zarnick's paper is a good theoretical reference for this program.

E. E. Zarnick (1978) formulated a mathematical model of forces acting on a planing craft. Zarnick's method assumes that wavelengths will be large with respect to the craft's length and that wave slopes will be small. Following the work of Martin (Martin, M., Theoretical Predictions of Motions of High-Speed Planing Boats in Waves. David W. Taylor Naval Ship Research and Development Center, DTNSRDC#76/0069, 1976), Zarnick (1978) developed a mathematical formulation for the instantaneous forces on a planing craft. In Zarnick's method, a planing craft is modeled as a series of strips or impacting wedges.

Following the work of Martin (1976), Zarnick (1978) developed a mathematical formulation for the instantaneous forces on a planing craft. Zarnick derived the normal hydrodynamic force per unit length as:

$$f = -\left\{\frac{D}{Dt}\left(m_a V\right) + C_{D,c}\rho b V^2\right\}$$
$$\text{where } \frac{D}{Dt}\left(m_a V\right) = m_a \dot{V} + \dot{m}_a V - \frac{\partial}{\partial \xi}\left(m_a V\right)\frac{d\xi}{dt} \tag{11}$$

Zarnick modeled sectional added mass as an impacting wedge:

$$m_a = k_a \frac{\pi}{2}\rho b^2 \text{ and } \dot{m}_a = k_a \pi \rho b \dot{b} \tag{12}$$

where k_a is an added mass coefficient. Zarnick used the value $k_a = 1.0$ from the derivation of Wagner (1932).

Since the horizontal component w_X of the wave orbital velocity is considered small with respect to $\dot{x}_{CG}$ only the vertical component w_Z is included. The boat relative velocities with the vertical wave component included are:

$$U = \dot{x}_{CG} * \cos(\theta) - (\dot{z} - w_Z) * \sin(\theta)$$
$$V = \dot{x}_{CG} * \sin(\theta) + (\dot{z} - w_Z) * \cos(\theta) - \dot{\theta}\xi \tag{13}$$

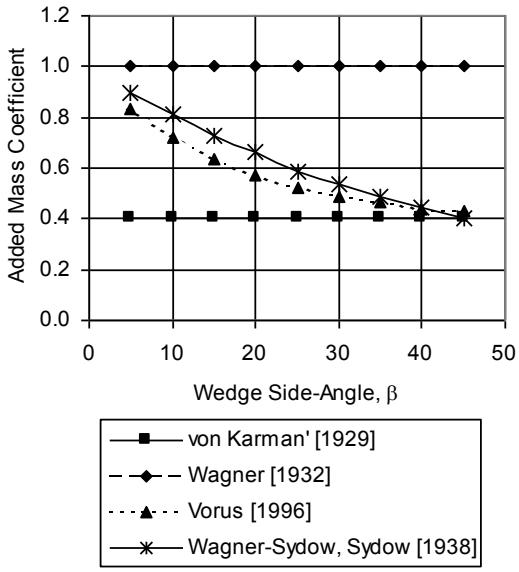

Figure 57 Added Mass Coefficient for Impacting Wedges, ka

Hydrostatic forces and moments must be included in the analysis, but are difficult to predict. Water rise at the bow of a planing vessel increases hydrostatic lift, flow separation at the stern decreases hydrostatic lift, and both cause an increase in pitching moment. These effects are speed dependent, and there is no single factor that can be used to correct the hydrostatics calculations for flow separation. In his work on rectangular planing surfaces, Shuford (1958) suggested that hydrostatic buoyancy should be halved in a dynamic simulation in order to achieve the correct total lift force. Zarnick (1978) found that use of an additional factor of one-half for the hydrostatic moment resulted in an accurate trim angle.

A1.2. Geometry Algorithms

The heart of the Planing Simulator system is a geometry program module that manages geometric entities, updates any dependencies when one of the entities is modified, and allows geometric operations such as calculating distances, intersections and areas based on the entities.

Each surface in the Planing Simulator is defined by a set of polynomials based on u and v:

$$X = fX(u, v),\ Y = fY(u, v),\ Z = fZ(u, v)$$
$$\text{where } u = [umin, umax],\ v = [vmin, vmax]$$

When the Planing Simulator updates the surface internally, it steps u from umin to umax in (udivisions*usubdivisions+1) steps, and it steps v from vmin to vmax in (vdivisions*vsubdivisions+1) steps, calculating (X, Y, Z) vertices at each step. It only displays vertices and lines between vertices at udivision/vdivision steps, but it keeps a record of all of the internal vertices. Surfaces thus are defined by triangles connecting the nearest vertices. This is a simple form of tessellation, a common practice in CAD software.

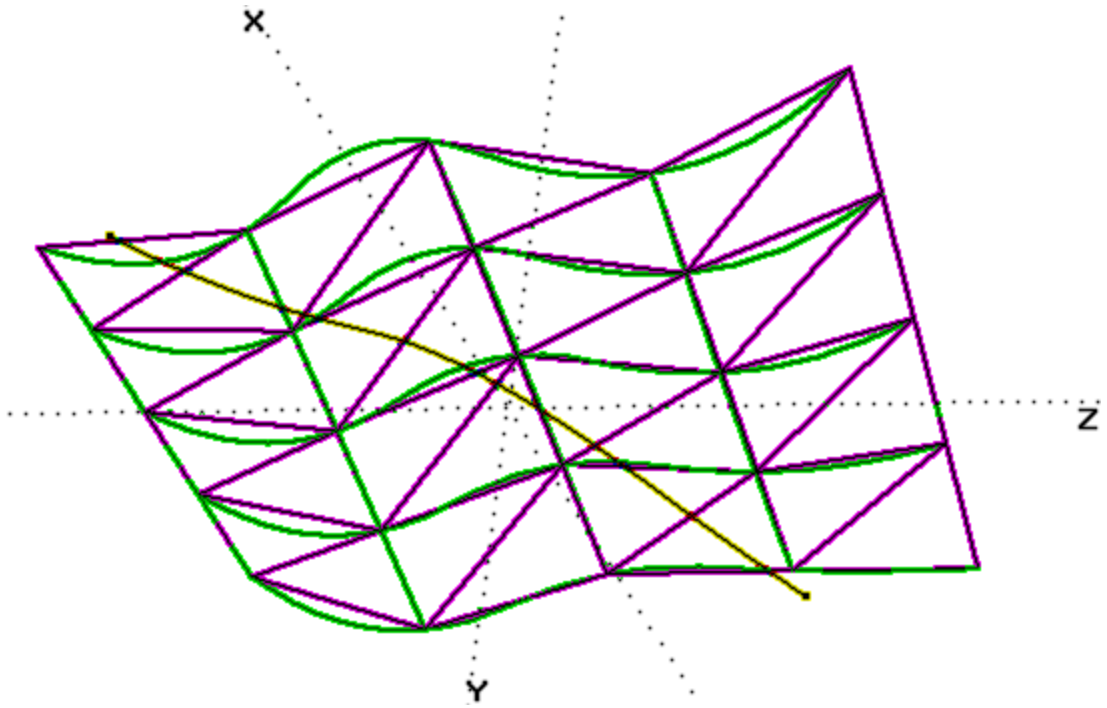

Figure 58 Tessellating a surface. Green lines represent constant U/V-parameter lines on a parametric (e.g. BSpline) surface. Surface is broken into triangles by finding vertices located in the surface, and connecting them with lines. Stations, waterlines and buttock lines found by computing intersections between triangle edges and cutting planes.

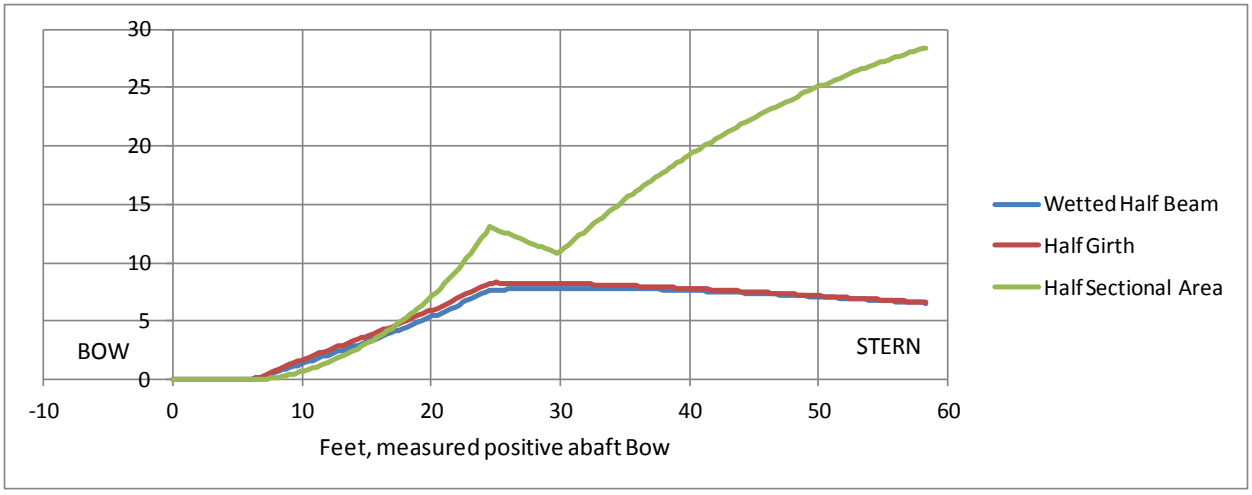

Figure 59 Precalculated geometric properties at each section. Geometry curves (e.g. BSpline curves) are preprocessed to minimize computation for individual time steps. The Mk III chine is first wet at about X=24 feet, and the chine would be submerged in calm water at about X=30 feet.

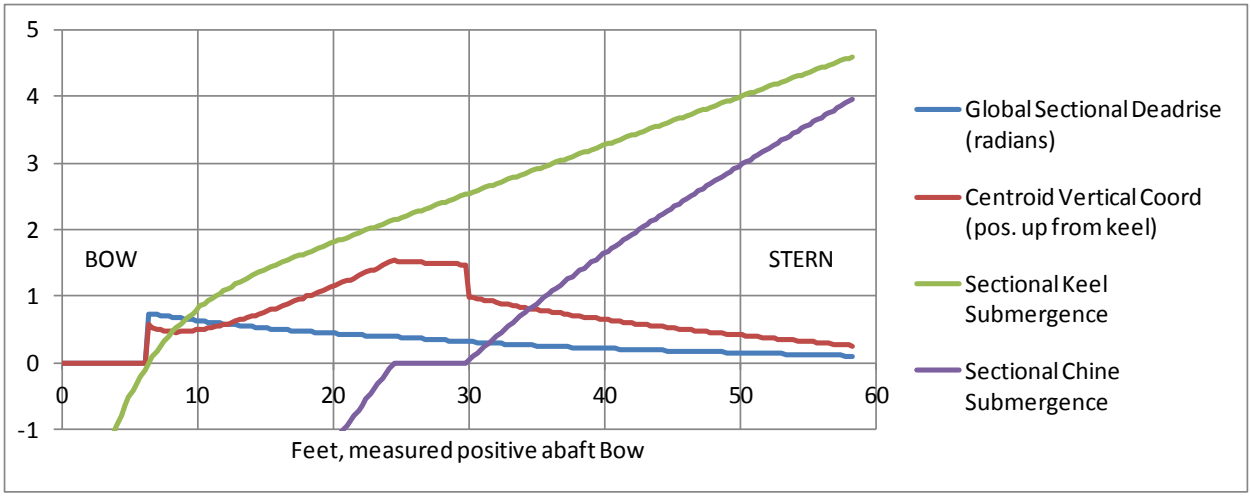

Figure 60 Precalculated geometric properties. Global deadrise is the slope of the line from the keel to the highest wetted point at a section. Positive submergence means that the keel or chine is below the pile-up water surface.

A1.3. Force Algorithms in the Planing Simulator

The Planing Simulator calculates five different forces acting on the hull and uses a weighted sum to calculate overall forces and moments to use in the equations of motion:

- Buoyancy
- Impacting Wedge in Chines-Dry Region
- Crossflow Drag in Chines-Wet Region
- Viscous Drag
- Dynamic lift due to Buttock Flow

Figure 61 and Figure 62 show the Mk III model from the SNAME Small Craft Datasheets as modeled in the Planing Simulator. This boat has significant chine warp, rocker and a tapered beam, all of which pose challenges to a planing boat simulator.

The boat was simulated with 65,000 lb. of load and was run at 20 knots, a low planing speed. The sectional forces calculated by the Planing Simulator are shown in Figure 63. This chart shows all five of the forces together to illustrate the relative importance of the forces. Following sections will describe each force individually.

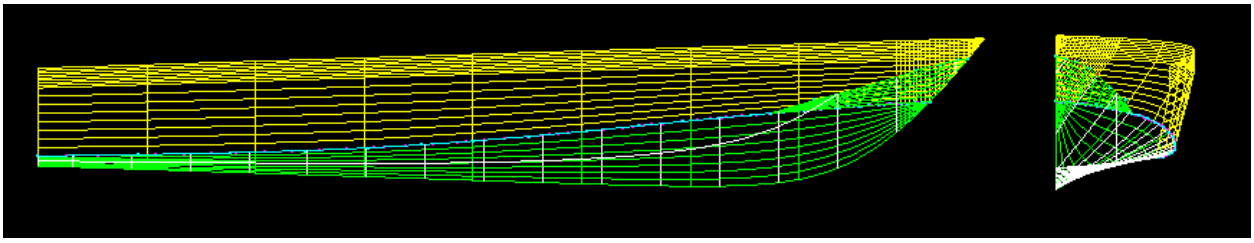

Figure 61 Profile and Bodyplan Views of Mk III model from SNAME Small Craft Datasheets

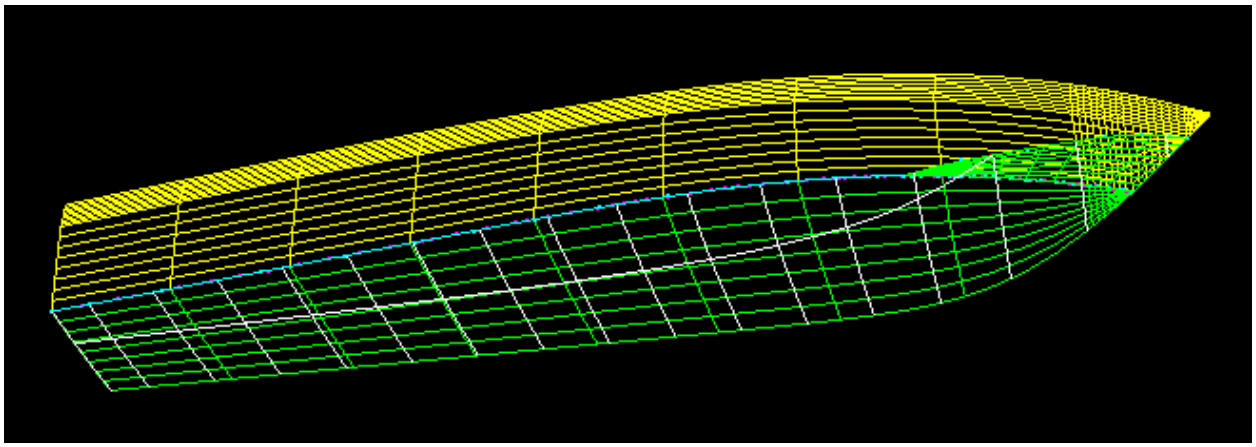

Figure 62 Perspective View of Mk III model from SNAME Small Craft Datasheets

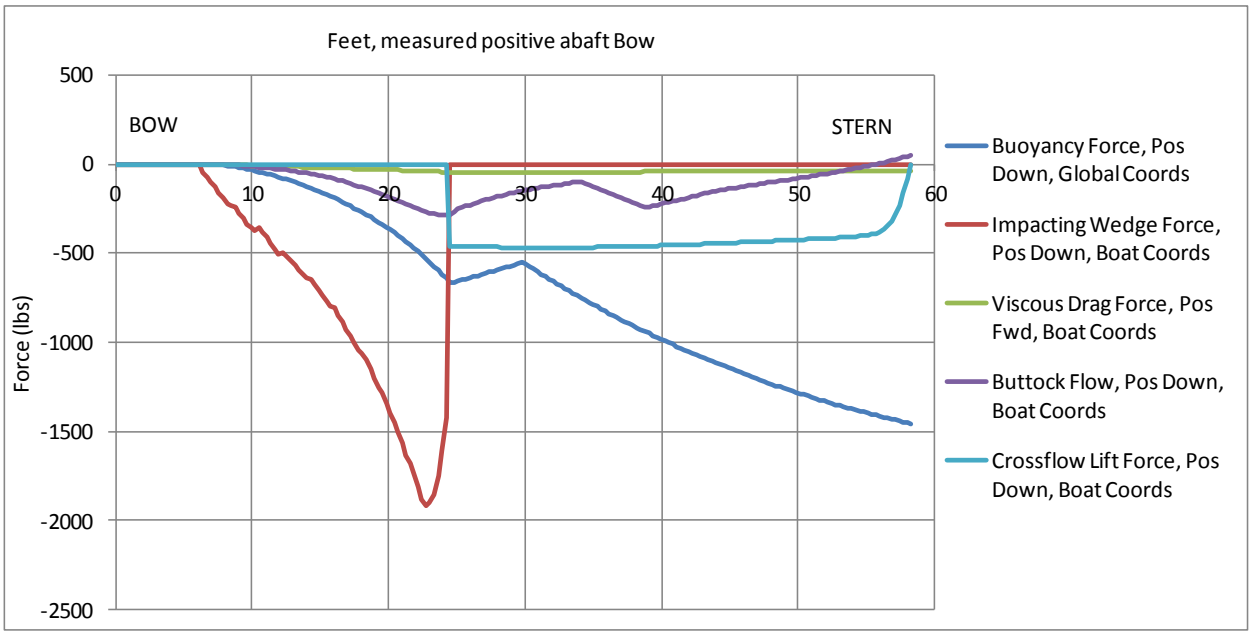

Figure 63 Relative forces obtained from simulation of Mk III. Calm water, 20 knots, 65,000 lbs. load. Force shown in inertial coordinates and design coordinates. Chine becomes wet at X=24, goes below calm-water at about X=30.

A1.4. Time-Derivative of Added Mass

To calculate the substantial derivative of the sectional momentum it is necessary to calculate the time derivative of the sectional added mass:

$$m_A = Cmy * [\ \pi/2 * \rho * b_{HCalm}{}^2\ ] \qquad (14)$$

where

$Cmy = Ka * WF^2$, Ka and WF are empirical functions of deadrise

$$d(m_A)/dt = \pi/2 * \rho * \{d(Cmy)/d(\beta) * d(\beta)/dt * b_{HPileup}{}^2 + Cmy * 2 * b_{HPileup} * d(b_{HPileup})/dt\} \quad (15)$$

Where

$$d(Cmy)/d(\beta) = d(\partial Ka)/ d\beta * WF^2 + 2 * Ka* WF * d(WF)/d\beta \quad (16)$$

A station is described by a piecewise linear curve connecting vertices that are found during the meshing operation. The global deadrise of a station is defined as the arctangent of the slope of the submerged portion of the station, $\Delta z/\Delta y = b_{HPileup} / T_{Pileup}$, where T_{Pileup} is the draft of the section including the piled up transverse waterject.

The time-derivative of deadrise at a station is calculated as:

$$d(\beta)/dt = d(\beta)/d(T_{Pileup}) * d(T_{Pileup})/dt \quad (17)$$

where

T_{Pileup} = wetted draft of section (including pileup)

$$d(\beta)/d(T_{Pileup}) = d(\text{atan}(b_{HPileup} / T_{Pileup}))/d(T_{Pileup})$$
$$= 1/(1+(b_{HPileup} / T_{Pileup})^2)*d(b_{HPileup} / T_{Pileup})/d(T_{Pileup})$$
$$= -1/(1+(b_{HPileup} / T_{Pileup})^2) * b_{HPileup} / T_{Pileup}{}^2 \quad (18)$$

$$d(b_{HPileup})/dt = d(b_{HPileup})/d(draft) * d(draft)/dt \quad (19)$$

where

d(WF)/d(β) = derivative of wetting factor regression model (above)

d(ka)/d(β) is closed form, comes from Vorus/Savander formulations

d(draft)/dt = draftDot (calculated in program)

A1.4.1. Impacting Wedge

In the following equations coefficients C_{BF} and C_{BM} correct the vertical force and pitching moment. Zarnick set these coefficients to 0.5 based upon the recommendation of Shuford.

A summary of the forces acting on the planing craft is:

$$F_N = \int_l \left\{ m_a \dot{V} + \dot{m}_a V - U \frac{\partial m_a V}{\partial \xi} + C_{D,c} \rho b V^2 \right\} d\xi$$

$$F_Z = -F_N * \cos(\theta) - \int_l \rho g C_{BF} a d\xi$$

$$F_X = -F_N * \sin(\theta)$$

$$F_\theta = \int_l \{ m_a \dot{V} + \dot{m}_a V - U \frac{\partial m_a V}{\partial \xi} + C_{D,c} \rho b V^2 - \rho g C_{BM} a * \cos(\theta) \} \xi \, d\xi \quad (20)$$

The vertical force F_Z is expanded as follows:

$$
\begin{aligned}
F_Z &= -F_N * \cos(\theta) - \int_l \rho g C_{BF} A d\xi \\
&= -\int_l \{(m_a \dot{V} + \dot{m}_a V - U \frac{\partial m_a V}{\partial \xi}) \cos(\theta) \\
&\quad + C_{D,c} \rho b V^2 \cos(\theta) + \rho g C_{BF} a\} \, d\xi
\end{aligned}
\tag{21}
$$

The time derivatives and partial derivatives of the boat-coordinate velocities are:

$$
\begin{aligned}
\dot{V} &= \ddot{x}_{CG} \sin(\theta) - \ddot{\theta}\xi + \ddot{z}_{CG} \cos(\theta) - \dot{w}_Z \cos(\theta) \\
&\quad + \dot{\theta}(\dot{x}_{CG} \cos(\theta) - \dot{z}_{CG} \sin(\theta)) + w_Z \dot{\theta} \sin(\theta) \\
\frac{\partial V}{\partial \xi} &= -\dot{\theta} - \frac{\partial w_Z}{\partial \xi} \cos(\theta) \\
\frac{\partial U}{\partial \xi} &= \frac{\partial w_Z}{\partial \xi} \sin(\theta)
\end{aligned}
\tag{22}
$$

- The vertical component of the wave orbital velocity can be described by:

$$
\begin{aligned}
\frac{dw_Z}{dt} &= \dot{w}_Z - U \frac{\partial w_Z}{\partial \xi} \\
\text{so } \dot{w}_Z &= \frac{dw_Z}{dt} + U \frac{\partial w_Z}{\partial \xi}
\end{aligned}
\tag{23}
$$

Making these substitutions and simplifying **YIELDS**:

$$
\begin{aligned}
F_N &= -M_a \cos(\theta) \ddot{z}_{CG} - M_a \sin(\theta) \ddot{x}_{CG} + Q_a \ddot{\theta} \\
&\quad + M_a \dot{\theta}(\dot{z}_{CG} \sin(\theta) - \dot{x}_{CG} \cos(\theta)) \\
&\quad + \int_l m_a \frac{dw_Z}{dt} \cos(\theta) d\xi - \int_l m_a w_Z \dot{\theta} \sin(\theta) d\xi \\
&\quad - \int_l m_a V \frac{\partial w_Z}{\partial \xi} \sin(\theta) d\xi + \int_l m_a U \frac{\partial w_Z}{\partial \xi} \cos(\theta) d\xi \\
&\quad + \int_l UV \frac{\partial m_a}{\partial \xi} d\xi - \int_l m_a U \dot{\theta} d\xi \\
&\quad - \int_l m_a U \frac{\partial w_Z}{\partial \xi} \cos(\theta) d\xi + \int_l m_a V \frac{\partial w_Z}{\partial \xi} \sin(\theta) d\xi \\
&\quad - \int_l V \dot{m}_a d\xi - \rho \int_l C_{D,c} b V^2 d\xi
\end{aligned}
\tag{24}
$$

Combining terms, replacing the total added mass with the equivalent integral of sectional added masses, and doing the same for the sectional moment of inertia yields:

$$
\begin{aligned}
F_N = &-\int_l m_a \cos(\theta)\ddot{z}_{CG}d\xi - \int_l m_a \sin(\theta)\ddot{x}_{CG}d\xi \\
&+ \int_l m_a \xi\ddot{\theta}d\xi + \int_l m_a \dot{\theta}(\dot{z}_{CG}\sin(\theta) - \dot{x}_{CG}\cos(\theta))d\xi \\
&+ \int_l m_a \frac{dw_Z}{dt}\cos(\theta)d\xi - \int_l m_a w_Z \dot{\theta}\sin(\theta)d\xi \\
&+ \int_l UV\frac{\partial m_a}{\partial \xi}d\xi - \int_l m_a U\dot{\theta}d\xi \\
&- \int_l V\dot{m}_a d\xi - \rho\int_l C_{D,c} bV^2 d\xi
\end{aligned}
\tag{25}
$$

The acceleration terms $\ddot{x}_{CG,}$ $\ddot{z}_{CG,}$ and $\ddot{\theta}$ are estimated using a numerical technique based on a running interpolation-polynomial estimate of state variable derivatives. The term $\frac{\partial m_a}{\partial \xi}$ is calculated using numerical derivatives.

Combining all terms into a single integral over the boat length l, a sectional hydrodynamic normal force can be calculated as:

$$
\begin{aligned}
f_N = &-m_a \cos(\theta)\ddot{z}_{CG} - m_a \sin(\theta)\ddot{x}_{CG} \\
&+ m_a \xi\ddot{\theta} + m_a \dot{\theta}(\dot{z}_{CG}\sin(\theta) - \dot{x}_{CG}\cos(\theta)) \\
&+ m_a \frac{dw_Z}{dt}\cos(\theta) - m_a w_Z \dot{\theta}\sin(\theta) \\
&+ UV\frac{\partial m_a}{\partial \xi} - m_a U\dot{\theta} \\
&- V\dot{m}_a - \rho C_{D,c} bV^2
\end{aligned}
\tag{26}
$$

The total normal force is $F_N = \int_l f_N d\xi$. A similar analysis is used to obtain an estimate of the instantaneous pitching moment.

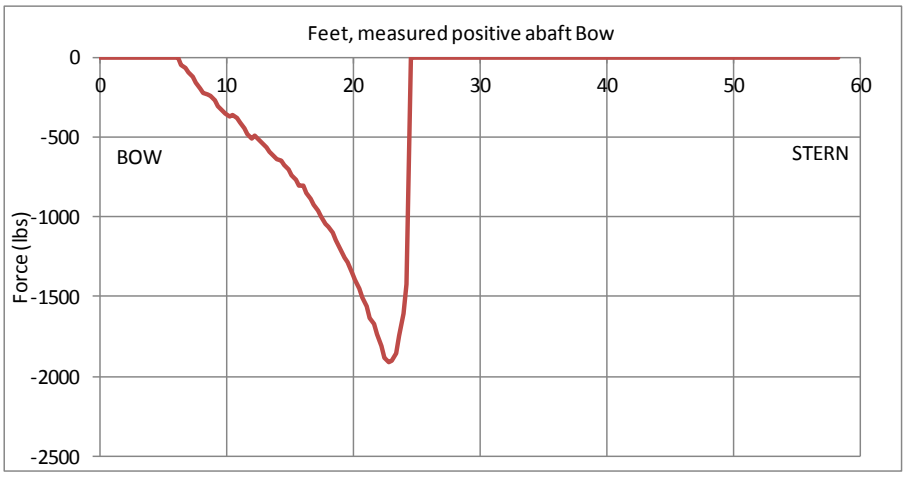

Figure 64 Impacting wedge calculated for Mk III running at 20 knots. Impacting wedge forces are only calculated in chines-dry region from the bow to X=24. Impacting wedge force is calculated in boat coordinates, positive down.

A.1.1 Wetting Factor and Added Mass in the Planing Simulator

The Planing Simulator combines semi-empirical algorithms to predict instantaneous forces and motions on a planing craft operating in irregular waves. By adding the force components and multiplying by the inverse of the sum of the inertial masses and the instantaneous added mass of the water, it is possible to predict the accelerations of the boat in three degrees of freedom. Integrating the accelerations produces the velocities (rates), and integrating again produces the time-dependent positions (angles).

The term "added mass" describes a fictional amount of fluid that moves synchronously with the movements of another object submerged in the fluid. In reality there is not a single volume of water that moves at the same rate as the object, adding to the apparent mass of the object, but rather a large mass of fluid particles that are set in motion at various speeds by the moving object. The aggregate hydrodynamic force applied to the object by these particles moving in their own trajectories can be expressed in terms of a fixed (smaller) mass that is moving exactly as the object moves. A two-dimensional flat plate oscillating at very high frequencies in an ideal fluid will cause a momentum change in the fluid such that the total derivative of the momentum change will appear to be caused by a constant mass moving in the same way as the plate. This effective mass will appear to equal that of a cylinder centered on the plate:

$$\begin{aligned} d(\text{momentum})/dt &= \text{sum}(d(m_1*v_1)/dt + d(m_2*d_2)/dt + \dots) \\ &= \text{sum}(m_{average})*d(v_{plate})/dt \end{aligned} \quad (27)$$

where

m_i is a particle of water moving at velocity v_i

$m_{average}$ is the apparent mass or "added mass" moving at v_{plate}, the speed of the plate

The amount of fluid that moves with a plate with non-zero thickness can be shown to be less than that associated with a thin flat plate:

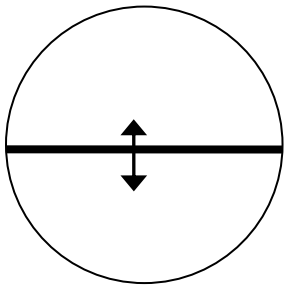

High Frequency Added Mass around a 2D flat plate. $m_A = \rho\pi r^2$

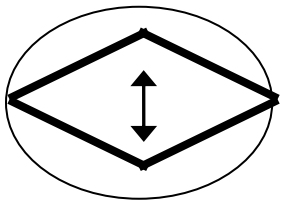

High Frequency Added Mass around a 2D flat plate with deadrise. $m_A = ka*\rho\pi r^2$

As a V-bottomed planing boat passes through the water, the water piles up transversely along the hull bottom (refer to Figure 65).

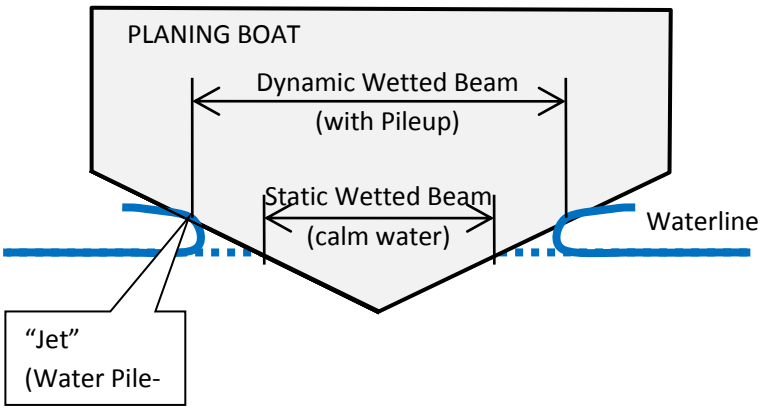

Figure 65 Water pile-up and transverse jets cause wetted-beam to be larger than static beam. The sectional added mass is the effective amount of water moving under the impacting wedge as it penetrates the surface.

The Planing Simulator calculates the added mass of a boat planing on the surface, so only one-half of the cylinder is used as the basis for the added mass. The sectional added mass is the product of the mass of a semicircle centered below the station (Area = $\pi/2 * \rho * b_{HCalm}{}^2$) and an added mass coefficient cmy that is a function of deadrise.

$$m_A = Cmy * \pi/2 * \rho * b_{HCalm}{}^2 \quad (28)$$

$$Cmy = Ka / WF^2 \quad (29)$$

$$Ka = f(\beta) \quad (30)$$

Where

m_A = sectional added mass
Cmy = vertical added mass coefficient
Ka = wetting coefficient, a function of global deadrise, β
ρ = density of water
$b_{HPileup}$ = dynamic half-wetted beam of the section (with "piled up" transverse jet)
b_{HCalm} = Static half-wetted beam of the section
β = global deadrise

Impacting wedge theory says that the forces on the Chines-Dry region of a planing craft arise from the change in momentum of the added mass of water associated with each section. This force is described mathematically as:

$$F = \frac{D(m*v)}{Dt} \quad (31)$$

Where "D/Dt" is the substantial derivative operator acting on the momentum, m*v:

$$\frac{Df}{Dt} \equiv \frac{\partial f}{\partial t} + \overline{v} \cdot \nabla f \quad (32)$$

As described in Section A1.2, this represents the force from successively deeper sections of the boat as it passes in front of a stationary observer. The velocity v is the vertical component of the velocity impacting on the hull (in boat-coordinates), and the mass m is the added mass of the water moving with the hull. In quasi-static planing operation (steady-state, no waves, constant heave, pitch and surge velocity), the added mass increases as the hull sections plunge successively deeper in the water, while the impacting rate of successive sections is constant.

Von Karman developed an expression for the added mass under an impacting wedge (Von Karman, 1929) based on a semicircle under the projected calm-water beam of the wedge:

$$m_A = \pi/2 * \rho * y^2/\tan(\beta)^2 \quad (33)$$

where

y = submergence = beam/tan(β),

so $y/\tan(\beta) = b_{HCalm}$ = Calm-water Half-Beam

β = deadrise of wedge (radians)

Wagner modified von Karman's solution by accounting for the effect of water pile-up on the edges of the wedge as it enters the water (Wagner, 1932):

$$m_A = \pi/2 * \rho * (\pi/2 * b_{HCalm})^2 \quad (34)$$

$$m_A = (\pi/2)^2 * [\ \pi/2 * \rho * b_{HCalm}{}^2\ ] \quad (35)$$

An added mass coefficient, Cm', is defined as the theoretical added mass / von Karman's added mass (which is the semicircle below the calm water projection). The added mass coefficient for Wagner's formulation is:

$$Cm' = (\pi/2)^2 \quad (36)$$

A wetting factor (WF) can be defined that relates the wetted beam including water pile-up to the calm water wetted beam. Using this wetting factor, an alternative added mass coefficient can be defined as:

$$Cmy = Ka * WF \quad (37)$$

where

Ka = added mass coefficient = f(β)

WF = water pileup (wetting) factor = f(β)

Zarnick assumed that the water pileup factor was π/2 so that the depth of penetration is:

$$d_e = \pi/2 * \text{draft} \quad (38)$$

where

d_e = effective draft

draft = calm water draft

π /2 = wetting factor.

Using this, the wetted beam of a wedge with a constant vertical velocity is

$b_{HPileup} = \pi/2 * b_{HCalm} = \pi/2 * \text{draft} * \cot(\beta)$

Zarnick modeled the added mass of a section as a semicircle whose width is the "wetted beam" of the section (Zarnick, 1978):

$$m_A = k_a * \pi/2 * \rho * b_{HPileup}{}^2 = k_a * \pi/2 * \rho * (\pi/2 * b_{HCalm})^2$$
$$= k_a * WF * \pi/2 * \rho * b_{HCalm}{}^2 \quad (39)$$

Where

k_a = 1 (in the original Zarnick formulation)

Using Zarnick's formulation the time-derivative of the sectional added mass is:

$$d(m_A)/dt = k_a * \pi * \rho * 2 * (\pi/2 * draft*\cot(\beta)) * d(\pi/2 * draft*\cot(\beta))/dt$$
$$= k_a * \pi * \rho * b_{HCalm} * d(\pi/2 * draft*\cot(\beta))/dt$$
$$= k_a * \pi * \rho * b_{HCalm} *(\pi/2 * \cot(\beta)) * d(draft))/dt$$
$$= k_a * \pi * \rho * b_{HCalm} *(\pi/2 * \cot(\beta)) * v \quad (40)$$

Where

v = Vertical velocity of section (in boat-coordinates)

A1.4.1.1 Wetting Factor

The "wetting factor" (WF) is defined as the ration between the dynamic wetted beam and the static (zero speed) wetted beam. The wetting factor is a non-linear function of the global deadrise β. Tveitnes investigated the water rise from impacting wedges (Tveitnes, et. al., 2008), and his results are summarized in Figure 66.

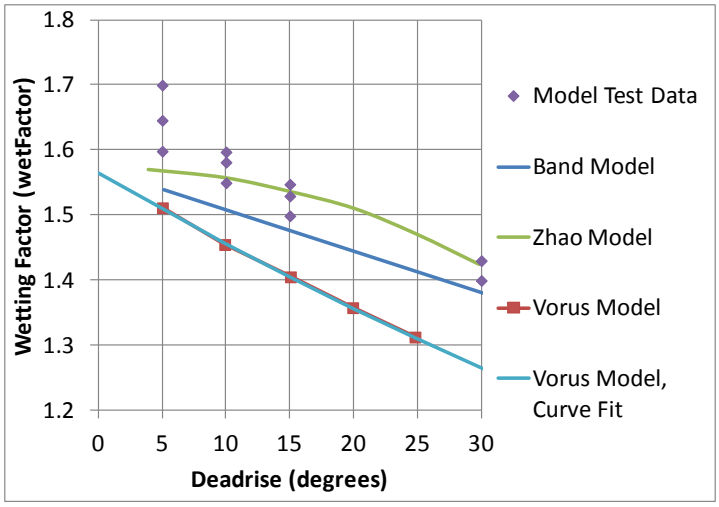

Figure 66 Wetting Factor (Dynamic Wetted Beam vs Static Wetted Beam)

Vorus developed a robust model for the wetting factor (Vorus, 1996) and his work was used as the basis for the wetting factor model in the Planing Simulator. Data calculated using Vorus's method was fit to a quadratic regression model of the form:

$$WF = d1 + \beta * (d2 + \beta * d3) \quad (41)$$

Where d1, d2, and d3 are regression coefficients and β is the overall sectional deadrise in radians. The coefficients for this model are listed in Table 11. Data points calculated using Vorus's model and a curve calculated from the Planing Simulator regression model are included in Figure 66.

Table 11 Regression coefficients for wetting factor model

Coefficient	Value
d1	1.565284483
d2	-0.647205817
d3	0.140480736

A1.4.1.2 Added Mass

The literature describes two different added mass factors, Cm' and Cmy. Cmy is the vertical added mass factor which is defined as Cm' * Wetting Factor, where wetting factor is defined above. The algorithm for modeling added mass in the Planing Simulator starts by calculating the wetted beam, which is then used along with Cm' to calculate instantaneous sectional added mass.

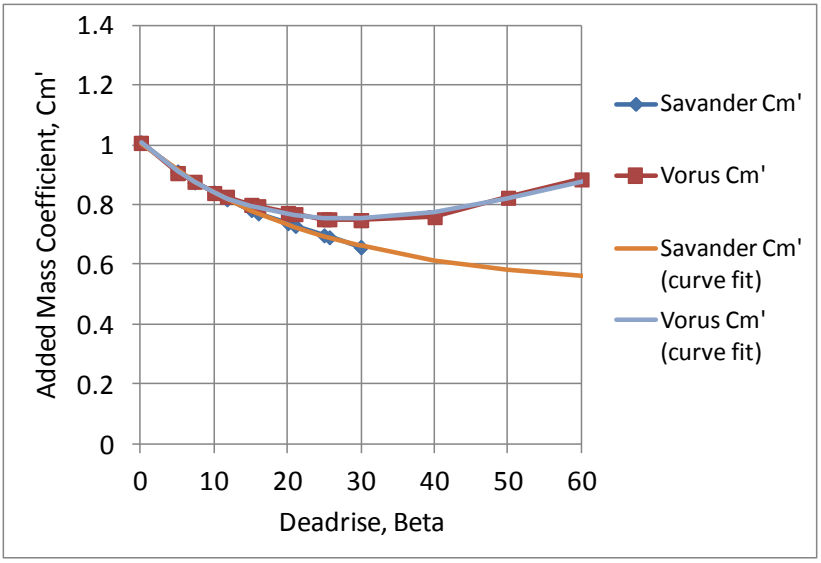

Figure 67 Added Mass coefficient versus deadrise

The relationships between several added mass formulations are shown in Figure 67. From the literature a common factor in added mass coefficient formulations is the basis function:

$$\text{Basis Function} = (\pi/(2*\beta)-1) * 2 *\tan(\beta)/\pi \quad (42)$$

Where

β = Deadrise defined by line connecting keel to farthest wetted point athwartships

This function was used as the basis for regression models of the Savander and Vorus formulations. As can be seen in Figure 67, the numerical approximations are quite close to formulations of Vorus and Savander. The Planing Simulator models the added mass coefficient Ka with an empirical model. d(ka)/d(β) is closed form, comes from Vorus/Savander formulations. For computational efficiency, the Planing Simulator precalculates the values of static wetted beam b_{HCalm} and dynamic wetted beam $b_{HPileup}$ versus submergence (draft) and creates spline models of the relationships. During each iteration in a time-domain simulation, the Planing Simulator finds the derivatives of b_H with respect to draft by differentiating the spline functions created for each section.

A1.5. Buoyancy

The Planing Simulator is intended to simulate high speed craft so the majority of the lift force arises from hydrodynamic mechanisms. Hydrostatic forces cannot be ignored, however, especially at lower planing speeds. In reality the hydrostatics and hydrodynamic forces cannot be separated, but for planing boats it is possible to make some simplifying assumptions about the hydrostatic forces and treat them separately from the hydrodynamic ones.

For most planing boats the water will separate off the bottom edge of the transom, so the wetted surface is not bow-stern symmetric. This effect is considered to be part of the impacting wedge formulation, so no hydrostatic "drag" is included in the Planing Simulator formulation.

Engineers calculate hydrostatic pressure by applying the Bernoulli Equation along a streamline starting at the free surface and ending at the point of interest. In the case of a planing craft, different results are obtained if the calm water surface is used as the starting point (Figure 68, A) than if the wetted surface at the boat hull is used as the starting point (Figure 68, B). By comparing simulation results for quasi-static (constant speed) operation, it was found that more accurate results are obtained using the pile-up wetted surface on the boat hull as the zero-pressure reference height for hydrostatic pressure calculations. As can be seen in Figure 68, this choice results in a lower hydrostatic bow-down moment than would be obtained by using the calm water surface as the reference plane.

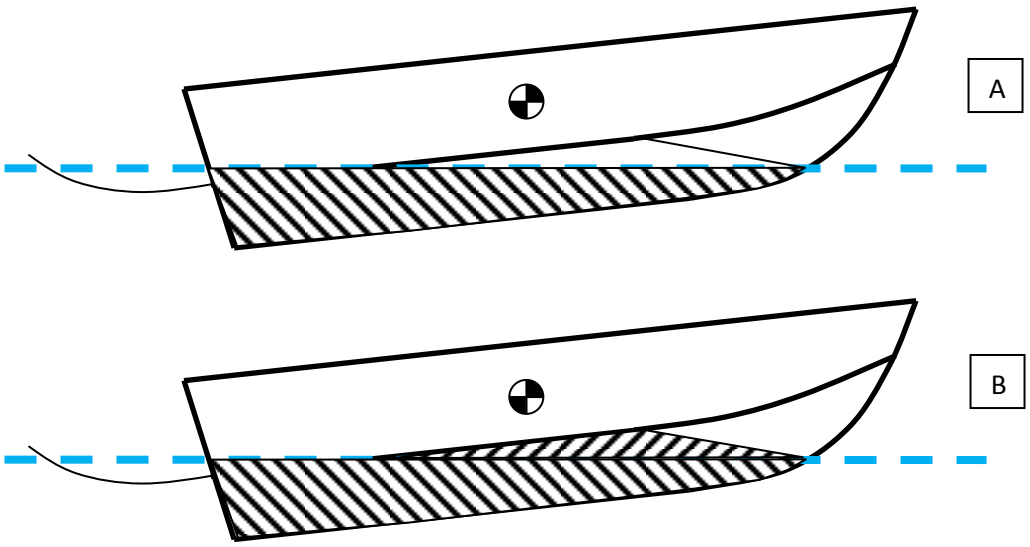

Figure 68 Calculating Displacement using calm waterline (top, A) or dynamic waterline (bottom, B). Buoyancy creates a larger bow-up moment in B than in A.

To illustrate the buoyancy force calculations, consider a Mk III simulation model. The buoyancy force at 20 knots and 65,000 pounds is charted in Figure 69. As sectional buoyancy force is directly proportional to the cross-sectional area, the buoyancy force is zero at the point on the left side of this chart where the keel first hits the water. Moving abaft this point the section area increases roughly by the square of the wetted beam. At approximately X=24, the piled up water touches the chine, corresponding to the peak in the shaded area in Figure 68 B. Moving further aft, the buoyancy force drops because the pile-up water separates off of the chine. At approximately X=30 the chine goes below the calm waterline and the buoyancy starts to rise accounting for the sectional area above the chine but below the calm waterline.

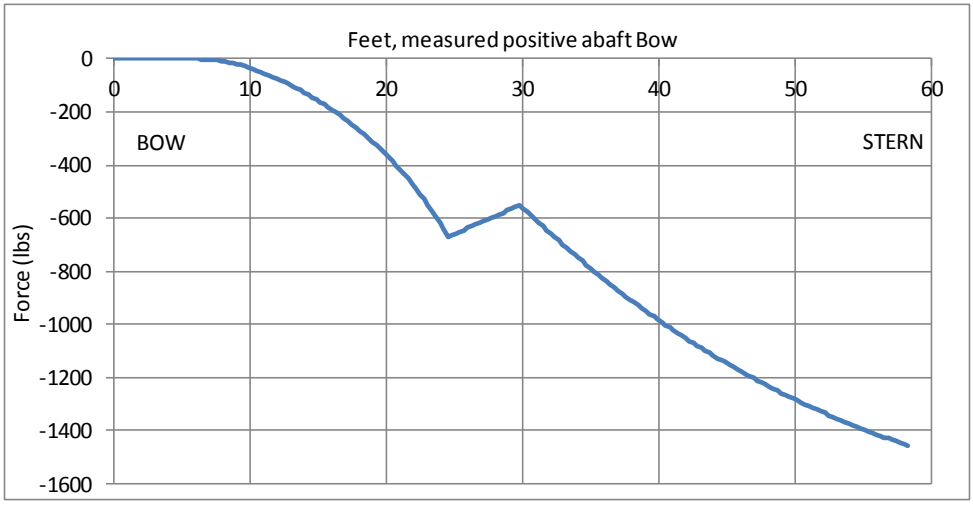

Figure 69 Buoyancy force calculated for Mk III running at 20 knots. Chine becomes wet at X=24, chine goes below calm-water plane at about X=30. Buoyancy force is calculated in global coordinates, positive down.

A.1.2 Buttock Flow

To better model dynamic lift and induced drag due to the flow of water along the bottom of planning hulls, a 2D panel code was introduced in the Planing Simulator. These forces are implicitly included in the added mass formulations in the chines-dry region, but better support for the lift from buttock curvature is required. A hybrid panel method has been employed to predict the lift and induce drag from flow along buttock lines.

A triangular mesh is generated from the hull geometry defined in the Planing Simulator to represent the hull surfaces. An array of 2D foils is created by intersecting the submerged portion of the mesh (using the calm water draft) along 7 buttock planes starting from the centerplane out to 98% of the maximum beam at the chine. The resulting points are mirrored across the calm waterline and these are fitted with a foil curve (Figure 70). Further foil curves are generated by generating buttock curves at the same buttock planes but fractions of the calm water drafts. Using a panel code derived from a constant-strength vortex method described in Katz (1991), a matrix of influence coefficients is calculated at the x-coordinates of a set of transverse sections along each buttock and at each draft for a range of trim angles ranging from -30 degrees to +30 degrees. (Refer to Table 12). These values are calculated in the Planing Simulator's Mesh command before making any analysis runs.

Table 12 Buttock flow panel coefficients are precalculated for each buttock line and draft combination at angles of attack in this table.

-30.0	-3.0	0.0	1.333	2.5	3.5	4.5	6.0
-20.0	-2.0	0.333	1.667	2.750	3.750	4.750	10.0
-10.0	-1.0	0.667	2.0	3.0	4.0	5.0	20.0
-5.0	-0.5	1.0	2.250	3.250	4.250	5.5	30.0

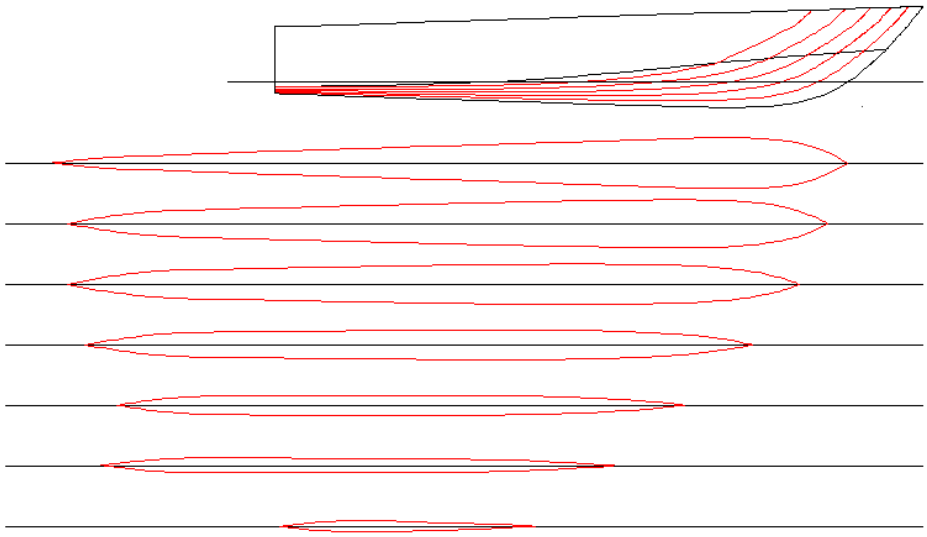

Figure 70 Planing hull with foils created from buttock curves.

At each time step of an analysis, a pressure coefficient (C_{ps0}) is calculated for each transverse section. The pressure coefficient is obtained by finding the instantaneous half-wetted beam, draft and trim angle of the section. Using the values obtained at the quarter-wetted beam, draft and trim angle, the pressure coefficient is interpolated from the matrix of influence coefficients previously calculated.

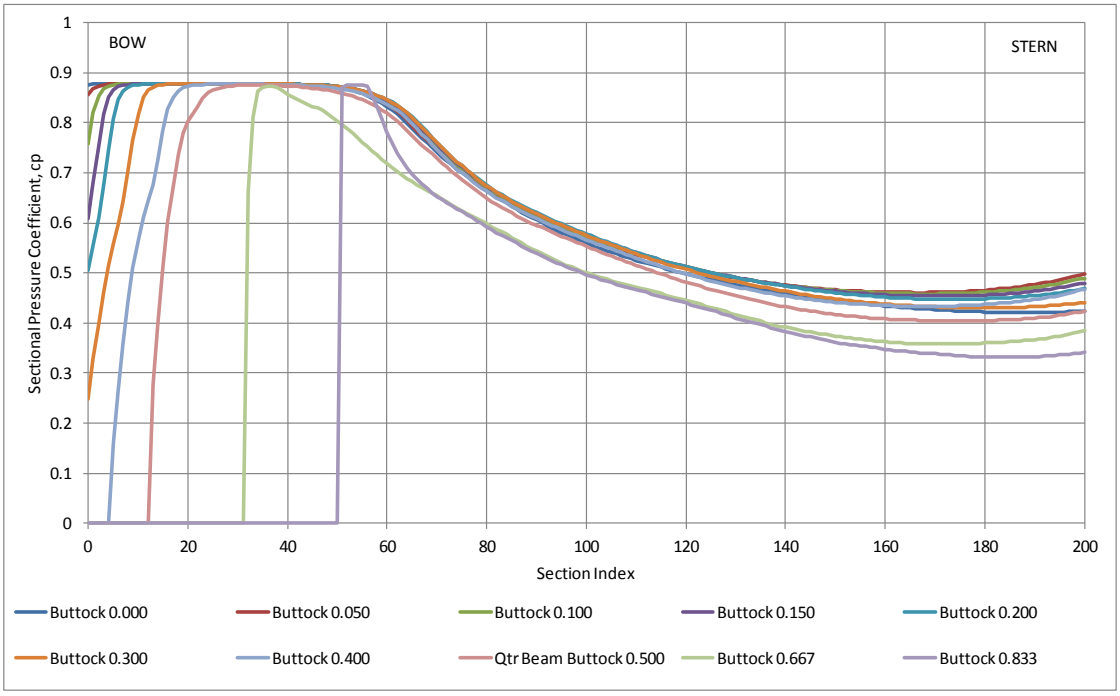

Figure 71 Pressure coefficients calculated using panel code along buttock foils at 4 degree trim. Buttocks are labeled by the fraction of the maximum beam (e.g. "Buttock 0.400" is located at 40% of BMax from centerplane).

A correction for low aspect ratio wings using Jones' approximation (Jones, 1946) is applied to the pressure coefficient:

$$AR = B_w/L_B \quad (43)$$

$$C_{ps} = 0.25C_{ps0}AR * \cos(\beta) \quad (44)$$

where,

B_w = section wetted beam

L_B = buttock length

AR = section aspect ratio

β = Global sectional deadrise (radians)

The panel force due to pressure at any given section is calculated with the following formula:

$$F_s = \frac{\rho}{2} C_{ps} U_\infty^2 B_w d\xi \quad (45)$$

where,

F_s = Panel force at given section

U_∞= Surge velocity

$d\xi$ = Panel length

Lift (L_S) and drag (D_S) forces are derived from this panel force and the slope of the buttock curve at the given section (α):

$$L_s = F_s cos\alpha \quad (46)$$

$$D_s = F_s sin\alpha \quad (47)$$

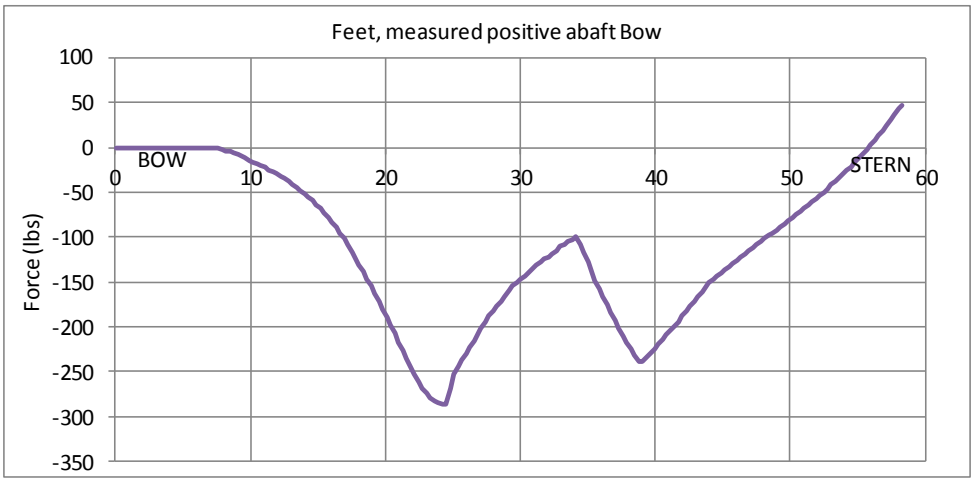

Figure 72 Sectional lift from buttock flow for Mk III running at 20 knots. Transition from chines-dry to chines-wet occurs at X=24. Buttock lift force calculated in boat coordinates, positive down. Transitions in pressure coefficient at approx. X=34 and X=38 from interpolation between buttocks at regular intervals.

A1.5.1. Crossflow Drag

The crossflow drag in the chines-wet-region is modeled with a drag coefficient, CDC, that varies along a straight line from the start of the chines-wet-region to the transom. Further, a blending function is applied

at a fraction of the beam forward of the transom so that the CDC coefficient drops smoothly to zero at the transom (Figure 73)

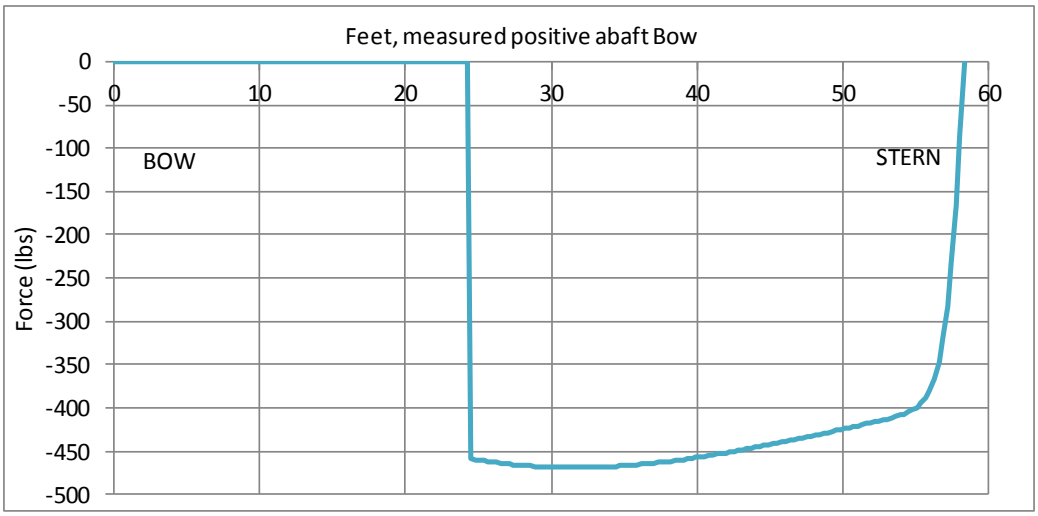

Figure 73 Section lift force from crossflow drag coefficient in chines-dry region. Force calculated by the Planing Simulator for Mk III running at 20 knots. The transition from chines-dry to chines-wet occurs at X=24. Lift force from crossflow drag is calculated in boat coordinates, positive down.

A.1.3 Viscous Drag

At each time step the mean wetted length, the Reynolds Number, and a friction coefficient can be calculated. The friction coefficient is calculated using the Prandtl-Schlichting line. For most of the hull this friction coefficient will be valid, but for highly curved sections the water flow will be significantly greater than the nominal water flow past the hull. A sectional friction force is calculated as:

$$f_D = \frac{1}{2} C_F \rho \, v_i^2 g_i \tag{48}$$

where f_D = Sectional friction drag

C_F = Overall friction coefficient

v_i = Sectional velocity (calculated from forward "cant" of surface normal)

g_i = Sectional wetted girth

An example of the shape of the viscous drag curve for a Mk III planing boat is shown in Figure 74.

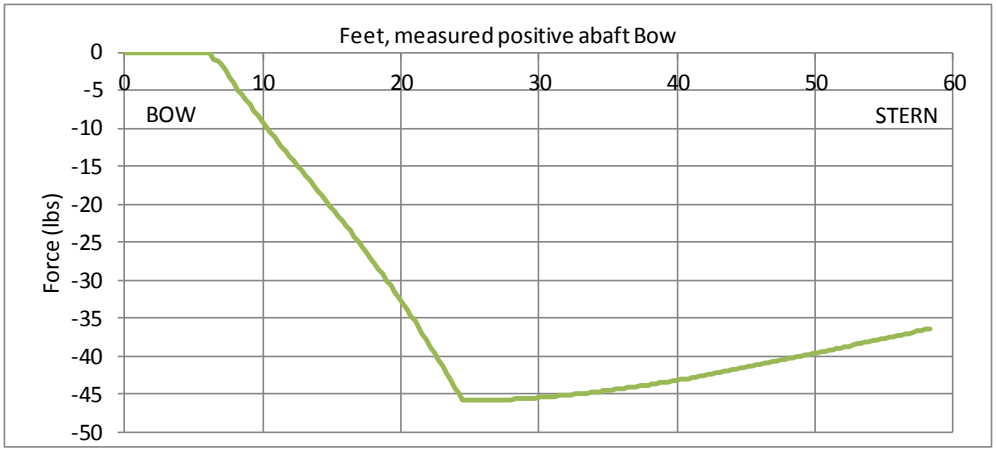

Figure 74 Viscous drag calculated by the Planing Simulator for Mk III running at 20 knots. The transition from chines-dry to chines-wet occurs at X=24.

A1.5.2. Combining Algorithms

The previous sections describe ways to predict forces from the impacting wedge, crossflow drag, buttock flow, viscous drag, and hydrostatic buoyancy algorithms. These forces must be blended so as to avoid double-counting physical phenomena. For example, the impacting wedge forces apply in the chines-dry region and the lift predicted by buttock flow cannot duplicate the predictions from the impacting wedge algorithm. On the other hand, the forces predicted by the buttock flow algorithms must be taken into account in order to predict negative gage patches on the hull.

Weighting coefficients for each of the force sources are specified:

1. Manually, usually by calibrating a model against measured data.
2. Automatically by comparing the principal characteristics of the hull being simulated with other hulls whose planing characteristics are known.

The automatic method is based on a database of model test data sorted by normalized principle characteristics. These principal characteristics are intended to be geometric or other physical characteristics of the hull

- They should be non-dimensional (if possible)
- They should describe most of the shape of the hull
- Must have physical definition (pass common sense test)

These characteristics are used in the calculation of the weighted forces, so they have to pertain to the wetted surface of the hull. For example, it is not appropriate to use the conventional projected planing area (area bounded by the transom and the chines, projected on the calm water surface) because it may be that the forward section of this area is never wet. If that is the case then the shape of that area would have no effect on the motions of the boat. Instead a better metric is the instantaneous waterplane area.

Normalization. Linear parameters such as mean wetted length are normalized by the maximum instantaneous beam. Angular parameters such as keel camber, chine warp and half angle of entrance are not normalized because they are unchanging as a function of the scale factor of the boat. Curvature values are calculated with 1/length dimensions, so they are normalized by multiplying by the beam.

The current hydrodynamic database consists of information from many dozens of model tests and includes several hundred data points. Research continues in this area.

SHIP STRUCTURE COMMITTEE LIAISON MEMBERS

LIAISON MEMBERS

American Society of Naval Engineers	Captain Dennis K. Kruse (USN Ret.)
Bath Iron Works	Mr. Steve Tarpy
Colorado School of Mines	Dr. Stephen Liu
Edison Welding Institute	Mr. Rich Green
International Maritime Organization	Mr. Igor Ponomarev
Int'l Ship and Offshore Structure Congress	Dr. Alaa Mansour
INTERTANKO	Mr. Dragos Rauta
Massachusetts Institute of Technology	
Memorial University of Newfoundland	Dr. M. R. Haddara
National Cargo Bureau	Captain Jim McNamara
National Transportation Safety Board - OMS	Dr. Jack Spencer
Office of Naval Research	Dr. Yapa Rajapaksie
Oil Companies International Maritime Forum	Mr. Phillip Murphy
Samsung Heavy Industries, Inc.	Dr. Satish Kumar
United States Coast Guard Academy	Commander Kurt Colella
United States Merchant Marine Academy	William Caliendo / Peter Web
United States Naval Academy	Dr. Ramswar Bhattacharyya
University of British Columbia	Dr. S. Calisal
University of California Berkeley	Dr. Robert Bea
Univ. of Houston - Composites Eng & Appl.	
University of Maryland	Dr. Bilal Ayyub
University of Michigan	Dr. Michael Bernitsas
Virginia Polytechnic and State Institute	Dr. Alan Brown
Webb Institute	Prof. Roger Compton

RECENT SHIP STRUCTURE COMMITTEE PUBLICATIONS

Ship Structure Committee Publications on the Web - All reports from SSC 1 to current are available to be downloaded from the Ship Structure Committee Web Site at URL: http://www.shipstructure.org
SSC 445 – SSC 393 are available on the SSC CD-ROM Library. Visit the National Technical Information Service (NTIS) Web Site for ordering hard copies of all SSC research reports at URL: http://www.ntis.gov

SSC Report No.	Report Bibliography
SSC 470	Finite Element Modeling Methods: Vibration Analysis For Ships Spence, J. H.; Favini, E. A.; Page, C. A. 2015
SSC 469	Strength And Fatigue Testing Of Composite Patches For Ship Plating Fracture Repair Karr, D.G.; Baloglu, C.; Cao, T.J.; Douglas, A.; Nielsen, K.; Ong, K.T.; Rohrback, B.; and Si, N. 2015
SSC 468	Development of a Structural Health Monitoring Prototype for Ship Structures Grisso, B.L 2013
SSC 467	Incorporation of Residual Stress Effects in a Plasticity and Ductile Fracture Model for Reliability Assessments of Aluminum Ship Hayden, M.J.; Gao, X,; Zhou, J.; Joyce, J.A. 2013
SSC 466	Mean Stress Assessment in Fatigue Analysis and Design Yuen, B.K.; Koko, T.S.; Polezhayeva, H.; Jiang, L 2013
SSC 465	Predictive Modeling Impact of Ice on Ship and Offshore Structures Bueno A. 2012
SSC 464	Design and Detailing for High Speed Aluminum Vessels Design Guide and Training Mish, Wh Jr., Lynch T., Hesse E., Kulis J., Wilde J., Snyder Z., Ruiz F. 2012
SSC 463	Marine Composites NDE, Inspection Techniques for Marine Composite Construction Greene, E 2012
SSC 462	Review of Current Practices of Fracture Repair Procedures for Ship Structures Wang, G, Khoo, E., ABS Corporate Technology 2012
SSC 461	Structural Challenges Faced By Arctic Ships, Kendrick A., Daley C. 2011
SSC 460	Effect of Welded Properties on Aluminum Structures, Sensharma P., Collette M., Harrington J. 2011
SSC 459	Reliability-Based Performance Assessment of Damaged Ships, Sun F., Pu Y., Chan H., Dow R.S., Shahid M., Das P.K. 2011